A comprehensive study on the size-dependent analysis of strain gradient multi-directional functionally graded microplates via finite element model

Armagan Karamanli[a*], Metin Aydogdu[b], Thuc P. Vo[c*]

[a]Faculty of Engineering and Natural Sciences, Mechatronics Engineering, Bahcesehir University, Istanbul, Turkey.

[b]Department of Mechanical Engineering, Trakya University, 22030 Edirne, Turkey

[c]School of Engineering and Mathematical Sciences, La Trobe University, Bundoora, VIC 3086, Australia

[*]Corresponding author. E-mail: armaganfatih.karamanli@eng.bau.edu.tr (A. Karamanli); t.vo@latrobe.edu.au (T. P. Vo)

Abstract

This paper presents a comprehensive study on bending, vibration and buckling behaviours of the multi-directional FG microplates. The material properties vary continuously both in-plane and through-thickness directions. Based on a quasi-3D shear and normal deformation plate theory and the modified strain gradient theory, a finite element model is proposed and employed to solve the problems of the multi-directional FG microplates with various boundary conditions. The verification is performed by comparing the numerical results with those from the previous studies. A number of numerical examples on the multi-directional FG microplates with nine boundary conditions and power-law index have been carried out. The effects of three material length scale parameters, aspect ratio, gradient indexes in spatial directions and boundary conditions on the displacements, natural frequencies and buckling loads of 1D, 2D and 3D-FG microplates are investigated in details. Some new results, which are not available in open literature, are provided as references for the future studies.

Keywords: Multi-directional FG microplates, modified strain gradient theory, bending, buckling, vibration, FEM

1. Introduction

Functionally graded materials (FGMs) have been used for micro/nano structures and their responses are size-dependent, which implies that classical elasticity theories fail to capture ([1- 3]). In order to solve these problems, various size-dependent elasticity theories are proposed, and their comprehensive review can be found in Ref. [4]. Among them, two theories, namely the Modified Couple Stress Theory (MCST) [5] and Modified Strain Gradient Theory (MSGT) [6] and are the most popular and widely used for the microstructures. It should be noted that the MSGT with three material length scale parameters (MLSPs), which are related to dilatation gradient, deviatoric gradient and symmetric rotation gradient tensors, is more general and complicated than the MCST with only one MLSP associated with rotation gradient. Moreover, the MSGT can be recovered to the MCST if the last two MLSPs are vanished. Besides, MSGT can give better prediction for very small plates at micron scale, especially when thickness is the same with MLSP. Due to this reason, the MSGT combined with the Classical Plate Theory (CPT), and First-order Shear Deformation Theory (FSDT) as well as several Higher-order Shear Deformation Theories (HSDTs) including Refined Plate Theory (RPT) and Third-order Shear Deformation Theory (TSDT) are employed by many researchers when dealing with the FG microplates. Mirsalehi et al. [7] developed CPT model to solve stability and dynamic responses of the FG microplates. The flexural response of the isotropic microplates was investigated using the extended Kantorovich technique and CPT by Movassagh and Mahmoodi [8]. Li et at. [9] developed strain gradient model using the neutral surface approach to provide bending solutions of bi-layered microplate. Kandaz and Dal [10] proposed different strain gradient finite element models to study the flexural responses of the isotropic microplates. Borjalilou and Asghari [11] investigated the effects of the small-scale on the thermoelastic damping for the isotropic microplates by using the CPT. By using the FSDT, Jiang and Wang [12] investigated the natural frequencies of the FG microplates. This theory was employed by Ashoori and Mahmoodi [13] to reveal a nonlinear strain gradient isotropic plate

formulation. Mohammadimehr et al. [14] employed generalized differential quadrature technique to investigate the dynamic stability of the annular carbon nanotube reinforced composite facesheets sandwich plates. The structural behaviours of the graphene nanoplatelets reinforced imperfect annular FG microplates were studied by using the FSDT and differential quadrature method [15]. Ghalebahman et al. [16] explored the natural frequencies of the composite micro-panels reinforced by boron nitride nanotubes considering the effect of an elastic foundation. Ansari et al. [17] proposed the FSDT model for thermal buckling of rectangular and later circular/annular FG microplates [18]. Shenas and Malekzadeh [19] focused on vibration responses of the FG quadrilateral microplates in thermal environment. In order to obtain more accurate results for the thick plates and ignore the shear correction factor in the FSDT, HSDTs are widely used. Sahmani and Ansari [20] derived the Navier solution for free vibration behaviour of the FG microplates. Zhang et al. ([21], [22]) used the TSDT to investigate structural responses of the FG square microplates with simply supported boundary conditions and later FG circular/annular microplates. Hughes et al. [23] proposed the Isogeometric analysis (IGA), which is employed by numerous researchers [24-32]. Thai et al. [26] developed IGA model based on the TSDT for linear analysis and later extended to transient analysis [27] and post-buckling behaviour [28] of the FG microplates. Thai et al. ([29], [30]) proposed a size-dependent IGA-RPT model for structural analyses of the FG sandwich microplates and FG-CNTRC microplates. Farzam and Hassani [31] used IGA-RPT to obtain deflections and buckling loads of the FG microplates under thermal conditions. Nguyen et al. [32] developed extended IGA for vibration of cracked FG microplates. Akgoz and Civalek [33] performed the mechanical analysis of the isotropic microplates using a sinusoidal plate theory. Li et al. [34] carried out analysis to explore the stability of the organic solar cell resting on an elastic foundation using a TSDT. The stability responses of the FG GNPs reinforced microplates were revealed by Arefi et al. [35] with the inclusion of the thermal effects. It should be mentioned that all of the above studies [12-35], the transverse displacement is assumed to

be constant and thus only shear deformation effect is considered, which means that normal deformation or thickness stretching effect is neglected. Carrera et al. [36] clearly identified the importance of this effect for the thick FG plates and concluded that it cannot be ignored. There are some studies taken into account both shear deformation and normal strain effects, which also called quasi-3D shear deformation theories, but limited to the MCST ([37]-[42]). Most of the above studies ([7]-[42]) reported on the FG microplates whose material distributions are assumed to be through-thickness (1D). Nowadays, many applications are demanding multi-directional FG structures whose material properties change in two or more directions [43]. This topic has attracted an increasing interest from researchers, who investigated the structural responses of the FG plates with in-plane (2D) and 3D stiffness variations ([44-67]). More details related to each paper can be found in recent review by Ghatage et al. [43]. Although there is large amount of studies on this topic, the only very few works dealing with 2D FG microplates but again limited to the MCST. Farzam and Hassani [68] proposed an IGA-RPT for linear analysis of in-plane FG porous microplates. Bakhsheshy and Mahbadi [69] derived Navier solution to study vibration of 2D FG microplates subjected to temperature distribution using the TSDT. It is clear that there is a gap related to the size-dependent behaviour of the multi-directional FG microplates using a quasi-3D shear deformation theory via the MSGT and finite element model (FEM), which are the main contributions of this paper.

In this work, a quasi-3D shear deformation theory and the MSGT is employed to study the size-dependent effects of the multi-directional FG microplates. The material properties vary continuously both in-plane and through-thickness directions. By considering both shear and normal deformation effects, the governing equations are derived and solved via FEM. A comprehensive study on the static, vibration and buckling behaviours of 1D, 2D and 3D-FG microplates is carried out. The verification is performed by comparing the numerical results with those from the MCST/MSGT. The effects of

material inhomogeneity, MLSPs, aspect ratio, gradient index, boundary conditions on the results are discussed.

2. Theoretical Formulation

A multi-directional FG microplate with its dimensions is illustrated in Fig. 1. $E, \rho \; and \; \nu$ are the Young's modulus, mass density and Poisson's ratio of the plate, respectively. The effective material properties of 3D-FG microplate can be described by:

$$P(x,y,z) = P_1 V_1(x,y,z) + P_2 V_2(x,y,z) \tag{1}$$

P_1 and P_2 indicate the material properties. V_1 and V_2 are the volume fractions of ceramic and metal and given by:

$$V_1(x,y,z) + V_2(x,y,z) = 1 \tag{2a}$$

$$V_1(z) = \left(\frac{x}{a}\right)^{p_x} \left(\frac{y}{b}\right)^{p_y} \left(\frac{1}{2} + \frac{z}{h}\right)^{p_z} \tag{2b}$$

where p_x, p_y and p_z are the associated gradient indexes in the *x*-, *y* and *z*-direction. It should be noted that the in-plane material inhomogeneity (2D-FG) is achieved by $p_z = 0$, while through-thickness one (1D-FG) is obtained by setting $p_x = p_y = 0$.

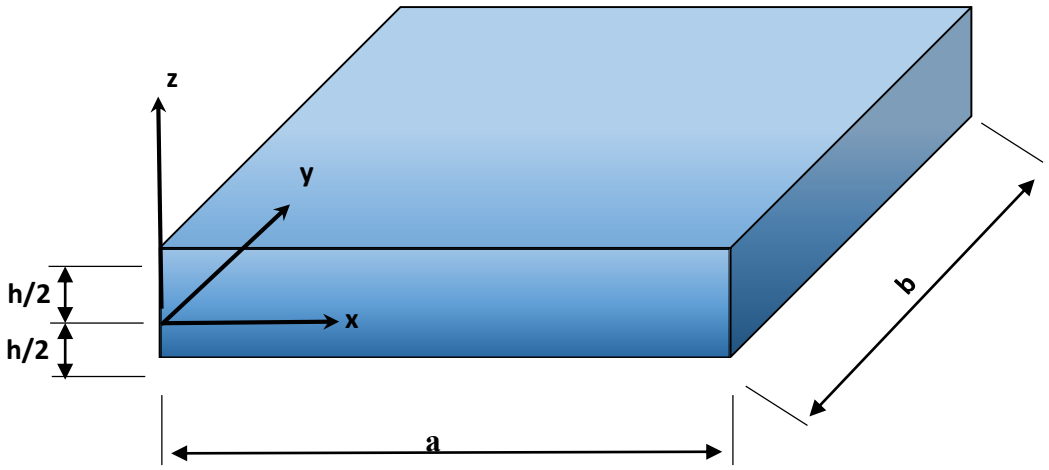

Figure 1. Multi-directional FG microplates with geometry and co-ordinate system

By using the Eqs. (1) and (2), the effective material properties can be obtained:

$$E(x,y,z) = (E_c - E_m)\left(\frac{x}{a}\right)^{p_x}\left(\frac{y}{b}\right)^{y}\left(\frac{1}{2}+\frac{z}{h}\right)^{p_z} + E_m \quad (3a)$$

$$\nu(x,y,z) = (\nu_c - \nu_m)\left(\frac{x}{a}\right)^{p_x}\left(\frac{y}{b}\right)^{y}\left(\frac{1}{2}+\frac{z}{h}\right)^{p_z} + \nu_m \quad (3b)$$

$$\rho(x,y,z) = (\rho_c - \rho_m)\left(\frac{x}{a}\right)^{p_x}\left(\frac{y}{b}\right)^{y}\left(\frac{1}{2}+\frac{z}{h}\right)^{p_z} + \rho_m \quad (3c)$$

By considering both shear and normal deformation effects, the following displacement field is used to investigate the structural responses of the multi-directional FG microplates [42]:

$$u_1(x,z,t) = U(x,y,z,t) = u(x,y,t) - \frac{4z^3}{3h^2}\frac{\partial w_b(x,y,t)}{\partial x} - \left(\frac{4z^3}{3h^2} - z\right)\frac{\partial w_s(x,y,t)}{\partial x}$$

$$= u - f_1 w_{b,x} - f_2 w_{s,x} \quad (4a)$$

$$u_2(x,z,t) = V(x,y,z,t) = v(x,y,t) - \frac{4z^3}{3h^2}\frac{\partial w_b(x,y,t)}{\partial y} - \left(\frac{4z^3}{3h^2} - z\right)\frac{\partial w_s(x,y,t)}{\partial y}$$

$$= v - f_1 w_{b,y} - f_2 w_{s,y} \quad (4b)$$

$$u_3(x,z,t) = W(x,y,z,t) = w_b(x,y,t) + w_s(x,y,t) + \left(1 - \frac{4z^2}{h^2}\right)w_z(x,y,t)$$

$$= w_b + w_s + f_3 w_z \quad (4c)$$

In the displacement field, the in-plane displacements are presented by u and v. Besides, the vertical displacement is given by three components, namely, bending, shear and normal deformations which are w_b, w_s and w_z ,respectively. f_1, f_2 and f_3 are the transverse shear and transverse normal strain shape function, respectively. If one sets $f_3 = 0$, the Third-order Shear Deformation Theory (TSDT) is obtained.

By using the MSGT [6], the strain energy ($\mathcal{U}$) of the multi-directional FG microplates can be expressed:

$$\mathcal{U} = \frac{1}{2}\int_V \left(\sigma_{ij}\varepsilon_{ij} + m_{ij}\chi_{ij} + \zeta_i\kappa_i + \tau_{ijk}\eta_{ijk}\right)d\mathcal{V}, \quad i,j,k = 1,2,3 \tag{5}$$

where σ_{ij} and ε_{ij} are the stress and strain tensors; m_{ij}, ζ_i and τ_{ijk} are the higher order stress tensors and χ_{ij}, κ_i and η_{ijk} are the symmetric curvature, dilatation gradient and deviatoric stretch gradient tensors, respectively.

Based on the displacement field (u_1, u_2, u_3), the strain tensors can be presented as follows:

$$\varepsilon_{ij} = \frac{1}{2}\left(\frac{\partial u_i}{\partial x_j} + \frac{\partial u_j}{\partial x_i}\right) \tag{6a}$$

$$\chi_{ij} = \frac{1}{4}\left(e_{imn}\frac{\partial^2 u_n}{\partial x_{mj}^2} + e_{jmn}\frac{\partial^2 u_n}{\partial x_{mi}^2}\right) \tag{6b}$$

$$\kappa_i = \frac{\partial \varepsilon_{mm}}{\partial x_i} \tag{6c}$$

$$\eta_{ijk} = \frac{1}{3}\left(\frac{\partial \varepsilon_{jk}}{\partial x_i} + \frac{\partial \varepsilon_{ki}}{\partial x_j} + \frac{\partial \varepsilon_{ij}}{\partial x_k}\right) - \frac{1}{15}\left[\delta_{ij}\left(\frac{\partial \varepsilon_{mm}}{\partial x_k} + 2\frac{\partial \varepsilon_{mk}}{\partial x_m}\right) + \delta_{jk}\left(\frac{\partial \varepsilon_{mm}}{\partial x_i} + 2\frac{\partial \varepsilon_{mi}}{\partial x_m}\right) + \delta_{ki}\left(\frac{\partial \varepsilon_{mm}}{\partial x_j} + 2\frac{\partial \varepsilon_{mj}}{\partial x_m}\right)\right] \tag{6d}$$

where e_{ijk} and δ_{ij} denote the permutation symbol and Kronecker delta, respectively.

Constitutive relations between stress and strain tensors:

$$\sigma_{ij} = \left(\frac{E(x,y,z)}{1+\nu(x,y,z)}\right)\varepsilon_{ij} + \left[\frac{\nu(x,y,z)E(x,y,z)}{(1+\nu(x,y,z))(1-2\nu(x,y,z))}\right]\varepsilon_{kk}\delta_{ij} \tag{7a}$$

$$m_{ij} = \left(\frac{E(x,y,z){\ell_1}^2}{1+\nu(x,y,z)}\right)\chi_{ij} \tag{7b}$$

$$\zeta_i = \left(\frac{E(x,y,z){\ell_2}^2}{1+\nu(x,y,z)}\right)\kappa_i \tag{7c}$$

$$\tau_{ijk} = \left(\frac{E(x,y,z){\ell_3}^2}{1+\nu(x,y,z)}\right)\eta_{ijk} \tag{7d}$$

where ℓ_1, ℓ_2 and ℓ_3 are the MLSPs related to the dilatation gradient, deviatoric stretch gradient and symmetric curvature, respectively. If one assigns $\ell_2 = \ell_3 = 0$, the MCST formulation is achieved.

The only nonzero strains can be obtained:

$$\varepsilon_{xx} = \frac{\partial U}{\partial x} = u_{,x} - f_1 w_{b,xx} - f_2 w_{s,xx} \tag{8a}$$

$$\varepsilon_{yy} = \frac{\partial V}{\partial y} = v_{,y} - f_1 w_{b,yy} - f_2 w_{s,yy} \tag{8b}$$

$$\varepsilon_{zz} = \frac{\partial W}{\partial z} = f_3{}' w_z \tag{8c}$$

$$\gamma_{xz} = \frac{\partial U}{\partial z} + \frac{\partial W}{\partial x} = (1 - f_1{}')\, w_{b,x} + (1 - f_2{}') w_{s,x} + f_3 w_{z,x} \tag{8d}$$

$$\gamma_{yz} = \frac{\partial V}{\partial z} + \frac{\partial W}{\partial y} = (1 - f_1{}')\, w_{b,y} + (1 - f_2{}') w_{s,y} + f_3 w_{z,y} \tag{8e}$$

$$\gamma_{xy} = \frac{\partial U}{\partial y} + \frac{\partial V}{\partial x} = u_{,y} + v_{,x} - 2 f_1 w_{b,xy} - 2 f_2 w_{s,xy} \tag{8f}$$

The components of the strain tensor associated with the higher order stress can be given by using Eq.(6):

$$\chi_{xx} = \frac{1}{2}\left[(1 + f_1{}')\, w_{b,xy} + (1 + f_2{}') w_{s,xy} + f_3 w_{z,xy}\right] \tag{9a}$$

$$\chi_{yy} = \frac{1}{2}\left[-(1 + f_1{}') w_{b,xy} - (1 + f_2{}') w_{s,xy} - f_3 w_{z,xy}\right] \tag{9b}$$

$$\chi_{xy} = \frac{1}{4}\left[(1 + f_1{}')\left(w_{b,yy} - w_{b,xx}\right) + (1 + f_2{}')\left(w_{s,yy} - w_{s,xx}\right) + f_3\left(w_{z,yy} - w_{z,xx}\right)\right] \tag{9c}$$

$$\chi_{yz} = \frac{1}{4}\left(-f_1{}'' w_{b,x} - f_2{}'' w_{s,x} - f_3{}' w_{z,x} + v_{,xy} - u_{,yy}\right) \tag{9d}$$

$$\chi_{xz} = \frac{1}{4}\left(f_1{}'' w_{b,y} + f_2{}'' w_{s,y} + f_3{}' w_{z,y} + v_{,xx} - u_{,xy}\right) \tag{9e}$$

$$\kappa_x = u_{,xx} + v_{,xy} - f_1 w_{b,xxx} - f_1 w_{b,xyy} - f_2 w_{s,xxx} - f_2 w_{s,xyy} + f_3{}' w_{z,x} \tag{9f}$$

$$\kappa_y = u_{,xy} + v_{,yy} - f_1 w_{b,xxy} - f_1 w_{b,yyy} - f_2 w_{s,xxy} - f_2 w_{s,yyy} + f_3{}' w_{z,y} \tag{9h}$$

$$\kappa_z = -f_1{}'w_{b,yy} - f_1{}'w_{b,xx} - f_2{}'w_{s,xx} - f_2{}'w_{s,yy} + f_3{}''w_z \tag{9g}$$

$$\eta_{xxx} = \frac{1}{5}\left[2u_{,xx} - u_{,yy} - 2v_{,xy} + f_1{}''w_{b,x} - 2f_1 w_{b,xxx} + 3f_1 w_{b,xyy} + f_2{}''w_{s,x} - 2f_2 w_{s,xxx} + 3f_2 w_{s,xyy} - 2f_3{}'w_{z,x}\right] \tag{9h}$$

$$\eta_{yyy} = \frac{1}{5}\left[-2u_{,xy} + 2v_{,yy} - v_{,xx} + f_1{}''w_{b,y} - 2f_1 w_{b,yyy} + 3f_1 w_{b,xxy} + f_2{}''w_{s,y} - 2f_2 w_{s,yyy} + 3f_2 w_{s,xxy} - 2f_3{}'w_{z,y}\right] \tag{9k}$$

$$\eta_{zzz} = \frac{1}{5}\left[(2f_1{}' - 1)w_{b,xx} + (2f_1{}' - 1)w_{b,yy} + (2f_2{}' - 1)w_{s,xx} + (2f_s{}' - 1)w_{s,yy} + 2f_3{}''w_z - f_3(w_{z,xx} + w_{z,yy})\right] \tag{9l}$$

$$\eta_{yyx} = \frac{1}{15}\left[4u_{,yy} - 3u_{,xx} + 8v_{,xy} + f_1{}''w_{b,x} + 3f_1 w_{b,xxx} - 12f_1 w_{b,xyy} + f_2{}''w_{s,x} + 3f_2 w_{s,xxx} - 12f_2 w_{s,xyy} - 2f_3{}'w_{z,x}\right] \tag{9m}$$

$$\eta_{zzx} = \frac{1}{15}\left[-3u_{,xx} - u_{,yy} - 2v_{,xy} - 4f_1{}''w_{b,x} + 3f_1 w_{b,xxx} + 3f_1 w_{b,xyy} - 4f_2{}''w_{s,x} + 3f_2 w_{s,xxx} + 3f_2 w_{s,xyy} + 8f_3{}'w_{z,x}\right] \tag{9n}$$

$$\eta_{xxy} = \frac{1}{15}\left[8u_{,xy} - 3v_{,yy} + 4v_{,xx} + f_1{}''w_{b,y} - 12f_1 w_{b,xxy} + 3f_1 w_{b,yyy} + f_2{}''w_{s,y} - 12f_2 w_{s,xxy} + 3f_2 w_{s,yyy} - 2f_3{}'w_{z,y}\right] \tag{9o}$$

$$\eta_{zzy} = \frac{1}{15}\left[-2u_{,xy} - 3v_{,yy} - v_{,xx} - 4f_1{}''w_{b,y} + 3f_1 w_{b,xxy} + 3f_1 w_{b,yyy} - 4f_2{}''w_{s,y} + 3f_2 w_{s,xxy} + 3f_2 w_{s,yyy} + 8f_3{}'w_{z,y}\right] \tag{9p}$$

$$\eta_{xxz} = \frac{1}{15}\left[(-8f_1{}' + 4)w_{b,xx} + (2f_1{}' - 1)w_{b,yy} + (-8f_2{}' + 4)w_{s,xx} + (2f_2{}' - 1)w_{s,yy} - 3f_3{}''w_z + 4f_3 w_{z,xx} - f_3 w_{z,yy}\right] \quad (9q)$$

$$\eta_{yyz} = \frac{1}{15}\left[(2f_1{}' - 1)w_{b,xx} + (-8f_1{}' + 4)w_{b,yy} + (2f_2{}' - 1)w_{s,xx} + (-8f_2{}' + 4)w_{s,yy} - 3f_3{}''w_z + 4f_3 w_{z,yy} - f_3 w_{z,xx}\right] \quad (9r)$$

$$\eta_{zzy} = \frac{1}{3}\left[(-2f_1{}' + 1)w_{b,xy} + (-2f_2{}' + 1)w_{s,xy} + f_3 w_{z,xy}\right] \quad (9s)$$

Constitutive relations between stress and strains of the multi-directional FG microplates:

$$\begin{Bmatrix}\sigma_{xx}\\ \sigma_{yy}\\ \sigma_{zz}\\ \sigma_{yz}\\ \sigma_{xz}\\ \sigma_{xy}\end{Bmatrix} = \begin{bmatrix} C_{11} & C_{12} & C_{13} & 0 & 0 & 0 \\ & C_{22} & C_{23} & 0 & 0 & 0 \\ & & C_{33} & 0 & 0 & 0 \\ & & & C_{44} & 0 & 0 \\ & & & & C_{55} & 0 \\ sym & & & & & C_{66} \end{bmatrix} \begin{Bmatrix}\varepsilon_{xx}\\ \varepsilon_{yy}\\ \varepsilon_{zz}\\ \gamma_{yz}\\ \gamma_{xz}\\ \gamma_{xy}\end{Bmatrix} \quad (10a)$$

$$\begin{Bmatrix}m_{xx}\\ m_{yy}\\ m_{yz}\\ m_{xz}\\ m_{xy}\end{Bmatrix} = \frac{E(x,y,z){\ell_1}^2}{1+\nu(x,y,z)} \begin{Bmatrix}\chi_{xx}\\ \chi_{yy}\\ \chi_{zy}\\ \chi_{xz}\\ \chi_{xy}\end{Bmatrix} \quad (10b)$$

$$\begin{Bmatrix}\zeta_x\\ \zeta_y\\ \zeta_z\end{Bmatrix} = \frac{E(x,y,z){\ell_2}^2}{1+\nu(x,y,z)} \begin{Bmatrix}\kappa_x\\ \kappa_y\\ \kappa_z\end{Bmatrix} \quad (10c)$$

$$\begin{Bmatrix}\tau_{xxx}\\ \tau_{yyy}\\ \tau_{zzz}\\ \tau_{yyx}\\ \tau_{zzx}\\ \tau_{xxy}\\ \tau_{zzy}\\ \tau_{xxz}\\ \tau_{yyz}\\ \tau_{xyz}\end{Bmatrix} = \frac{E(x,y,z){\ell_3}^2}{1+\nu(x,y,z)} \begin{Bmatrix}\eta_{xxx}\\ \eta_{yyy}\\ \eta_{zzz}\\ \eta_{yyx}\\ \eta_{zzx}\\ \eta_{xxy}\\ \eta_{zzy}\\ \eta_{xxz}\\ \eta_{yyz}\\ \eta_{xyz}\end{Bmatrix} \quad (10d)$$

where C_{ij} are given by:

$$C_{11}(x,y,z) = C_{22}(x,y,z) = C_{33}(x,y,z) = \frac{E(x,y,z)(1-v(x,y,z))}{(1-2v(x,y,z))(1+v(x,y,z))} \quad (11a)$$

$$C_{12}(x,y,z) = C_{13}(x,y,z) = C_{23}(x,y,z) = \frac{E(x,y,z)v(x,y,z)}{(1-2v(x,y,z))(1+v(x,y,z))} \quad (11b)$$

$$C_{44}(x,y,z) = C_{55}(x,y,z) = C_{66}(x,y,z) = \frac{E(x,y,z)}{2(1+v(x,y,z))} \quad (11c)$$

Based on the displacement field given in Eq. (4), the following expression of $\mathcal{U}$ can be derived:

$$\begin{aligned}\mathcal{U} = \frac{1}{2}\int_V \Big[& C_{11}\{\varepsilon_{xx}^2 + \varepsilon_{yy}^2 + \varepsilon_{zz}^2\} + 2C_{12}\{\varepsilon_{xx}\varepsilon_{yy} + \varepsilon_{yy}\varepsilon_{zz} + \varepsilon_{xx}\varepsilon_{zz}\} + C_{44}\{\gamma_{xy}^2 + \gamma_{xz}^2 + \gamma_{yz}^2\} \\ & + Q_\chi\{\chi_{xx}^2 + \chi_{yy}^2 + 2\chi_{xz}\chi_{xz} + 2\chi_{xy}\chi_{xy} + 2\chi_{zy}\chi_{zy}\} + Q_\gamma\{\gamma_x^2 + \gamma_y^2 + \gamma_z^2\} \\ & + Q_\eta\{{\eta_{xxx}}^2 + {\eta_{yyy}}^2 + {\eta_{zzz}}^2 + 3{\eta_{yyx}}^2 + 3{\eta_{zzx}}^2 + 3{\eta_{xxy}}^2 + 3{\eta_{zzy}}^2 + 3{\eta_{xxz}}^2 \\ & + 3{\eta_{yyz}}^2 + 6{\eta_{xyz}}^2\}\Big]\, dV \end{aligned} \quad (12)$$

where

$$Q_\chi = \frac{E(x,y,z){\ell_1}^2}{1+\nu(x,y,z)} \quad (13a)$$

$$Q_\gamma = \frac{E(x,y,z){\ell_2}^2}{1+\nu(x,y,z)} \quad (13b)$$

$$Q_\eta = \frac{E(x,y,z){\ell_3}^2}{1+\nu(x,y,z)} \quad (13c)$$

The kinetic energy (*K*) for the multi-directional FG microplates is then obtained as

$$K = \frac{1}{2}\int_V \rho\Big[\{(\dot{u})^2 + (f_1)^2(\dot{w}_{b,x})^2 + (f_2)^2(\dot{w}_{s,x})^2 - 2f_1\dot{u}\dot{w}_{b,x} - 2f_2\dot{u}\dot{w}_{s,x} + 2f_1f_2\dot{w}_{b,x}\dot{w}_{s,x}\}$$
$$+ \{(\dot{v})^2 + (f_1)^2(\dot{w}_{b,y})^2 + (f_2)^2(\dot{w}_{s,y})^2 - 2f_1\dot{v}\dot{w}_{b,y} - 2f_2\dot{v}\dot{w}_{s,y} + 2f_1f_2\dot{w}_{b,y}\dot{w}_{s,y}\}$$
$$+ \{(\dot{w}_b)^2 + (\dot{w}_s)^2 + (f_3)^2(\dot{w}_z)^2 + 2\dot{w}_b\dot{w}_s + 2f_3\dot{w}_b\dot{w}_z$$
$$+ 2f_3\dot{w}_s\dot{w}_z\}\Big]dV \qquad (14)$$

where an over dot denotes time derivative.

The potential energy (V) by the external forces can be given by:

$$V = -\frac{1}{2}\int_A \left[N_x\left\{\left(\frac{\partial w_b}{\partial x}\right)^2 + \left(\frac{\partial w_s}{\partial x}\right)^2 + \left(\frac{\partial w_z}{\partial x}\right)^2 + 2\frac{\partial w_b}{\partial x}\frac{\partial w_s}{\partial x} + 2\frac{\partial w_b}{\partial x}\frac{\partial w_z}{\partial x} + 2\frac{\partial w_s}{\partial x}\frac{\partial w_z}{\partial x} + \right\}\right.$$
$$+ N_y\left\{\left(\frac{\partial w_b}{\partial y}\right)^2 + \left(\frac{\partial w_s}{\partial y}\right)^2 + \left(\frac{\partial w_z}{\partial y}\right)^2 + 2\frac{\partial w_b}{\partial y}\frac{\partial w_s}{\partial y} + 2\frac{\partial w_b}{\partial y}\frac{\partial w_z}{\partial y} + 2\frac{\partial w_s}{\partial y}\frac{\partial w_z}{\partial y}\right\}$$
$$+ 2N_{xy}\left\{\frac{\partial w_b}{\partial x}\frac{\partial w_b}{\partial y} + \frac{\partial w_b}{\partial x}\frac{\partial w_s}{\partial y} + \frac{\partial w_b}{\partial y}\frac{\partial w_s}{\partial x} + \frac{\partial w_s}{\partial x}\frac{\partial w_s}{\partial y} + \frac{\partial w_b}{\partial x}\frac{\partial w_z}{\partial y} + \frac{\partial w_s}{\partial x}\frac{\partial w_z}{\partial y}\right.$$
$$\left.\left. + \frac{\partial w_z}{\partial x}\frac{\partial w_z}{\partial y} + \frac{\partial w_z}{\partial x}\frac{\partial w_b}{\partial y} + \frac{\partial w_z}{\partial x}\frac{\partial w_s}{\partial y}\right\}\right] dA - \int_A q(w_b + w_s + f_3(z)w_z)dA \qquad (15)$$

where q is the distributed load and N_x, N_y and N_{xy} can be described as in-plane loads. Three cases are considered for stability analysis including uniaxial load: $N_x = \gamma_1 N_0$ and biaxial loads: $N_x = \gamma_1 N_0$, $N_y = \gamma_2 N_0$ as well as shear load: $N_{xy} = \gamma_3 N_0$ where γ_1, γ_2 and γ_3 are the coefficients.

3. Strain Gradient FEM Formulation

By using the conforming shape functions, the displacement functions $u(x, y, t)$, $v(x, y, t)$, $w_b(x, y, t)$, $w_s(x, y, t)$ and $w_z(x, y, t)$ can be expressed via natural frequency (ω), nodal displacements ($u_j, v_j, w_{b\,j}, w_{s\,j}, w_{z_j}$) and interpolation functions (φ_j):

$$u(x,y,t) = \sum_{j=1}^{16} u_j \varphi_j(x,y) e^{i\omega t}, \tag{16a}$$

$$v(x,y,t) = \sum_{j=1}^{16} v_j \varphi_j(x,y) e^{i\omega t}, \tag{16b}$$

$$w_b(x,y,t) = \sum_{j=1}^{16} w_{b_j} \varphi_j(x,y) e^{i\omega t}, \tag{16c}$$

$$w_s(x,y,t) = \sum_{j=1}^{16} w_{s_j} \varphi_j(x,y) e^{i\omega t}, \tag{16d}$$

$$w_z(x,y,t) = \sum_{j=1}^{16} w_{z_j} \varphi_j(x,y) e^{i\omega t}, \tag{16e}$$

where

$$u_j = \left[u, u_{,x}, u_{,y}, u_{,xy}\right] \tag{17a}$$

$$v_j = \left[v, v_{,x}, v_{,y}, v_{,xy}\right] \tag{17b}$$

$$w_{b_j} = \left[w_b, w_{b,x}, w_{b,y}, w_{b,xy}\right] \tag{17c}$$

$$w_{s_j} = \left[w_s, w_{s,x}, w_{s,y}, w_{s,xy}\right] \tag{17d}$$

$$w_{z_j} = \left[w_z, w_{z,x}, w_{z,y}, w_{z,xy}\right] \tag{17e}$$

The interpolation functions for a conforming element can be given by using the natural coordinates (ξ, ϑ):

$$\varphi_j = \frac{1}{16}\left(\xi + \xi_j\right)^2 \left(\xi\xi_j - 2\right)\left(\vartheta + \vartheta_j\right)^2 \left(\vartheta\vartheta_j - 2\right), \qquad j = 1, 5, 9, 13 \tag{18a}$$

$$\varphi_j = \frac{1}{16}\xi_j\left(\xi + \xi_j\right)^2 \left(1 - \xi\xi_j\right)\left(\vartheta + \vartheta_j\right)^2 \left(\vartheta\vartheta_j - 2\right), \qquad j = 2, 6, 10, 14 \tag{18b}$$

$$\varphi_j = \frac{1}{16}\vartheta_j\left(\xi + \xi_j\right)^2 \left(\xi\xi_j - 2\right)\left(\vartheta + \vartheta_j\right)^2 \left(1 - \vartheta\vartheta_j\right), \qquad j = 3, 7, 11, 15 \tag{18c}$$

$$\varphi_j = \frac{1}{16}\xi_j\vartheta_j\left(\xi+\xi_j\right)^2\left(1-\xi\xi_j\right)\left(\vartheta+\vartheta_j\right)^2\left(1-\vartheta\vartheta_j\right), \qquad j=4,8,12,16 \tag{18d}$$

By using the Lagrange's equations, governing equations for static, vibration and buckling analysis can be obtained through total energy functional (Π):

$$\Pi = U + V - K \tag{19a}$$

$$\frac{\partial \Pi}{\partial q_j} - \frac{\partial}{\partial t}\left(\frac{\partial \Pi}{\partial \dot{q}_j}\right) = 0 \tag{19b}$$

where q_j representing the values of $(u_j, v_j, w_{b\,j}, w_{s\,j}, w_{z_j})$.

Eq. (19) leads to the following equation, which uses to determine the displacements, frequencies and buckling loads:

$$\left(\begin{bmatrix} [K_{11}] & [K_{12}] & [K_{13}] & [K_{14}] & [K_{15}] \\ [K_{12}]^T & [K_{22}] & [K_{23}] & [K_{24}] & [K_{25}] \\ [K_{13}]^T & [K_{23}]^T & [K_{33}] & [K_{34}] & [K_{35}] \\ [K_{14}]^T & [K_{24}]^T & [K_{34}]^T & [K_{44}] & [K_{45}] \\ [K_{15}]^T & [K_{25}]^T & [K_{35}]^T & [K_{45}]^T & [K_{55}] \end{bmatrix} - N_0 \begin{bmatrix} [0] & [0] & [0] & [0] & [0] \\ [0]^T & [0] & [0] & [0] & [0] \\ [0]^T & [0]^T & [G_{33}] & [G_{34}] & [G_{35}] \\ [0]^T & [0]^T & [G_{34}]^T & [G_{44}] & [G_{45}] \\ [0]^T & [0]^T & [G_{35}]^T & [G_{45}]^T & [G_{55}] \end{bmatrix}\right.$$

$$\left. - \omega^2 \begin{bmatrix} [M_{11}] & [M_{12}] & [M_{13}] & [M_{14}] & [M_{15}] \\ [M_{12}]^T & [M_{22}] & [M_{23}] & [M_{24}] & [M_{25}] \\ [M_{13}]^T & [M_{23}]^T & [M_{33}] & [M_{34}] & [M_{35}] \\ [M_{14}]^T & [M_{24}]^T & [M_{34}]^T & [M_{44}] & [M_{45}] \\ [M_{15}]^T & [M_{25}]^T & [M_{35}]^T & [M_{45}]^T & [M_{55}] \end{bmatrix} \begin{Bmatrix} \{u_j\} \\ \{v_j\} \\ \{w_{b\,j}\} \\ \{w_{s\,j}\} \\ \{w_{z\,j}\} \end{Bmatrix} \right) = \begin{Bmatrix} \{0\} \\ \{0\} \\ \{F_3\} \\ \{F_4\} \\ \{0\} \end{Bmatrix} \tag{20}$$

where $[K_{kl}]$, $[M_{kl}]$ and $[G_{kl}]$ are the stiffness, mass and geometric stiffness matrices and F_k is the nodal force vector, respectively.

Nine BCs are considered in Fig. 2 and given below:

Simply Supported (S):

$$u = v = w_b = w_{b,y} = \ w_s = w_{s,y} = w_z = w_{z,y} = 0 \ at \ x = 0 \ and \ x = a$$

$$u = v = w_b = w_{b,x} = \ w_s = w_{s,x} = w_z = w_{z,x} = 0 \ at \ y = 0 \ and \ y = a$$

Clamped (C):

$$u = v = w_b = w_{b,x} = w_{b,y} = \ w_s = w_{s,x} = w_{s,y} = w_z = w_{z,x} = w_{z,y} = 0 \ at \ x = 0, a \ and \ y = 0, a$$

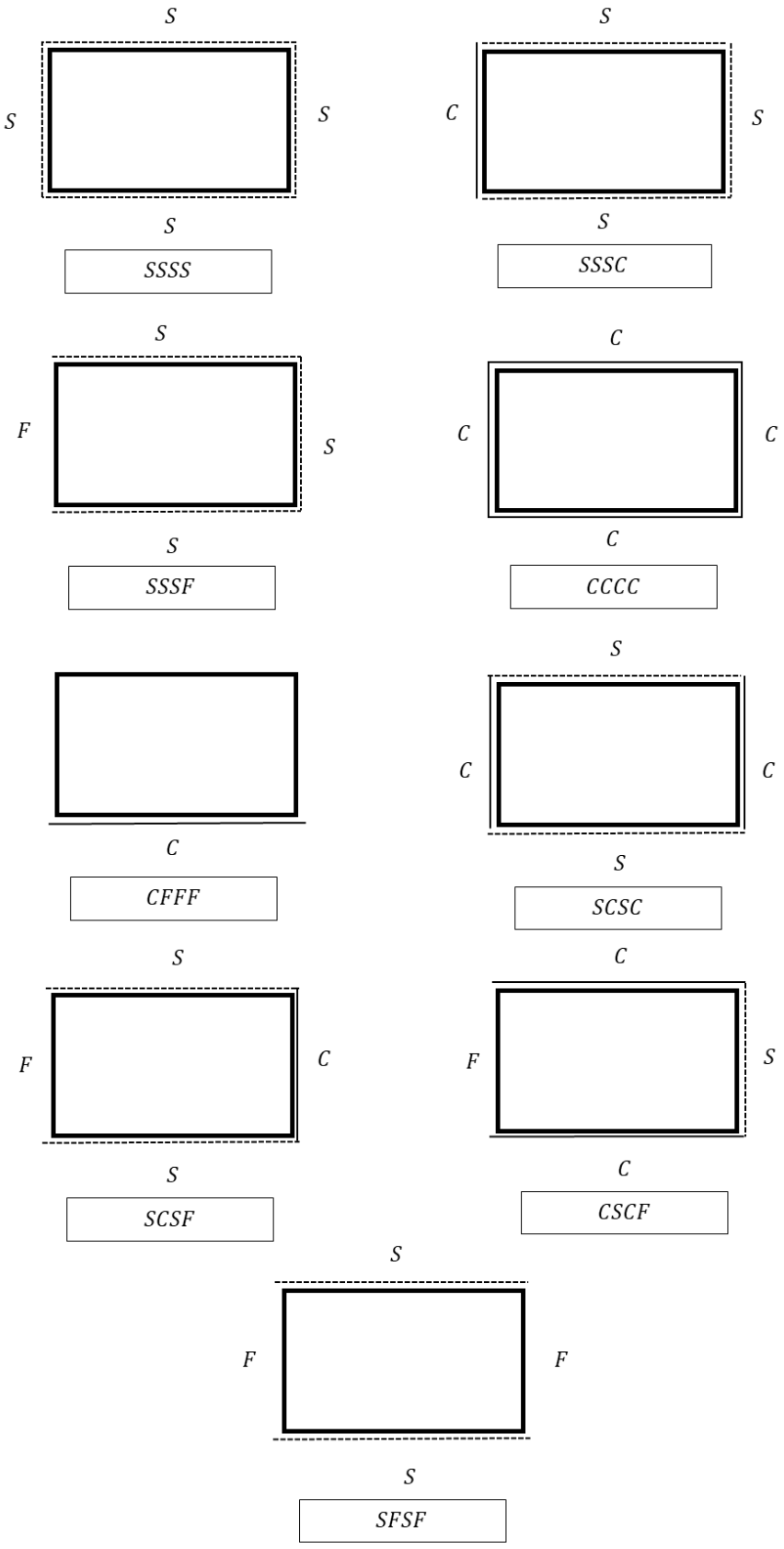

Figure 2. Boundary conditions (BCs) for the multi-directional FG microplates

4. Numerical Examples

In this section, a comprehensive study on the structural analysis of 1D, 2D, and 3D-FG microplates made of Al/Al_2O_3 is presented to illustrate convergence and validate the accuracy of the proposed strain gradient FEM model. Material properties are given by (Al: $E_m = 70\ GPa$, $\nu_m = 0.3$, $\rho_m = 2702\ kg/m^3$; Al_2O_3: $E_c = 380\ GPa$, $\nu_c = 0.3$, $\rho_c = 3800\ kg/m^3$). Nine boundary conditions (BCs) given in Fig. 2 are considered. All three MLSPs have the same value $\ell = \ell_1 = \ell_2 = \ell_3 = 15\ \mu m$. The following non-dimensional frequencies, buckling load and displacement parameters are used:

$$\text{DFF: } \lambda = \frac{\omega a^2}{h}\sqrt{\frac{\rho_c}{E_c}} \tag{21a}$$

$$\text{DCBL: } N_{cr} = N_0\frac{a^2}{E_m h^3} \tag{21b}$$

$$\text{DCD: } \overline{w} = w\frac{10E_c h^3}{qa^4} \tag{21c}$$

4.1 Convergence study

A SUS304/Si_3N_4 2D-FG plates with various BCs (SSSS, CCCC, SCSF and SSSC) are considered to study the convergence characteristics of the present solution method. The material properties are given by (SUS304: $E_m = 201.04\ GPa$, $\nu_m = 0.3262$, $\rho_m = 8166\ kg/m^3$; Si_3N_4: $E_c = 348.43\ GPa$, $\nu_c = 0.24$, $\rho_c = 2370\ kg/m^3$). The results are obtained in Tables 1 and 2 by using various uniform mesh sizes (4x4, 6x6, 8x8 and 10x10). It can be seen that they converge gradually with increase in number of elements and they are in excellent agreement with open literature [56, 57], who used IGA-RPT ($\varepsilon_z = 0$). It is also observed that the present theory associated with the normal deformation effect produces results which are slightly different from ones without it. The mesh size (10x10) is used in the following numerical examples.

Table 1. Convergence study on the DFFs $\left(\Omega = \omega \frac{a^2}{\pi^2}\sqrt{\frac{\rho_c h}{D_c}}\right)$ and DCBLs $\left(N_{cr} = N_0 \frac{a^2}{\pi^2 D_c}\right)$ of the SUS304/Si_3N_4 2D-FG square plates for various BCs, p_x and p_y. $(a/h = 10,\ D_c = \frac{E_c h^3}{12(1-\nu_c^2)})$

BCs	Theory	Number of Element	p_y	p_x			
				0	0.5	1	2
DFF							
SSSC	Present - $\varepsilon_z \neq 0$	4x4	0	2.2993	1.5837	1.3430	1.1602
		6x6		2.3051	1.5869	1.3452	1.1615
		8x8		2.3054	1.5866	1.3446	1.1606
		10x10		2.3049	1.5859	1.3438	1.1597
	IGA - RPT ([57])			2.2824	1.5657	1.3269	1.1448
	Present - $\varepsilon_z \neq 0$	4x4	0.5	1.5360	1.3010	1.1895	1.0890
		6x6		1.5393	1.3036	1.1914	1.0902
		8x8		1.5395	1.3034	1.1910	1.0894
		10x10		1.5392	1.3028	1.1903	1.0886
	IGA - RPT ([57])			1.5255	1.2882	1.1761	1.0744
	Present - $\varepsilon_z \neq 0$	4x4	1	1.3010	1.1792	1.1147	1.0516
		6x6		1.3037	1.1815	1.1165	1.0527
		8x8		1.3038	1.1813	1.1160	1.0520
		10x10		1.3036	1.1808	1.1154	1.0512
	IGA - RPT ([57])			1.2945	1.1695	1.1032	1.038
	Present - $\varepsilon_z \neq 0$	4x4	2	1.1311	1.0773	1.0470	1.0155
		6x6		1.1334	1.0793	1.0486	1.0165
		8x8		1.1335	1.0791	1.0482	1.0158
		10x10		1.1333	1.0787	1.0476	1.0150
	IGA - RPT ([57])			1.1265	1.0693	1.0368	1.0026
DCBL							
SCSF (1, 1, 0)	Present - $\varepsilon_z \neq 0$	4x4	0	0.9515	0.8640	0.8074	0.7353
		6x6		1.0692	0.9729	0.9135	0.8397
		8x8		1.1116	1.0106	0.9499	0.8758
		10x10		1.1313	1.0278	0.9663	0.8921
	IGA - RPT ([57])			1.1288	1.0231	0.9627	0.8905
	Present - $\varepsilon_z \neq 0$	4x4	0.5	0.7747	0.7280	0.6965	0.6551
		6x6		0.8743	0.8230	0.7898	0.7471
		8x8		0.9115	0.8576	0.8236	0.7805
		10x10		0.9291	0.8738	0.8393	0.7960
	IGA - RPT ([57])			0.9256	0.8694	0.8356	0.7936
		4x4	1	0.7045	0.6719	0.6497	0.6202
		6x6		0.7938	0.7583	0.7351	0.7049
		8x8		0.8271	0.7900	0.7663	0.7360
	Present - $\varepsilon_z \neq 0$	10x10		0.8429	0.8049	0.7809	0.7505
	IGA - RPT ([57])			0.8394	0.8007	0.7772	0.7477
	Present - $\varepsilon_z \neq 0$	4x4	2	0.6435	0.6224	0.6078	0.5882
		6x6		0.7227	0.7002	0.6853	0.6658
		8x8		0.7520	0.7288	0.7138	0.6944
		10x10		0.7659	0.7422	0.7271	0.7077
	IGA - RPT ([57])			0.7615	0.7374	0.7227	0.7041

Table 2. Convergence study on the DCDs $\left(\overline{w} = w\frac{h^2 E_c}{q_0 a^3}\right)$ of the SUS304/Si_3N_4 2D-FG square plates subjected to sinusoidally distributed load for various BCs, p_x and p_y $(a/h = 5)$

BCs	Theory	Number of Element	p_y	p_x			
				0	0.5	1	2
SSSS	Present - $\varepsilon_z \neq 0$	4x4	0	0.1726	0.2034	0.2219	0.2434
		6x6		0.1723	0.2031	0.2215	0.2430
		8x8		0.1723	0.2031	0.2215	0.2429
		10x10		0.1723	0.2030	0.2215	0.2429
	IGA - RPT ([56])	-		0.1752	0.2075	0.2264	0.2485
	Present - $\varepsilon_z \neq 0$	4x4	0.5	0.2035	0.2274	0.2414	0.2572
		6x6		0.2031	0.2270	0.2410	0.2568
		8x8		0.2031	0.2270	0.2409	0.2567
		10x10		0.2030	0.2270	0.2409	0.2567
	IGA - RPT ([56])	-		0.2075	0.2324	0.2467	0.2628
	Present - $\varepsilon_z \neq 0$	4x4	1	0.2219	0.2414	0.2524	0.2646
		6x6		0.2215	0.2410	0.2520	0.2641
		8x8		0.2215	0.2409	0.2519	0.2640
		10x10		0.2215	0.2409	0.2519	0.2640
	IGA - RPT ([56])	-		0.2264	0.2467	0.2579	0.2703
	Present - $\varepsilon_z \neq 0$	4x4	2	0.2434	0.2572	0.2645	0.2724
		6x6		0.2430	0.2567	0.2641	0.2719
		8x8		0.2429	0.2567	0.2640	0.2718
		10x10		0.2429	0.2567	0.2640	0.2718
	IGA - RPT ([56])	-		0.2485	0.2628	0.2703	0.2783
CCCC	Present - $\varepsilon_z \neq 0$	4x4	0	0.0791	0.0930	0.1016	0.1118
		6x6		0.0782	0.0922	0.1008	0.1110
		8x8		0.0783	0.0923	0.1010	0.1113
		10x10		0.0784	0.0925	0.1012	0.1115
	IGA - RPT ([56])	-		0.0823	0.0983	0.1079	0.1191
	Present - $\varepsilon_z \neq 0$	4x4	0.5	0.0930	0.1038	0.1102	0.1176
		6x6		0.0922	0.1030	0.1095	0.1169
		8x8		0.0923	0.1033	0.1098	0.1173
		10x10		0.0925	0.1035	0.1101	0.1175
	IGA - RPT ([56])	-		0.0983	0.1108	0.1179	0.1259
	Present - $\varepsilon_z \neq 0$	4x4	1	0.1016	0.1102	0.1153	0.1210
		6x6		0.1008	0.1095	0.1146	0.1203
		8x8		0.1010	0.1098	0.1150	0.1207
		10x10		0.1012	0.1101	0.1153	0.1210
	IGA - RPT ([56])	-		0.1079	0.1179	0.1235	0.1298
	Present - $\varepsilon_z \neq 0$	4x4	2	0.1118	0.1176	0.1210	0.1247
		6x6		0.1110	0.1169	0.1203	0.1241
		8x8		0.1113	0.1173	0.1207	0.1246
		10x10		0.1115	0.1175	0.1210	0.1249
	IGA - RPT ([56])	-		0.1191	0.1259	0.1298	0.1341

4.2 1D FG microplates

Since the DCDs, DFFs and DCBLs of the FG square microplates using a quasi-3D shear deformation theory and MSGT are not available in the open literature, verification is carried out with some authors using the RPT [21, 29] and TSDT [26]. In Tables 3-6, the results of Al/Al_2O_3 FG microplates are calculated for four different BCs, namely, SSSS, CCCC, SCSC and SFSF for various a/h, p_z and h/ℓ ratios. The obtained results are compared with those available using IGA and analytical solutions. It should be noted that these available results are again limited to $\varepsilon_z = 0$. The normal deformation effect can be easily detected, especially for $h/\ell = 5$. Even the strong size effect is considered, the present results still show very good agreement with those from previous studies. It is also observed that the results from the present quasi-3D (Q3D) shear deformation theory overestimate the displacements and underestimate buckling loads and frequencies of the FG microplates. It means that softening behaviours are observed using the present size-dependent theory. It can be concluded that the strain gradient FEM model of the FG square microplates is verified.

Some new results for various BCs (SSSC, CSCF, SCSF, SSSF and CFFF), a/h, p_z and h/ℓ are presented in Tables 7-9 for the first time. DCDs are computed for the FG microplates subjected to uniformly distributed load. The bifurcation buckling analysis are carried for uniaxial, biaxial and shear buckling loadings. These computed results can be used in the future studies for benchmark.

Table 3. Verification studies for the DCDs of the Al/Al_2O_3 FG square microplates subjected to sinusoidally distributed load for various BCs, a/h, h/ℓ and p_z

a/h	h/ℓ	Theory	SSSS			CCCC			SCSC			SFSF		
			p_z =1	2	10	p_z =1	2	10	p_z =1	2	10	p_z =1	2	10
5	10	IGA – TSDT ([26])	0.5709	0.7379	1.0668	0.2603	0.3383	0.5214	0.3498	0.4539	0.6892	1.3833	1.7837	2.5108
		IGA – RPT ([29])	0.5670	0.7332	1.0609	0.2523	0.3284	0.5071	-	-	-	-	-	-
		Present - $\varepsilon_z \neq 0$	0.5272	0.6803	1.0115	0.2326	0.3009	0.4732	0.3055	0.4022	0.6533	1.2907	1.6687	2.5558
	5	IGA – TSDT ([26])	0.3977	0.5107	0.7678	0.1774	0.2267	0.3505	0.2393	0.3058	0.4703	0.9564	1.2306	1.8256
		IGA – RPT ([29])	0.3908	0.5021	0.7548	0.1704	0.2183	0.3378	-	-	-	-	-	-
		Present - $\varepsilon_z \neq 0$	0.3690	0.4736	0.7205	0.1612	0.2050	0.3202	0.2137	0.2770	0.4560	0.9029	1.1652	1.8483
	2	IGA – TSDT ([26])	0.1286	0.1627	0.2614	0.0559	0.0693	0.1081	0.0758	0.0942	0.1483	0.3058	0.3905	0.6311
		IGA – RPT ([29])	0.1252	0.1580	0.2510	0.0537	0.0663	0.1019	-	-	-	-	-	-
		Present - $\varepsilon_z \neq 0$	0.1243	0.1569	0.2514	0.0536	0.0659	0.1029	0.0718	0.0900	0.1523	0.3058	0.3902	0.6633
	1	IGA – TSDT ([26])	0.0378	0.0475	0.0781	0.0163	0.0200	0.0313	0.0222	0.0272	0.0432	0.0896	0.1138	0.1895
		IGA – RPT ([29])	0.0369	0.0460	0.0743	0.0158	0.0192	0.0292	-	-	-	-	-	-
		Present - $\varepsilon_z \neq 0$	0.0372	0.0465	0.0763	0.0160	0.0194	0.0304	0.0215	0.0265	0.0453	0.0917	0.1163	0.2031
10	10	IGA – TSDT ([26])	-	-	-	0.1951	0.2517	0.3582	0.2724	0.3513	0.4961	1.2851	1.6518	2.2577
		IGA – RPT ([29])	0.5004	0.6439	0.8879	0.1915	0.2472	0.3510	-	-	-	-	-	-
		Present - $\varepsilon_z \neq 0$	0.4638	0.5946	0.8293	0.1738	0.2221	0.3214	0.2435	0.3144	0.4797	1.1979	1.5371	2.2955
	5	IGA – TSDT ([26])	-	-	-	0.1349	0.1733	0.2584	0.1886	0.2425	0.3604	0.8861	1.1408	1.6705
		IGA – RPT ([29])	0.3453	0.4446	0.6535	0.1318	0.1694	0.2523	-	-	-	-	-	-
		Present - $\varepsilon_z \neq 0$	0.3230	0.4153	0.6080	0.1216	0.1551	0.2321	0.1702	0.2195	0.3465	0.8319	1.0713	1.6705
	2	IGA – TSDT ([26])	-	-	-	0.0430	0.0547	0.0884	0.0602	0.0768	0.1246	0.2801	0.361	0.5938
		IGA – RPT ([29])	0.1095	0.1407	0.2298	0.0419	0.0532	0.0854	-	-	-	-	-	-
		Present - $\varepsilon_z \neq 0$	0.1083	0.1392	0.2258	0.0409	0.0517	0.0833	0.0572	0.0732	0.1240	0.2779	0.3583	0.6099
	1	IGA – TSDT ([26])	-	-	-	0.0126	0.0159	0.0265	0.0176	0.0223	0.0375	0.0815	0.1050	0.1800
		IGA – RPT ([29])	0.0320	0.0409	0.0694	0.0123	0.0155	0.0254	-	-	-	-	-	-
		Present - $\varepsilon_z \neq 0$	0.0323	0.0414	0.0702	0.0122	0.0154	0.0256	0.0171	0.0217	0.0379	0.0828	0.1067	0.1881

Table 4. Verification studies on the DFFs of Al/Al_2O_3 FG square microplates for various BCs, $a/h, h/\ell$ and p_z

a/h	h/ℓ	Theory	SSSS			CCCC			SCSC			SFSF		
			p_z =1	2	10	p_z =1	2	10	p_z =1	2	10	p_z =1	2	10
5	10	IGA – TSDT ([26])	0.1766	0.1596	0.1394	0.2805	0.2530	0.2133	0.2339	0.2111	0.1795	0.0908	0.0823	0.0727
		IGA – RPT ([29])	0.1772	0.1601	0.1397	-	-	-	-	-	-	-	-	-
		Present - $\varepsilon_z \neq 0$	0.1834	0.1660	0.1440	0.2952	0.2662	0.2231	0.2516	0.2273	0.1930	0.0986	0.0920	0.0780
	5	IGA – TSDT ([26])	0.2118	0.1920	0.1642	0.3414	0.3107	0.2617	0.2836	0.2579	0.2179	0.1096	0.0993	0.0854
		IGA – RPT ([29])	0.2136	0.1935	0.1655	-	-	-	-	-	-	-	-	-
		Present - $\varepsilon_z \neq 0$	0.2197	0.1992	0.1705	0.3555	0.3234	0.2720	0.3016	0.2741	0.2318	0.1169	0.1084	0.0908
	2	IGA – TSDT ([26])	0.3729	0.3402	0.2807	0.6122	0.5655	0.4739	0.5058	0.4657	0.3883	0.1947	0.1769	0.1454
		IGA – RPT ([29])	0.3778	0.3449	0.2861	-	-	-	-	-	-	-	-	-
		Present - $\varepsilon_z \neq 0$	0.3792	0.3465	0.2875	0.6202	0.5737	0.4814	0.5220	0.4806	0.4015	0.1978	0.1818	0.1481
	1	IGA – TSDT ([26])	0.6867	0.6266	0.5111	1.1357	1.0553	0.8819	0.9396	0.8666	0.7231	0.3600	0.3277	0.2652
		IGA – RPT ([29])	0.6948	0.6360	0.5230	-	-	-	-	-	-	-	-	-
		Present - $\varepsilon_z \neq 0$	0.6933	0.6251	0.5198	1.1396	1.0615	0.8398	0.9592	0.8700	0.6860	0.3576	0.3212	0.2545
10	10	IGA – TSDT ([26])	0.0478	0.0434	0.0387	0.0828	0.0749	0.0656	0.0676	0.0612	0.0539	0.0237	0.0215	0.0193
		IGA – RPT ([29])	0.0479	0.0435	0.0387	-	-	-	-	-	-	-	-	-
		Present - $\varepsilon_z \neq 0$	0.0498	0.0452	0.0399	0.0873	0.0792	0.0691	0.0717	0.0651	0.0572	0.0258	0.0242	0.0207
	5	IGA – TSDT ([26])	0.0573	0.0520	0.0449	0.0996	0.0904	0.0774	0.0813	0.0737	0.0633	0.0286	0.0260	0.0225
		IGA – RPT ([29])	0.0577	0.0523	0.0451	-	-	-	-	-	-	-	-	-
		Present - $\varepsilon_z \neq 0$	0.0597	0.0541	0.0466	0.1044	0.0948	0.0814	0.0858	0.0779	0.0671	0.0306	0.0285	0.0240
	2	IGA – TSDT ([26])	0.1013	0.0918	0.0750	0.1764	0.1610	0.1327	0.1439	0.1311	0.1078	0.0511	0.0463	0.0378
		IGA – RPT ([29])	0.1024	0.0930	0.0761	-	-	-	-	-	-	-	-	-
		Present - $\varepsilon_z \neq 0$	0.1030	0.0935	0.0766	0.1804	0.1647	0.1364	0.1482	0.1349	0.1113	0.0521	0.0477	0.0386
	1	IGA – TSDT ([26])	0.1873	0.1698	0.1359	0.3263	0.2986	0.2428	0.2662	0.2431	0.1966	0.0948	0.0859	0.0686
		IGA – RPT ([29])	0.1896	0.1722	0.1384	-	-	-	-	-	-	-	-	-
		Present - $\varepsilon_z \neq 0$	0.1888	0.1714	0.1376	0.3305	0.3025	0.2464	0.2713	0.2474	0.2004	0.0948	0.0862	0.0687

Table 5. Verification studies on the DCBLs $(\gamma_1, \gamma_2, \gamma_3)$ of SSSS Al/Al_2O_3 FG square microplates for various $a/h, h/\ell$ and p_z

a/h	h/ℓ	Theory	$(\gamma_1 = 1, \gamma_2 = 0, \gamma_3 = 0)$				$(\gamma_1 = 1, \gamma_2 = 1, \gamma_3 = 0)$			
			p_z =1	2	5	10	p_z =1	2	5	10
5	10	Navier – RPT ([21])	9.7211	7.5208	5.9295	5.2075	4.8605	3.7604	2.9647	2.6038
		IGA – TSDT ([26])	9.6338	7.4530	5.8718	5.1551	4.8169	3.7265	2.9359	2.5775
		IGA – RPT ([29])	9.7001	7.5009	5.9051	5.1838	4.8500	3.7504	2.9525	2.5919
		Present - $\varepsilon_z \neq 0$	10.2353	7.8727	5.9958	5.0104	5.1180	3.9367	2.9982	2.5054
	5	Navier – RPT ([21])	14.1785	11.0452	8.5527	7.3746	7.0893	5.5226	4.2764	3.6873
		IGA – TSDT ([26])	13.8259	10.7648	8.3136	7.1586	6.9129	5.3824	4.1568	3.5793
		IGA – RPT ([29])	14.0645	10.9449	8.4499	7.2790	7.0323	5.4725	4.2250	3.6395
		Present - $\varepsilon_z \neq 0$	14.7419	11.4080	8.6245	7.0902	7.3712	5.7043	4.3124	3.5453
	1	Navier – RPT ([21])	154.2099	123.1490	92.0898	75.9013	77.1050	61.5745	46.0450	37.9506
		IGA – TSDT ([26])	145.1577	115.5208	85.6764	70.2680	72.5812	57.7620	42.8394	35.1350
		IGA – RPT ([29])	148.6460	119.0692	89.4137	73.7216	74.3253	59.5363	44.7082	36.8621
		Present - $\varepsilon_z \neq 0$	147.1293	117.3357	86.6470	68.0471	73.5667	58.6695	43.3246	34.0245
10	10	Navier – RPT ([21])	10.9968	8.5479	6.9549	6.2026	5.4984	4.2740	3.4774	3.1013
		IGA – TSDT ([26])	10.9375	8.4979	6.9131	6.1674	5.4688	4.2490	3.4565	3.0837
		IGA – RPT ([29])	10.9906	8.5419	6.9468	6.1945	5.4953	4.2710	3.4734	3.0972
		Present - $\varepsilon_z \neq 0$	11.7985	9.2050	7.4511	6.5948	5.8995	4.6026	3.7257	3.2976
	5	Navier – RPT ([21])	15.9590	12.4000	9.7100	8.4445	7.9795	6.2000	4.8550	4.2222
		IGA – TSDT ([26])	15.7204	12.1985	9.5425	8.3032	7.8602	6.0993	4.7712	4.1516
		IGA – RPT ([29])	15.9260	12.3708	9.6789	8.4150	7.9630	6.1854	4.8395	4.2075
		Present - $\varepsilon_z \neq 0$	16.9789	13.2060	10.3663	9.0166	8.4897	6.6032	5.1833	4.5084
	1	Navier – RPT ([21])	173.7865	135.4673	97.6728	79.7717	86.8932	67.7337	48.8364	39.8858
		IGA – TSDT ([26])	167.6943	130.3251	93.4952	76.2541	83.8473	65.1626	46.7476	38.1271
		IGA – RPT ([29])	171.9637	134.2383	96.9802	79.2302	85.9820	67.1192	48.4902	39.6151
		Present - $\varepsilon_z \neq 0$	170.1274	132.6443	95.7409	78.2450	85.0655	66.3235	47.8713	39.1232

Table 6. Verification studies on the DCBLs ($\gamma_1 = 1, \gamma_2 = 1, \gamma_3 = 0$) of Al/Al_2O_3 FG square microplates for various BCs, a/h, h/ℓ and p_z

BCs	h/ℓ	Theory	$a/h = 5$				$a/h = 10$			
			p_z =1	2	5	10	p_z =1	2	5	10
CCCC	10	IGA – TSDT ([26])	10.0195	7.7033	5.8049	4.9931	13.3681	10.3593	8.2536	7.2866
		Present - $\varepsilon_z \neq 0$	10.6891	8.2193	6.1133	5.1435	14.5732	11.3262	8.9741	7.7788
	5	IGA – TSDT ([26])	14.6224	11.4380	8.6877	7.3912	19.2892	15.0090	11.6489	10.0669
		Present - $\varepsilon_z \neq 0$	15.4782	12.0940	9.1209	7.6262	20.9136	16.2835	12.6585	10.8313
	2	IGA – TSDT ([26])	46.2244	37.3139	28.7174	23.9520	60.2751	47.3980	35.3088	29.3375
		Present - $\varepsilon_z \neq 0$	46.7248	37.8127	29.0612	23.9076	62.2595	48.9942	36.6495	30.3543
	1	IGA – TSDT ([26])	158.2961	129.4025	100.0113	82.7755	205.9116	162.8077	119.6213	97.9102
		Present - $\varepsilon_z \neq 0$	157.2106	129.0896	99.6593	81.3716	208.5288	165.0517	121.4706	99.1111
SCSC	10	IGA – TSDT ([26])	7.7207	5.9489	4.5337	3.9175	9.8829	7.6662	6.1422	5.4356
		Present - $\varepsilon_z \neq 0$	8.5555	6.5987	4.9961	4.2380	10.9106	8.4920	6.7981	5.9891
	5	IGA – TSDT ([26])	11.2293	8.7862	6.7019	5.7108	14.2540	11.0923	8.6285	7.4639
		Present - $\varepsilon_z \neq 0$	12.3229	9.6186	7.3147	6.1542	15.6529	12.1823	9.5192	8.2540
	2	IGA – TSDT ([26])	35.3135	28.4258	21.7214	18.0594	44.5632	34.9766	25.9432	21.5220
		Present - $\varepsilon_z \neq 0$	36.8137	29.5955	22.5955	18.6202	46.6746	36.5684	27.2445	22.7191
	1	IGA – TSDT ([26])	120.7061	98.3027	75.1539	61.9117	152.3305	120.0884	87.6253	71.5538
		Present - $\varepsilon_z \neq 0$	123.3254	100.4291	76.6500	62.5715	156.5403	123.1277	89.9437	73.6807
SFSF	10	IGA – TSDT ([26])	2.4376	1.8914	1.5183	1.3451	2.6119	2.0317	1.6607	1.4846
		Present - $\varepsilon_z \neq 0$	2.8454	2.3388	1.8373	1.5344	3.0617	2.5362	2.0316	1.7032
	5	IGA – TSDT ([26])	3.5659	2.7714	2.1546	1.8657	3.8161	2.9628	2.3205	2.0195
		Present - $\varepsilon_z \neq 0$	4.0281	3.2736	2.5225	2.0907	4.3419	3.5389	2.7511	2.2846
	2	IGA – TSDT ([26])	11.3053	8.8367	6.5469	5.4432	12.1872	9.4445	6.9127	5.7355
		Present - $\varepsilon_z \neq 0$	11.6654	9.2993	6.8983	5.6375	12.6934	10.0284	7.3601	6.0082
	1	IGA – TSDT ([26])	38.7359	30.3991	22.1888	18.1692	42.0090	32.5562	23.2915	18.9829
		Present - $\varepsilon_z \neq 0$	38.5538	30.5236	22.2509	18.0775	42.1839	32.9060	23.5595	19.0977

Table 7. DCDs and DFFs of the Al/Al_2O_3 FG square microplates subjected to uniformly distributed load for various BCs, a/h, h/ℓ and p_z

BCs	h/ℓ	DCD								DFF							
		$a/h=5$				$a/h=10$				$a/h=5$				$a/h=10$			
		p_z =1	2	5	10	p_z =1	2	5	10	p_z =1	2	5	10	p_z =1	2	5	10
SSSC	1	0.0421	0.0521	0.0690	0.0841	0.0354	0.0451	0.0622	0.0762	20.0987	18.2360	15.9056	14.6537	22.4688	20.4761	17.9765	16.4810
	2	0.1400	0.1743	0.2297	0.2773	0.1177	0.1497	0.2018	0.2440	11.1283	10.2468	9.1926	8.4980	12.3216	11.2474	9.9853	9.2156
	5	0.4085	0.5160	0.6735	0.7963	0.3436	0.4333	0.5553	0.6510	6.5017	5.9537	5.3747	5.0178	7.2160	6.6170	6.0247	5.6427
	10	0.5787	0.7343	0.9565	1.1217	0.4881	0.6117	0.7648	0.8853	5.4528	4.9845	4.5060	4.2230	6.0547	5.5707	5.1336	4.8373
CSCF	1	0.0379	0.0465	0.0609	0.0740	0.0298	0.0378	0.0517	0.0632	19.3532	17.9484	16.1228	14.8409	21.8471	19.8362	17.2154	15.7363
	2	0.1265	0.1570	0.2054	0.2469	0.0995	0.1268	0.1702	0.2043	10.5474	9.6867	8.5310	7.8295	11.9432	10.8797	9.6762	8.9642
	5	0.3739	0.4779	0.6266	0.7353	0.2946	0.3778	0.4838	0.5590	6.0941	5.5405	4.9924	4.6844	6.8832	6.2497	5.6935	5.3797
	10	0.5344	0.6919	0.9123	1.0611	0.4207	0.5396	0.6753	0.7683	5.0715	4.5824	4.1257	3.8911	5.7343	5.2049	4.8022	4.5772
SCSF	1	0.0793	0.0992	0.1337	0.1635	0.0696	0.0891	0.1237	0.1519	11.6551	10.5947	9.2935	8.5629	12.5045	11.3618	9.9246	9.0824
	2	0.2633	0.3301	0.4397	0.5326	0.2320	0.2953	0.4003	0.4855	6.4188	5.8811	5.2312	4.8213	6.8258	6.2254	5.5030	5.0638
	5	0.7672	0.9630	1.2506	1.4828	0.6802	0.8522	1.0917	1.2874	3.7234	3.4249	3.1015	2.8884	3.9487	3.6376	3.3113	3.0878
	10	1.0860	1.3605	1.7467	2.0521	0.9665	1.1988	1.4932	1.7391	3.1166	2.8755	2.6290	2.4616	3.3024	3.0600	2.8298	2.6569
SSSF	1	0.1072	0.1345	0.1828	0.2246	0.0964	0.1234	0.1719	0.2118	10.8697	9.9550	8.7742	8.0362	11.5239	10.4788	9.1489	8.3620
	2	0.3532	0.4417	0.5913	0.7213	0.3189	0.4037	0.5483	0.6698	5.9674	5.4826	4.8739	4.4765	6.3138	5.7733	5.1024	4.6825
	5	1.0086	1.2468	1.6188	1.9448	0.9164	1.1288	1.4495	1.7373	3.4927	3.2329	2.9265	2.7099	3.6868	3.4178	3.1085	2.8812
	10	1.4140	1.7342	2.2217	2.6520	1.2917	1.5680	1.9603	2.3298	2.9351	2.7292	2.4933	2.3184	3.0946	2.8898	2.6676	2.4855
CFFF	1	0.5880	0.7508	1.0360	1.2683	0.5531	0.7141	0.9983	1.2239	3.3187	2.9940	2.5873	2.3619	3.4220	3.0968	2.6975	2.4720
	2	1.9734	2.5262	3.4103	4.0971	1.8632	2.4041	3.2711	3.9293	1.8218	1.6528	1.4633	1.3553	1.8645	1.6882	1.4913	1.3808
	5	5.8992	7.5814	9.6830	11.1467	5.6043	7.2102	9.1515	10.4890	1.0533	0.9554	0.8730	0.8270	1.0750	0.9753	0.8930	0.8468
	10	8.4589	10.8649	13.4813	15.2336	8.0508	10.3158	12.6140	14.1583	0.8791	0.7985	0.7420	0.7100	0.8963	0.8151	0.7609	0.7292

Table 8. DCBLs of the Al/Al_2O_3 FG square microplates for various BCs, h/ℓ and p_z $(a/h = 5)$

BCs	h/ℓ	$\gamma_1 = 1, \gamma_2 = 0, \gamma_3 = 0$				$\gamma_1 = 1, \gamma_2 = 1, \gamma_3 = 0$				$\gamma_1 = 1, \gamma_2 = 1, \gamma_3 = 1$			
		p_z =1	2	5	10	p_z =1	2	5	10	p_z =1	2	5	10
SSSC	1	167.3783	135.6341	102.5064	84.1037	93.2891	75.4748	56.9281	46.6912	85.2520	69.1915	52.4581	43.0996
	2	50.2651	40.4528	30.7363	25.4381	28.0503	22.5399	17.1044	14.1574	25.5225	20.5527	15.6484	12.9700
	5	17.1083	13.5734	10.3525	8.7167	9.5851	7.6003	5.8119	4.9026	8.6042	6.8060	5.1838	4.3733
	10	11.9496	9.4337	7.1742	6.0749	6.7188	5.3075	4.0644	3.4533	5.9777	4.6914	3.5522	3.0147
CSCF	1	142.2816	114.6269	86.8128	71.7602	106.7973	85.8571	64.7638	53.4343	72.6624	56.0246	40.1447	32.9768
	2	41.6324	33.1906	25.1781	21.0076	31.3668	24.9654	18.8919	15.7484	20.7322	16.0835	11.8904	9.9456
	5	13.0941	10.2014	7.7922	6.6612	9.9503	7.7512	5.9374	5.0848	6.1003	4.7761	3.8182	3.3506
	10	8.7478	6.7484	5.1819	4.4853	6.6911	5.1672	3.9964	3.4723	3.9239	3.0793	2.5651	2.3106
SCSF	1	99.0100	78.6885	58.1648	47.6586	48.3634	38.2680	28.0211	22.8638	38.5597	29.7654	21.2109	17.3126
	2	28.8668	22.8580	17.0606	14.1150	14.3408	11.3645	8.4410	6.9466	11.0796	8.6186	6.3236	5.2416
	5	9.0625	7.1371	5.4804	4.6550	4.7016	3.7551	2.8955	2.4369	3.3661	2.6593	2.1023	1.8149
	10	6.1416	4.8310	3.7742	3.2535	3.2524	2.6129	2.0601	1.7565	2.2400	1.7812	1.4673	1.2963
SSSF	1	97.2896	77.3250	57.1959	46.8900	44.4227	35.1937	25.7257	20.9349	38.0444	29.3714	20.9257	17.0741
	2	28.4094	22.4825	16.7915	13.9077	13.2872	10.5734	7.8491	6.4304	10.9360	8.5131	6.2454	5.1724
	5	8.9494	7.0367	5.4079	4.6020	4.4481	3.5854	2.7621	2.3050	3.3271	2.6333	2.0810	1.7930
	10	6.0716	4.7676	3.7290	3.2209	3.1015	2.5191	1.9822	1.6727	2.2161	1.7660	1.4539	1.2814
CFFF	1	28.0616	21.8634	15.7685	12.8846	10.5850	8.2138	5.8864	4.8012	3.5329	2.7243	1.9375	1.5792
	2	8.1600	6.3480	4.6702	3.8794	3.1425	2.4381	1.7928	1.4916	1.0301	0.7960	0.5818	0.4835
	5	2.5528	1.9832	1.5496	1.3457	1.0402	0.8084	0.6358	0.5541	0.3263	0.2535	0.1997	0.1743
	10	1.7296	1.3451	1.0919	0.9717	0.7205	0.5621	0.4588	0.4084	0.2223	0.1735	0.1428	0.1278

Table 9. DCBLs of the Al/Al_2O_3 FG square microplates for various BCs, h/ℓ and p_z $(a/h = 10)$

BCs	h/ℓ	$\gamma_1 = 1, \gamma_2 = 0, \gamma_3 = 0$				$\gamma_1 = 1, \gamma_2 = 1, \gamma_3 = 0$				$\gamma_1 = 1, \gamma_2 = 1, \gamma_3 = 1$			
		p_z =1	2	5	10	p_z =1	2	5	10	p_z =1	2	5	10
SSSC	1	202.5793	159.1404	115.5142	94.1860	111.8915	87.8212	63.6872	51.9269	104.1781	81.9388	59.6114	48.6482
	2	60.9347	48.0188	35.6213	29.4249	33.6498	26.4946	19.6434	16.2311	31.2958	24.6624	18.3229	15.1559
	5	20.9044	16.6273	12.9489	11.0008	11.5422	9.1732	7.1504	6.0822	10.6976	8.4822	6.6039	5.6250
	10	14.6801	11.7569	9.3682	8.0491	8.1110	6.4906	5.1824	4.4608	7.5031	5.9803	4.7594	4.1025
CSCF	1	167.3421	131.0619	95.3041	78.0716	125.2844	98.0020	71.1133	58.2089	63.5509	48.9706	34.9022	28.5273
	2	48.9424	38.2191	28.3162	23.5780	36.6370	28.5837	21.1447	17.5976	18.3490	14.1805	10.3910	8.6541
	5	15.5231	12.0706	9.4217	8.1704	11.6135	9.0287	7.0522	6.1192	5.6399	4.3867	3.4636	3.0262
	10	10.5220	8.1831	6.5896	5.8333	7.8800	6.1287	4.9474	4.3864	3.7712	2.9438	2.4275	2.1762
SCSF	1	110.8941	86.4227	62.1047	50.5736	52.8444	41.1517	29.4813	23.9539	35.8462	27.6689	19.6606	15.9989
	2	32.2878	25.2245	18.5094	15.2769	15.6050	12.2410	8.9740	7.3705	10.3968	8.0690	5.8887	4.8679
	5	10.1833	8.0263	6.2498	5.3470	5.0944	4.0751	3.1728	2.6806	3.2486	2.5555	2.0062	1.7288
	10	6.9630	5.5212	4.4574	3.8922	3.5303	2.8548	2.3016	1.9764	2.2067	1.7485	1.4335	1.2647
SSSF	1	109.0803	84.9899	61.0891	49.7675	48.4633	37.7918	27.0670	21.9562	35.3478	27.2904	19.3909	15.7751
	2	31.7968	24.8213	18.2218	15.0562	14.4369	11.3757	8.3419	6.8232	10.2585	7.9676	5.8143	4.8026
	5	10.0540	7.9094	6.1632	5.2840	4.8078	3.8836	3.0198	2.5275	3.2106	2.5302	1.9856	1.7078
	10	6.8765	5.4407	4.3957	3.8467	3.3553	2.7448	2.2062	1.8721	2.1829	1.7335	1.4203	1.2501
CFFF	1	28.9078	22.3491	15.9369	12.9872	10.8515	8.3807	5.9710	4.8664	3.4836	2.6859	1.9089	1.5549
	2	8.3810	6.4847	4.7394	3.9338	3.2123	2.4843	1.8204	1.5145	1.0167	0.7853	0.5735	0.4764
	5	2.6162	2.0314	1.5943	1.3888	1.0584	0.8224	0.6482	0.5658	0.3231	0.2509	0.1975	0.1723
	10	1.7764	1.3838	1.1348	1.0149	0.7325	0.5719	0.4693	0.4188	0.2208	0.1723	0.1417	0.1269

The effect of h/ℓ on the DCDs, DCBLs and DFFs of the SSSC, CSCF, SCSF and SSSF FG square microplates are illustrated in Fig. 3. With the increasing of h/ℓ, the variation on the DCBLs and DFFs decreases. For the DCBLs, it is clear that while $h/\ell \geq 10$, their variations are almost invisible for all BCs. However, regarding to DCDs and DFFs, the variations become negligible as $h/\ell \geq 20$ in all cases. It is interesting to see that the effect of the variation of h/ℓ on the structural responses depending BCs. The most significant on the DCDs is SSSF, while on the DCBLs is CSCF and finally on the DFFs is SSSC, respectively.

Transverse deformations of the FG square microplates under the sinusoidally distributed load for nine BCs are plotted in Fig. 4. It can be observed that when the FG square microplate has a free edge, the maximum deflection is observed close to this edge. The maximum transverse deflections are always obtained in the middle of the microplate which has the symmetric BCs such as SSSS, CCCC and SCSC. Only for the SSSC FG square microplate, the maximum deflection is occurred close to its right edge.

The vibration mode shapes of the CCCC FG microplates are depicted in Fig. 5 based on the present Q3D shear deformation theory and TSDT for classical, MCST and MSGT. It should be noticed that even though their fundamental frequencies in these cases are totally different, the mode shapes are almost identical no matter what the shear deformation theories (Q3D, TSDT) or continuum theories (Classical, MCST and MSGT) are considered.

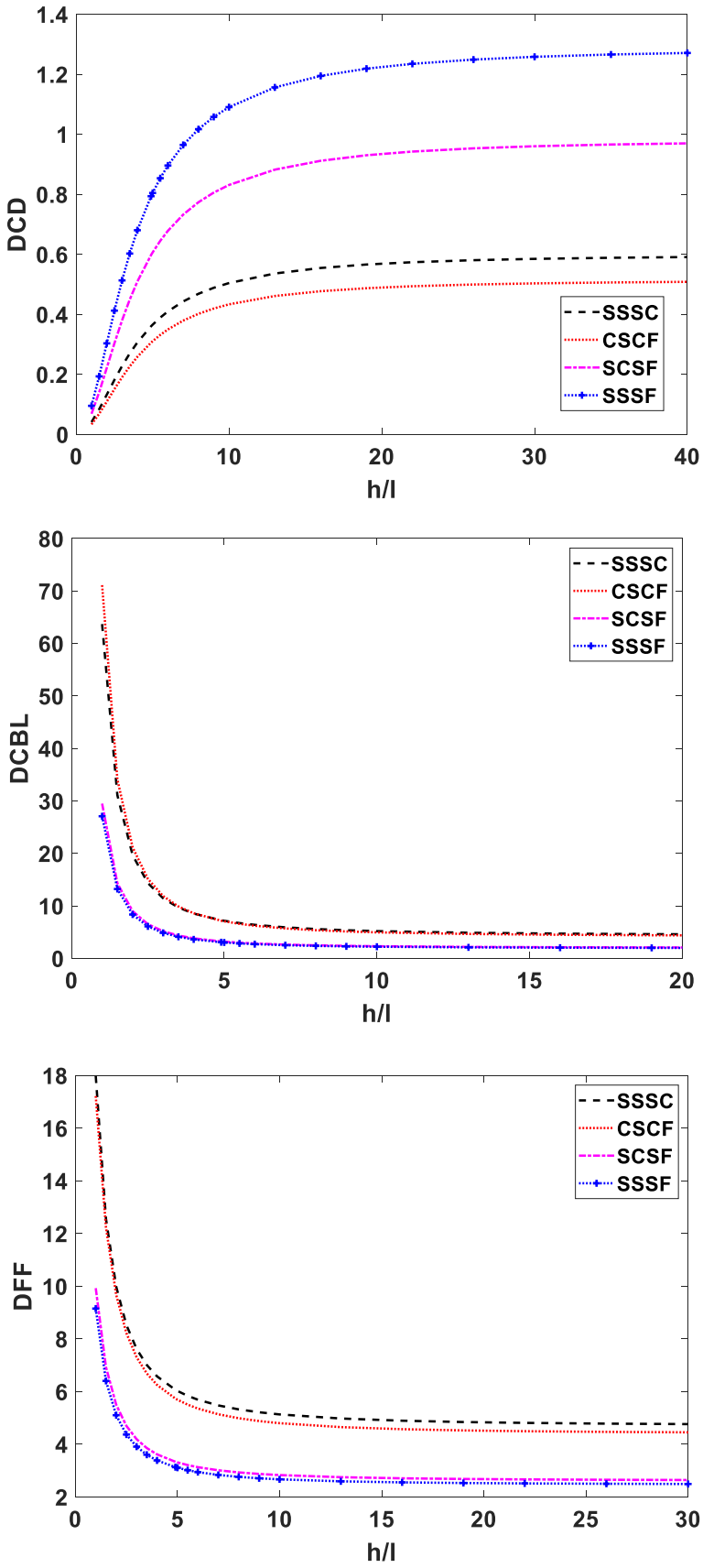

Figure 3. DCDs (sinusoidally distributed load), DCBLs (biaxial) and DFFs of FG microplates with respect to h/ℓ_m $(a/h = 10, p_z = 5)$

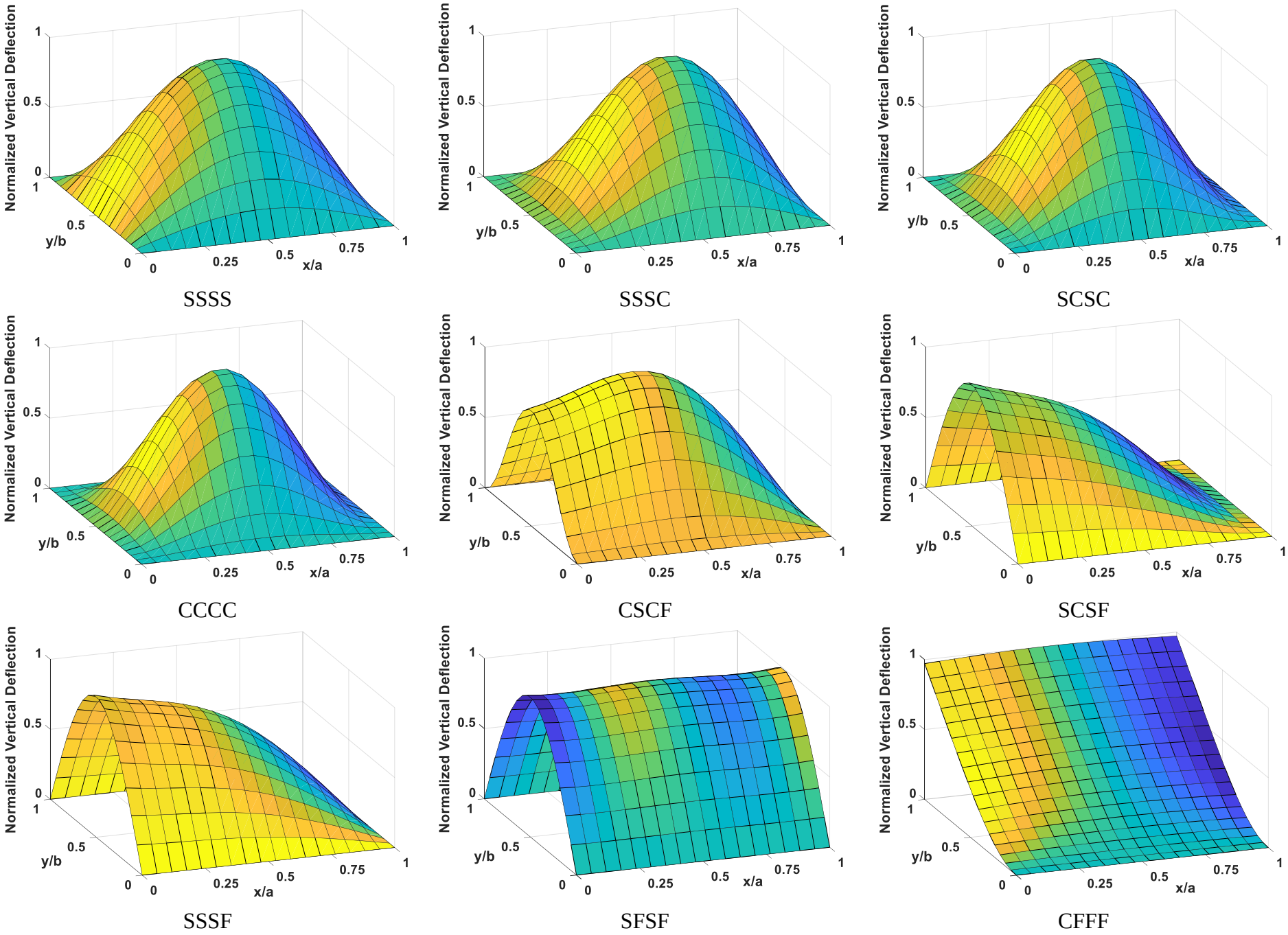

Figure 4. Transverse deformations (sinusoidally distributed load) of the FG microplates ($a/h = 10,\ p_z = 5, h/\ell_m = 1$)

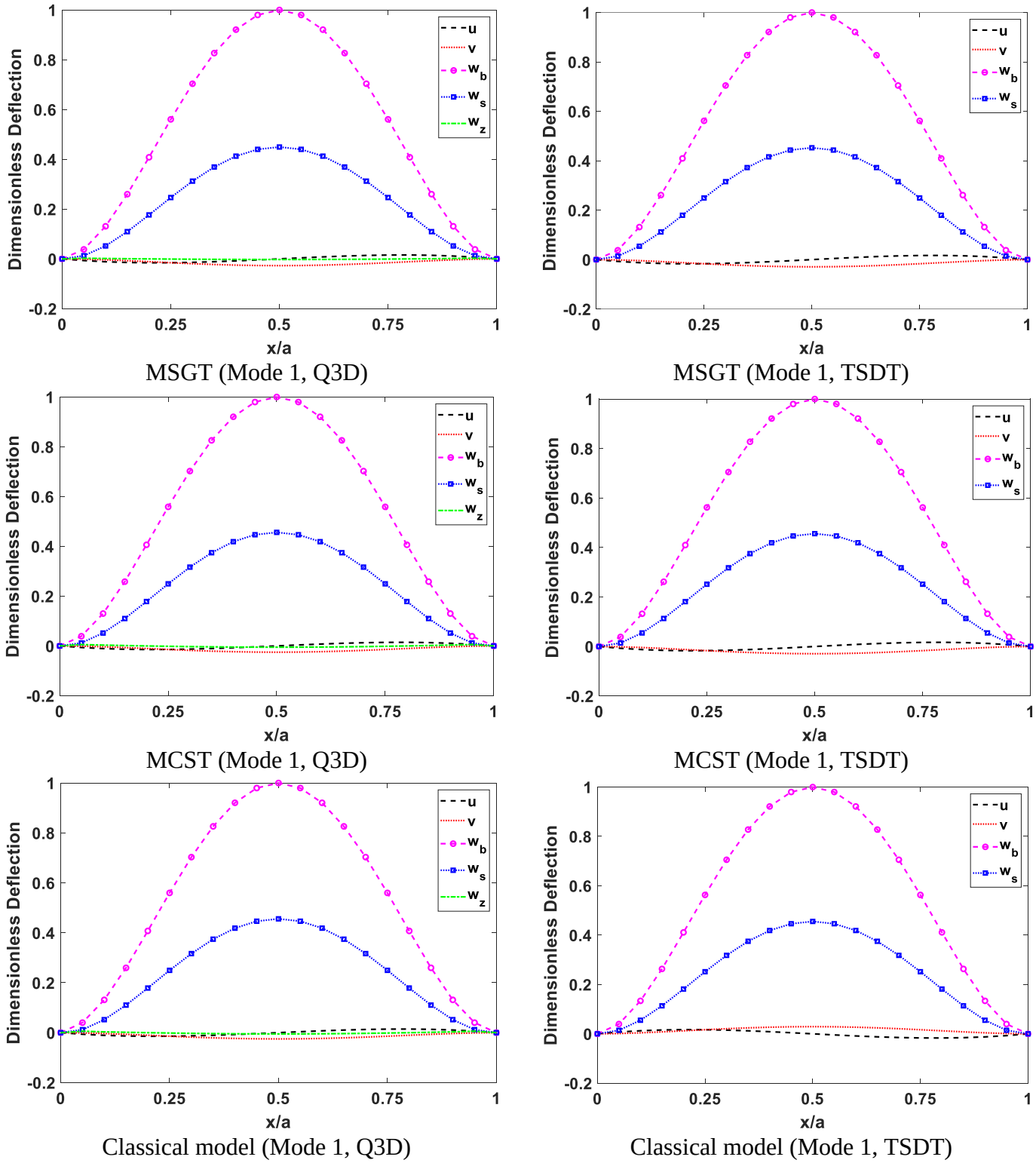

Figure 5. Vibration mode shape along the x-axis (x, b/4, 0) of clamped square FG microplates $(a/h = 10,\ p_z = 1, h/\ell_m = 8)$

4.3 2D FG microplates

Since there is no available results regarding to analysis of 2D-FG square strain gradient microplates, the developed FEM model is validated again the results generated by the IGA-RPT and MCST [68] for SSSS and CCCC microplates with various p_x, p_y and a/h in Tables 10 and 11. For the DCBLs, due the lack of available results for the SSSS microplates, the verification is carried out only for CCCC ones. It is observed that an excellent agreement is found for all cases with the MCST. The present DCDs obtained by the MCST considering the normal deformation is negligibly higher than those without it ($\varepsilon_z = 0$). However, the difference between computed results based on the MSGT and MCST is significant due the formulation of the MSGT, which increases the stiffness of the structure. It is observed that the effect of the MSGT on the stiffness of the SSSS 2D-FG square microplates is more pronounce than the CCCC ones.

The DCDs, DCBLs and DFFs of the 2D-FG square microplates for nine BCs are presented in Tables 12-14 with respect to the variation of the gradient indexes in both directions, h/ℓ and a/h. As it is expected, the highest DFFs and DCBLS and the lowest DCDs are always obtained for the CCCC microplate. Moreover, the lowest stiffness is detected for CFFF one. Some new results, which are not available in open literature, are provided as references for the future studies.

The effect of p_x and p_y on the results of the 2D-FD square microplates are investigated in Fig. 6 with respect to various h/ℓ ratios. The findings show that with the decreasing of the small size effect, the effects of the gradient indexes on the mechanical behaviours of the 2D-FG microplates becomes significant. Besides, the effect of p_x on the DCDs is more noticeable than those of p_y due the sinusoidally distributed load.

The ratios of DCDs, DCBLs and DFFs for SSSS, SCSC and CCCC 2D-FG microplates with respect to various h/ℓ ratios based on the MSCT and MSGT are plotted in Fig. 7. It is observed that these

ratios obtain the maximum/minimum value when $h/\ell = 1$, which also implies that the most significant size effect occurs when plate's thickness is the same with MLSP. With an increment of h/ℓ, the ratios of DCBLs and DFFs approach to unity approximately at h/ℓ=20, which is faster than those of DFFs at h/ℓ=40. It also means that MSGT should be used for vibration and buckling analysis of 2D-FG microplates when $h/\ell \leq 20$ and bending one when $h/\ell \leq 40$. When h/ℓ > 40, the difference between these theories becomes negligible and MCST will be efficient to deal with the microplates

The effect of h/ℓ on the results of SCSC, CSCF, SCSF and SFSF 2D-FG microplates are shown in Fig. 8. This effect becomes significant on the DCBLs and DFFs of microplates with the inclusion of clamped edge. On the other hand, it is more pronounced for the DCDs of microplates with the free edge (SFSF, SCSF) than those with clamped edge (SCSC) of all BCs. The variations on the DCBLs and DFFs due the variation of h/ℓ are not detected as $h/\ell \geq 15$. However, for the DCDs, h/ℓ should be greater than 20 to observe the same response.

The first three vibration mode shapes of SSSC and CSCF 2D-FG microplates and buckling mode shapes of SSSS, SCSC and CCCC 2D-FG microplates subjected to various loading conditions are illustrated in Figs. 9 and 10. Unlike the 1D-FG microplates, the maximum deflections are obtained in different locations of the microplates depending on the BCs.

Table 10. Verification studies on the DCDs $\left(\bar{w} = w\frac{10h^3E_c}{q_0a^4}\right)$ and DFFs $\left(\Omega = \omega\frac{a^2}{h}\sqrt{\frac{\rho_c}{E_c}}\right)$ of Al/Al_2O_3 2D-FG square microplates subjected to sinusoidally distributed load for various BCs, h/ℓ, p_x and p_y $(a/h = 20, \ell = 17.6\mu m)$

BCs	h/ℓ	Theory	$p_x = p_y$			
			1	2	5	10
DCD						
SSSS	10	IGA – RPT (MCST, [68])	0.7452	1.0676	1.3421	1.4205
		Present - $\varepsilon_z \neq 0$ (MCST)	0.7442	1.0743	1.3514	1.4302
		Present - $\varepsilon_z \neq 0$ (MSGT)	0.6328	0.9210	1.1584	1.2206
	5	IGA – RPT (MCST, [68])	0.6643	0.9398	1.1817	1.2582
		Present - $\varepsilon_z \neq 0$ (MCST)	0.6637	0.9465	1.1913	1.2689
		Present - $\varepsilon_z \neq 0$ (MSGT)	0.4537	0.6596	0.8297	0.8747
	1	IGA – RPT (MCST, [68])	0.1486	0.1954	0.2464	0.2714
		Present - $\varepsilon_z \neq 0$ (MCST)	0.1489	0.1972	0.2500	0.2762
		Present - $\varepsilon_z \neq 0$ (MSGT)	0.0496	0.0716	0.0900	0.0953
CCCC	10	IGA – RPT (MCST, [68])	0.2735	0.3904	0.5054	0.5325
		Present - $\varepsilon_z \neq 0$ (MCST)	0.2656	0.3829	0.4958	0.5198
		Present - $\varepsilon_z \neq 0$ (MSGT)	0.2287	0.3305	0.4273	0.4475
	5	IGA – RPT (MCST, [68])	0.2433	0.3459	0.4483	0.4733
		Present - $\varepsilon_z \neq 0$ (MCST)	0.2370	0.3403	0.4413	0.4637
		Present - $\varepsilon_z \neq 0$ (MSGT)	0.1652	0.2387	0.3086	0.3233
	1	IGA – RPT (MCST, [68])	0.0538	0.0744	0.0973	0.1040
		Present - $\varepsilon_z \neq 0$ (MCST)	0.0536	0.0749	0.0981	0.1044
		Present - $\varepsilon_z \neq 0$ (MSGT)	0.0181	0.0260	0.0337	0.0354
DFF						
SSSS	10	IGA – RPT (MCST, [68])	4.0928	3.5589	3.2383	3.1471
		Present - $\varepsilon_z \neq 0$ (MCST)	4.0939	3.5478	3.2263	3.1341
		Present - $\varepsilon_z \neq 0$ (MSGT)	4.4404	3.8327	3.4850	3.3927
	5	IGA – RPT (MCST, [68])	4.3350	3.7917	3.4515	3.3448
		Present - $\varepsilon_z \neq 0$ (MCST)	4.3351	3.7791	3.4368	3.3282
		Present - $\varepsilon_z \neq 0$ (MSGT)	5.2450	4.5293	4.1183	4.0083
	1	IGA – RPT (MCST, [68])	9.1675	8.3089	7.5624	7.2102
		Present - $\varepsilon_z \neq 0$ (MCST)	9.1541	8.2718	7.5066	7.1414
		Present - $\varepsilon_z \neq 0$ (MSGT)	15.8591	13.7515	12.5041	12.1439
CCCC	10	IGA – RPT (MCST, [68])	7.2790	6.3720	5.7213	5.5687
		Present - $\varepsilon_z \neq 0$ (MCST)	7.4059	6.4546	5.7902	5.6477
		Present - $\varepsilon_z \neq 0$ (MSGT)	7.9728	6.9419	6.2313	6.0810
	5	IGA – RPT (MCST, [68])	7.7191	6.7704	6.0755	5.9078
		Present - $\varepsilon_z \neq 0$ (MCST)	7.8386	6.8456	6.1367	5.9799
		Present - $\varepsilon_z \neq 0$ (MSGT)	9.3734	8.1632	7.3273	7.1494
	1	IGA – RPT (MCST, [68])	16.4438	14.5978	13.0521	12.6175
		Present - $\varepsilon_z \neq 0$ (MCST)	16.4672	14.5663	13.0025	12.5936
		Present - $\varepsilon_z \neq 0$ (MSGT)	28.3493	24.7124	22.1699	21.6183

Table 11. Verification studies on the DCBLs $\left(N_{cr} = N_0 \frac{a^2}{h^3 E_m}\right)$ of Al/Al_2O_3 2D-FG square microplates for various BCs, $h/\ell, p_x$ and p_y $(a/h = 20, \ell = 17.6\mu m)$

BCs	h/ℓ	Theory	$\gamma_1 = 1, \gamma_2 = 1, \gamma_3 = 0$				$\gamma_1 = 1, \gamma_2 = 0, \gamma_3 = 0$				$\gamma_1 = 1, \gamma_2 = 1, \gamma_3 = 1$			
			$p_x = p_y$				$p_x = p_y$				$p_x = p_y$			
			1	2	5	10	1	2	5	10	1	2	5	10
CCCC	10	IGA – RPT (MCST, [68])	8.8687	6.3433	5.0893	4.8664	-	-	-	-	-	-	-	-
		Present - $\varepsilon_z \neq 0$ (MCST)	9.0568	6.4073	5.1392	4.9366	16.5660	11.7411	9.5746	9.2455	7.6989	5.3675	4.3534	4.2378
		Present - $\varepsilon_z \neq 0$ (MSGT)	10.5176	7.4359	5.9725	5.7412	19.3095	13.6744	11.1666	10.7909	8.9836	6.2562	5.0778	4.9450
	5	IGA – RPT (MCST, [68])	9.9704	7.1575	5.7343	5.4733	-	-	-	-	-	-	-	-
		Present - $\varepsilon_z \neq 0$ (MCST)	10.1459	7.2064	5.7711	5.5338	18.5824	13.2139	10.7593	10.3742	8.6225	6.0320	4.8890	4.7546
		Present - $\varepsilon_z \neq 0$ (MSGT)	14.6183	10.3441	8.3075	7.9833	26.8667	19.0414	15.5477	15.0205	12.5009	8.7106	7.0693	6.8831
	2	IGA – RPT (MCST, [68])	17.6755	12.8522	10.2446	9.7189	-	-	-	-	-	-	-	-
		Present - $\varepsilon_z \neq 0$ (MCST)	17.7506	12.7860	10.1842	8.7057	32.6542	23.4964	19.0317	18.2574	15.0720	10.6728	8.6293	8.3645
		Present - $\varepsilon_z \neq 0$ (MSGT)	40.8720	28.9694	23.2439	22.3167	75.2608	53.4129	43.5651	42.0537	35.0100	24.4236	19.8087	19.2769
	1	IGA – RPT (MCST, [68])	45.1685	33.1734	26.3384	24.8709	-	-	-	-	-	-	-	-
		Present - $\varepsilon_z \neq 0$ (MCST)	44.8195	32.6467	25.8966	24.5622	82.6898	60.0684	48.4691	46.3162	38.0157	27.1844	21.9405	21.2114
		Present - $\varepsilon_z \neq 0$ (MSGT)	133.8858	94.9596	76.1596	73.0940	246.6920	175.1737	142.8087	137.8075	114.7422	80.0866	64.9356	63.1783
SSSS	10	Present - $\varepsilon_z \neq 0$ (MCST)	3.4622	2.4782	2.0344	1.9232	6.7697	4.8831	4.0571	3.8444	3.2580	2.2956	1.8957	1.8128
		Present - $\varepsilon_z \neq 0$ (MSGT)	4.0756	2.8963	2.3769	2.2558	7.9677	5.7092	4.7420	4.5095	3.8381	2.6853	2.2183	2.1288
	5	Present - $\varepsilon_z \neq 0$ (MCST)	3.8824	2.8092	2.3063	2.1681	7.5928	5.5314	4.5966	4.3332	3.6489	2.5985	2.1440	2.0400
		Present - $\varepsilon_z \neq 0$ (MSGT)	5.6894	4.0464	3.3205	3.1500	11.1237	7.9764	6.6244	6.2973	5.3580	3.7519	3.0990	2.9727
	2	Present - $\varepsilon_z \neq 0$ (MCST)	6.8224	5.1222	4.1979	3.8752	13.3514	10.0599	8.3458	7.7402	6.3842	4.7143	3.8730	3.6259
		Present - $\varepsilon_z \neq 0$ (MSGT)	15.8990	11.3655	9.3267	8.8240	31.0942	22.4003	18.6024	17.6390	14.9694	10.5357	8.6979	8.3229
	1	Present - $\varepsilon_z \neq 0$ (MCST)	17.3170	13.3710	10.9237	9.9557	33.9054	26.2036	21.6679	19.8737	16.1472	12.2571	10.0233	9.2794
		Present - $\varepsilon_z \neq 0$ (MSGT)	52.0430	37.2907	30.6009	28.9159	101.7940	73.4893	61.0275	57.8010	48.9936	34.5628	28.5276	27.2671

Table 12. DCDs of the Al/Al_2O_3 2D-FG square microplates subjected to uniformly distributed load for various BCs, a/h, p_x, p_y *and* h/ℓ

BCs	h/ℓ	$a/h=5$					$a/h=10$					$a/h=20$				
		(p_x,p_y)					(p_x,p_y)					(p_x,p_y)				
		(1,1)	(2,2)	(2,1)	(5,1)	(5,2)	(1,1)	(2,2)	(2,1)	(5,1)	(5,2)	(1,1)	(2,2)	(2,1)	(5,1)	(5,2)
CCCC	1	0.0363	0.0519	0.0447	0.0573	0.0618	0.0277	0.0396	0.0341	0.0436	0.0470	0.0252	0.0360	0.0310	0.0395	0.0426
	2	0.1203	0.1726	0.1484	0.1904	0.2054	0.0908	0.1300	0.1119	0.1431	0.1543	0.0826	0.1179	0.1016	0.1296	0.1398
	5	0.3488	0.5016	0.4308	0.5541	0.5972	0.2558	0.3663	0.3153	0.4035	0.4349	0.2306	0.3296	0.2840	0.3626	0.3908
	10	0.4932	0.7091	0.6090	0.7837	0.8445	0.3560	0.5098	0.4389	0.5617	0.6052	0.3193	0.4567	0.3935	0.5026	0.5415
SCSC	1	0.0505	0.0718	0.0612	0.0765	0.0836	0.0404	0.0575	0.0488	0.0606	0.0664	0.0378	0.0537	0.0455	0.0563	0.0618
	2	0.1664	0.2370	0.2017	0.2527	0.2759	0.1325	0.1886	0.1600	0.1988	0.2178	0.1238	0.1760	0.1491	0.1845	0.2025
	5	0.4730	0.6763	0.5747	0.7220	0.7879	0.3714	0.5302	0.4491	0.5588	0.6120	0.3453	0.4924	0.4165	0.5163	0.5664
	10	0.6607	0.9453	0.8028	1.0092	1.1012	0.5163	0.7373	0.6242	0.7769	0.8510	0.4788	0.6832	0.5778	0.7165	0.7859
SSSC	1	0.0697	0.0980	0.0850	0.1072	0.1145	0.0589	0.0828	0.0719	0.0907	0.0964	0.0563	0.0790	0.0686	0.0865	0.0918
	2	0.2291	0.3227	0.2798	0.3536	0.3773	0.1930	0.2717	0.2358	0.2980	0.3165	0.1843	0.2590	0.2250	0.2841	0.3013
	5	0.6462	0.9153	0.7920	1.0062	1.0722	0.5408	0.7643	0.6623	0.8403	0.8917	0.5144	0.7263	0.6297	0.7983	0.8461
	10	0.8997	1.2760	1.1034	1.4044	1.4953	0.7529	1.0649	0.9225	1.1714	1.2427	0.7154	1.0109	0.8763	1.1117	1.1780
SSSS	1	0.0938	0.1336	0.1156	0.1470	0.1569	0.0818	0.1170	0.1014	0.1291	0.1373	0.0789	0.1130	0.0979	0.1248	0.1325
	2	0.3075	0.4392	0.3799	0.4841	0.5164	0.2679	0.3842	0.3325	0.4245	0.4511	0.2582	0.3708	0.3209	0.4098	0.4350
	5	0.8623	1.2402	1.0709	1.3721	1.4609	0.7492	1.0810	0.9339	1.1976	1.2709	0.7210	1.0414	0.8999	1.1540	1.2235
	10	1.1966	1.7252	1.4887	1.9113	2.0333	1.0441	1.5085	1.3028	1.6722	1.7740	1.0058	1.4540	1.2561	1.6120	1.7087
CSCF	1	0.0630	0.0886	0.0783	0.1004	0.1062	0.0499	0.0698	0.0622	0.0797	0.0837	0.0465	0.0647	0.0580	0.0742	0.0776
	2	0.2074	0.2917	0.2580	0.3310	0.3499	0.1635	0.2287	0.2041	0.2613	0.2743	0.1523	0.2122	0.1903	0.2432	0.2545
	5	0.5877	0.8284	0.7327	0.9424	0.9947	0.4590	0.6417	0.5738	0.7349	0.7699	0.4259	0.5934	0.5331	0.6813	0.7116
	10	0.8205	1.1568	1.0236	1.3181	1.3903	0.6378	0.8917	0.7978	1.0219	1.0700	0.5901	0.8224	0.7389	0.9446	0.9863
SCSF	1	0.1272	0.1802	0.1543	0.1931	0.2111	0.1122	0.1587	0.1359	0.1688	0.1847	0.1085	0.1534	0.1313	0.1626	0.1781
	5	1.1997	1.6965	1.4573	1.8130	1.9766	1.0592	1.4945	1.2840	1.5832	1.7293	1.0240	1.4439	1.2405	1.5252	1.6671
	10	1.6731	2.3660	2.0328	2.5266	2.7543	1.4796	2.0873	1.7938	2.2102	2.4138	1.4302	2.0163	1.7328	2.1295	2.3269
SFSF	1	0.2828	0.4145	0.3449	0.4338	0.4789	0.2571	0.3794	0.3138	0.3942	0.4365	0.2512	0.3715	0.3066	0.3851	0.4269
	2	0.9250	1.3552	1.1285	1.4188	1.5649	0.8444	1.2453	1.0308	1.2941	1.4321	0.8258	1.2203	1.0081	1.2652	1.4015
	5	2.5897	3.7907	3.1628	3.9708	4.3724	2.3860	3.5134	2.9140	3.6521	4.0357	2.3367	3.4469	2.8538	3.5749	3.9545
	10	3.5961	5.2662	4.3937	5.5156	6.0718	3.3331	4.9080	4.0713	5.1011	5.6360	3.2675	4.8188	3.9908	4.9976	5.5274
SSSF	1	0.1772	0.2484	0.2175	0.2741	0.2913	0.1607	0.2249	0.1976	0.2483	0.2628	0.1568	0.2193	0.1928	0.2421	0.2559
	2	0.5842	0.8189	0.7177	0.9039	0.9594	0.5307	0.7425	0.6530	0.8197	0.8666	0.5178	0.7242	0.6375	0.7995	0.8443
	5	1.6629	2.3313	2.0490	2.5755	2.7245	1.5151	2.1200	1.8688	2.3404	2.4680	1.4788	2.0681	1.8244	2.2825	2.4048
	10	2.3179	3.2502	2.8588	3.5929	3.7965	2.1200	2.9665	2.6160	3.2753	3.4520	2.0705	2.8954	2.5552	3.1957	3.3656
CFFF	1	1.4467	1.7771	1.5582	1.6923	1.8170	1.3789	1.6794	1.4793	1.5986	1.7126	1.3671	1.6577	1.4640	1.5785	1.6888
	2	4.7434	5.8264	5.1090	5.5483	5.9571	4.5271	5.5124	4.8569	5.2483	5.6219	4.4891	5.4430	4.8077	5.1841	5.5462
	5	13.3203	16.3545	14.3452	15.5733	16.7183	12.7384	15.5019	13.6667	14.7664	15.8123	12.6139	15.3002	13.5153	14.5793	15.5960
	10	18.5237	22.7229	19.9401	21.6338	23.2185	17.6986	21.5404	18.9897	20.5182	21.9704	17.4887	21.2359	18.7471	20.2326	21.6490

Table 13. DFFs of the Al/Al_2O_3 2D-FG square microplates for various BCs, $a/h, p_x, p_y$ and h/ℓ

BCs	h/ℓ	$a/h=5$					$a/h=10$					$a/h=20$				
		(p_x,p_y)					(p_x,p_y)					(p_x,p_y)				
		(1,1)	(2,2)	(2,1)	(5,1)	(5,2)	(1,1)	(2,2)	(2,1)	(5,1)	(5,2)	(1,1)	(2,2)	(2,1)	(5,1)	(5,2)
CCCC	1	23.8654	21.0540	22.2381	20.4351	19.7331	26.8033	23.3411	24.7441	22.5234	21.7883	28.3459	24.7123	26.1884	23.8583	23.0759
	2	12.6736	11.0256	11.6923	10.6316	10.2881	14.7913	12.8776	13.6520	12.4248	12.0211	15.6618	13.6501	14.4659	13.1763	12.7461
	5	7.4009	6.4339	6.8232	6.2012	6.0039	8.8077	7.6659	8.1266	7.3943	7.1565	9.3724	8.1630	8.6518	7.8768	7.6223
	10	6.2065	5.3990	5.7240	5.2042	5.0394	7.4655	6.4989	6.8889	6.2684	6.0674	7.9656	6.9363	7.3519	6.6921	6.4764
SCSC	1	19.4425	16.9681	18.0971	16.6382	15.9987	22.0336	19.2143	20.5346	18.9242	18.1660	22.9780	20.0422	21.4411	19.7915	18.9795
	2	10.6911	9.3243	9.9462	9.1402	8.7907	12.1688	10.6063	11.3376	10.4463	10.0284	12.6989	11.0705	11.8456	10.9315	10.4840
	5	6.3114	5.4975	5.8660	5.3861	5.1825	7.2623	6.3235	6.7627	6.2285	5.9804	7.6018	6.6191	7.0857	6.5352	6.2690
	10	5.3266	4.6399	4.9512	4.5464	4.3749	6.1581	5.3615	5.7347	5.2816	5.0713	6.4551	5.6192	6.0160	5.5475	5.3218
SSSC	1	17.3442	15.3300	16.1963	14.8964	14.3332	18.2576	15.9753	16.9524	15.4677	15.0089	18.8152	16.4683	17.4724	15.9384	15.4782
	2	9.1143	7.9703	8.4631	7.7235	7.4808	10.0859	8.8163	9.3597	8.5320	8.2803	10.3991	9.0927	9.6514	8.7959	8.5431
	5	5.4078	4.7175	5.0140	4.5652	4.4245	6.0234	5.2540	5.5832	5.0789	4.9311	6.2234	5.4292	5.7687	5.2465	5.0972
	10	4.5719	3.9868	4.2380	3.8563	3.7387	5.1027	4.4495	4.7291	4.3003	4.1757	5.2761	4.6009	4.8896	4.4453	4.3190
SSSS	1	14.1941	12.3511	13.0755	11.9144	11.5788	15.4561	13.4147	14.2057	12.9214	12.5762	15.8573	13.7500	14.5623	13.2384	12.8914
	2	7.8293	6.8039	7.2053	6.5593	6.3766	8.5411	7.4033	7.8425	7.1271	6.9385	8.7654	7.5908	8.0420	7.3044	7.1146
	5	4.6590	4.0366	4.2778	3.8857	3.7805	5.1050	4.4121	4.6775	4.2422	4.1323	5.2449	4.5292	4.8023	4.3533	4.2422
	10	3.9431	3.4134	3.6179	3.2842	3.1964	4.3219	3.7332	3.9582	3.5885	3.4961	4.4403	3.8327	4.0642	3.6831	3.5895
CSCF	1	14.5819	12.9024	13.2684	12.3539	12.2264	16.3602	14.5461	14.9012	13.9356	13.8179	16.9478	15.1023	15.4422	14.4693	14.3600
	5	4.6982	4.1681	4.2772	3.9962	3.9594	5.3105	4.7351	4.8397	4.5419	4.5087	5.5080	4.9205	5.0209	4.7203	4.6896
	10	3.9534	3.5102	3.5995	3.3663	3.3363	4.4867	4.0023	4.0887	3.8398	3.8127	4.6655	4.1687	4.2526	4.0000	3.9747
SCSF	1	9.2014	8.0291	8.3902	7.7280	7.5666	9.7684	8.5329	8.9142	8.2276	8.0529	9.9360	8.6815	9.0702	8.3761	8.1963
	5	2.9365	2.5714	2.6795	2.4816	2.4333	3.1217	2.7349	2.8508	2.6433	2.5902	3.1759	2.7827	2.9011	2.6907	2.6360
	10	2.4743	2.1682	2.2582	2.0936	2.0533	2.6331	2.3077	2.4049	2.2310	2.1864	2.6797	2.3486	2.4480	2.2714	2.2255
SFSF	1	7.2992	6.2507	6.7182	6.1483	5.9027	7.7092	6.5844	7.0944	6.4968	6.2277	7.8211	6.6735	7.1973	6.5919	6.3151
	2	4.0217	3.4467	3.7009	3.3903	3.2567	4.2408	3.6249	3.9022	3.5767	3.4302	4.3005	3.6725	3.9571	3.6275	3.4769
	5	2.3814	2.0451	2.1906	2.0119	1.9351	2.5038	2.1442	2.3034	2.1158	2.0315	2.5377	2.1714	2.3346	2.1446	2.0579
	10	2.0142	1.7303	1.8527	1.7027	1.6381	2.1151	1.8118	1.9457	1.7880	1.7170	2.1435	1.8345	1.9719	1.8120	1.7390
SSSF	1	8.4950	7.4361	7.7441	7.1191	7.0035	8.9741	7.8654	8.1817	7.5324	7.4167	9.1120	7.9888	8.3080	7.6513	7.5354
	5	2.7213	2.3890	2.4798	2.2908	2.2585	2.8753	2.5258	2.6206	2.4226	2.3894	2.9193	2.5649	2.6610	2.4603	2.4268
	10	2.2943	2.0155	2.0906	1.9331	1.9067	2.4251	2.1310	2.2103	2.0443	2.0167	2.4626	2.1641	2.2446	2.0762	2.0483
CFFF	1	2.2391	2.0519	2.1920	2.1338	2.0566	2.2806	2.0958	2.2362	2.1812	2.1038	2.2875	2.1053	2.2445	2.1911	2.1144
	5	0.7387	0.6770	0.7231	0.7041	0.6787	0.7506	0.6900	0.7360	0.7179	0.6926	0.7531	0.6930	0.7388	0.7211	0.6960
	10	0.6265	0.5742	0.6133	0.5972	0.5757	0.6365	0.5850	0.6240	0.6086	0.5872	0.6390	0.5877	0.6267	0.6116	0.5902

Table 14. DCBLs of the Al/Al_2O_3 2D-FG square microplates for various BCs, p_x, p_y *and* h/ℓ $(a/h = 10)$

BCs	h/ℓ	$(\gamma_1 = 1, \gamma_2 = 0, \gamma_3 = 0)$					$(\gamma_1 = 1, \gamma_2 = 1, \gamma_3 = 0)$					$(\gamma_1 = 1, \gamma_2 = 1, \gamma_3 = 1)$				
		(p_x, p_y)					(p_x, p_y)					(p_x, p_y)				
		(1,1)	(2,2)	(2,1)	(5,1)	(5,2)	(1,1)	(2,2)	(2,1)	(5,1)	(5,2)	(1,1)	(2,2)	(2,1)	(5,1)	(5,2)
CCCC	1	217.3249	154.4228	170.7548	136.6028	132.2397	120.7495	85.6311	97.6842	77.9763	73.7531	101.3593	70.6679	81.1852	64.8569	61.1495
	2	66.0540	46.9201	51.8773	41.5154	40.2010	36.7901	26.0767	29.7453	23.7387	22.4626	30.7939	21.4645	24.6535	19.6939	18.5775
	5	23.2369	16.5023	18.2354	14.6136	14.1622	13.0462	9.2382	10.5351	8.4044	7.9612	10.8250	7.5468	8.6606	6.9203	6.5368
	10	16.5412	11.7518	12.9796	10.4126	10.0944	9.3392	6.6111	7.5383	6.0129	5.6981	7.7058	5.3764	6.1661	4.9293	4.6591
SCSC	1	158.6471	112.5316	127.6056	102.4286	97.1129	88.1194	63.8791	73.9217	60.9138	56.7340	78.2822	55.5561	64.7686	52.9833	49.1883
	2	48.3549	34.2631	38.8619	31.1872	29.5763	26.8745	19.4667	22.5348	18.5639	17.2942	23.8421	16.9078	19.7172	16.1241	14.9736
	5	17.1558	12.1293	13.7609	11.0395	10.4773	9.5581	6.9131	8.0081	6.5934	6.1464	8.4445	5.9803	6.9777	5.7026	5.2999
	10	12.2530	8.6585	9.8224	7.8808	7.4816	6.8473	4.9515	5.7368	4.7232	4.4041	6.0337	4.2730	4.9860	4.0748	3.7882
SSSC	1	131.3893	92.1398	107.4444	84.1078	78.2743	67.4175	48.3327	56.3278	45.1621	42.0782	61.5891	43.4162	50.8897	40.6728	37.7653
	5	14.2760	9.9414	11.6218	9.0442	8.4269	7.3315	5.2243	6.1060	4.8674	4.5403	6.6757	4.6794	5.4993	4.3735	4.0657
	10	10.2070	7.1008	8.3022	6.4563	6.0178	5.2495	3.7375	4.3704	3.4809	3.2478	4.7724	3.3431	3.9303	3.1237	2.9047
SSSS	1	96.5252	70.1503	77.2909	63.8697	61.4569	49.6833	35.7427	40.5256	32.9154	31.2053	46.4534	32.8783	37.5671	30.4976	28.7790
	2	29.4615	21.3692	23.5499	19.4430	18.7157	15.1686	10.8872	12.3507	10.0162	9.5005	14.1781	10.0119	11.4458	9.2795	8.7609
	5	10.5016	7.5857	8.3618	6.8916	6.6404	5.4122	3.8650	4.3895	3.5480	3.3692	5.0534	3.5506	4.0637	3.2852	3.1051
	10	7.5098	5.4210	5.9744	4.9238	4.7459	3.8720	2.7625	3.1378	2.5349	2.4079	3.6129	2.5359	2.9029	2.3458	2.2179
CSCF	1	70.1988	56.5506	58.3546	54.0124	53.7050	51.8709	41.8435	43.0339	40.0555	39.9189	24.7639	20.7644	21.1185	20.1602	20.1392
	5	7.0293	5.6656	5.8443	5.4139	5.3859	5.1869	4.1983	4.3134	4.0240	4.0107	2.3854	2.0101	2.0422	1.9542	1.9524
	10	4.9339	3.9758	4.1008	3.7990	3.7800	3.6501	2.9543	3.0352	2.8313	2.8220	1.6582	1.3983	1.4204	1.3595	1.3582
SCSF	1	47.7442	37.5004	38.8497	35.3010	35.1350	25.2329	19.2799	20.5129	17.8473	17.4449	15.0052	12.1085	12.5159	11.5411	11.4534
	5	4.6507	3.6617	3.7922	3.4495	3.4340	2.4897	1.9168	2.0304	1.7835	1.7474	1.4485	1.1759	1.2137	1.1242	1.1158
	10	3.2781	2.5828	2.6745	2.4336	2.4228	1.7608	1.3572	1.4368	1.2636	1.2383	1.0171	0.8267	0.8531	0.7908	0.7849
SFSF	1	46.1659	36.0414	37.7156	33.9813	33.3979	22.6114	16.5721	18.3871	15.6699	14.8772	14.5529	11.7133	12.1329	11.1951	11.1033
	5	4.5035	3.5279	3.6902	3.3332	3.2745	2.2742	1.6994	1.8510	1.6024	1.5403	1.4049	1.1376	1.1762	1.0901	1.0815
	10	3.1759	2.4900	2.6041	2.3533	2.3120	1.6112	1.2068	1.3118	1.1378	1.0952	0.9866	0.7998	0.8268	0.7668	0.7608
SSSF	1	47.6452	37.3267	38.7625	35.0865	34.8493	23.6001	17.9947	19.1630	16.5440	16.2057	14.7132	11.8955	12.2622	11.3176	11.2619
	2	14.0801	11.0410	11.4615	10.3820	10.3145	7.0081	5.3582	5.6940	4.9341	4.8389	4.3331	3.5094	3.6159	3.3419	3.3257
	5	4.6492	3.6546	3.7906	3.4397	3.4192	2.3393	1.7994	1.9037	1.6628	1.6347	1.4189	1.1541	1.1877	1.1011	1.0960
	10	3.2781	2.5789	2.6743	2.4279	2.4137	1.6549	1.2746	1.3475	1.1786	1.1592	0.9963	0.8113	0.8347	0.7745	0.7709
CFFF	1	15.3929	11.3382	13.0263	11.0145	10.1897	5.2255	3.9407	4.6514	4.0611	3.6992	1.7917	1.3297	1.5563	1.3313	1.2161
	2	4.5639	3.3641	3.8644	3.2689	3.0236	1.5885	1.1980	1.4136	1.2342	1.1244	0.5364	0.3982	0.4658	0.3984	0.3640
	5	1.5211	1.1234	1.2896	1.0921	1.0100	0.5612	0.4231	0.4990	0.4355	0.3969	0.1829	0.1358	0.1587	0.1357	0.1240
	10	1.0748	0.7944	0.9116	0.7722	0.7144	0.4024	0.3032	0.3577	0.3121	0.2844	0.1300	0.0966	0.1128	0.0964	0.0882

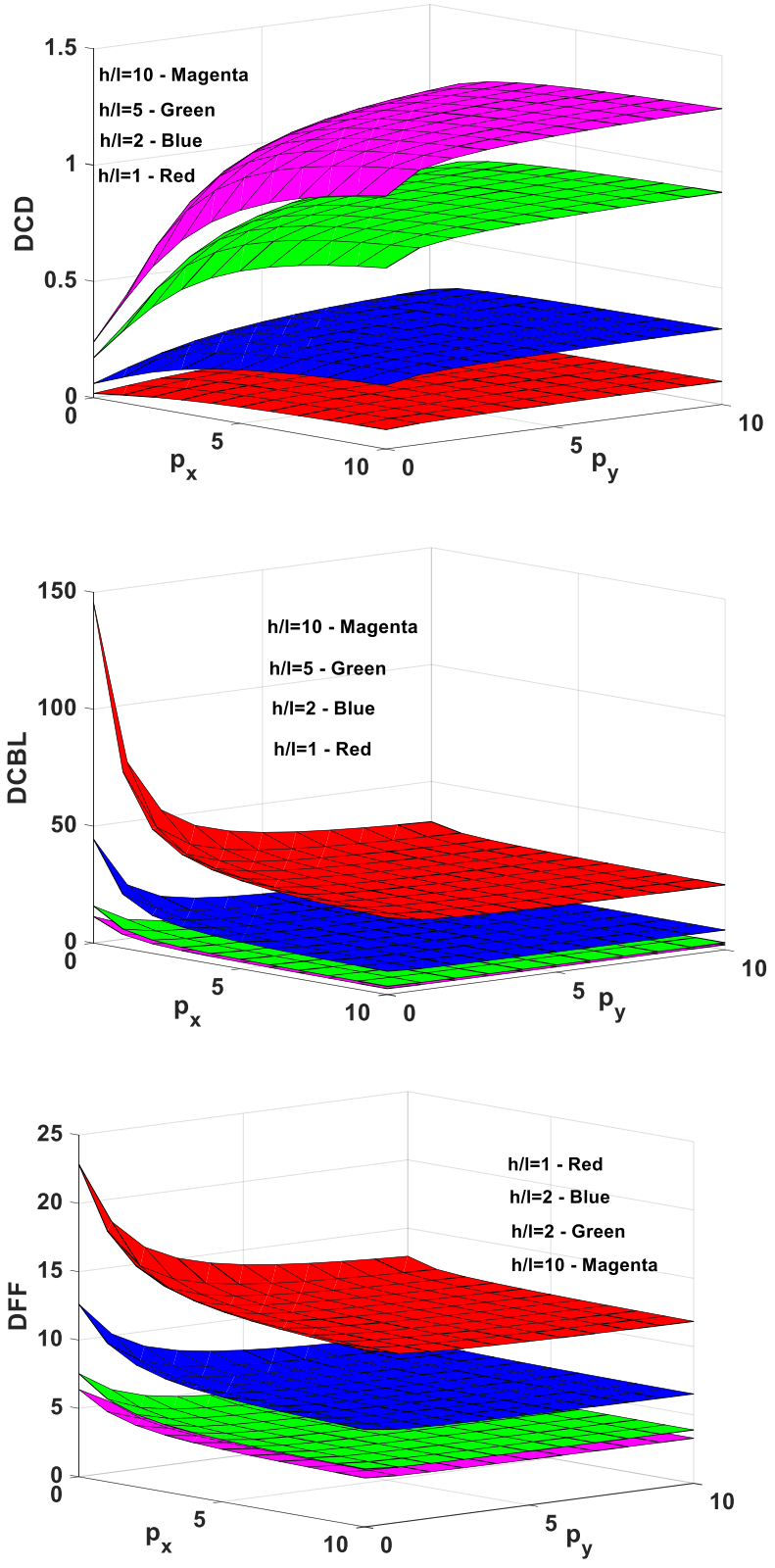

Figure 6. DCDs (sinusoidally distributed load), DCBLs (biaxial) and DFFs of SSSS 2D-FG microplates with respect to p_x and p_y $(a/h = 10,\ h/\ell_m = 1,2,8)$

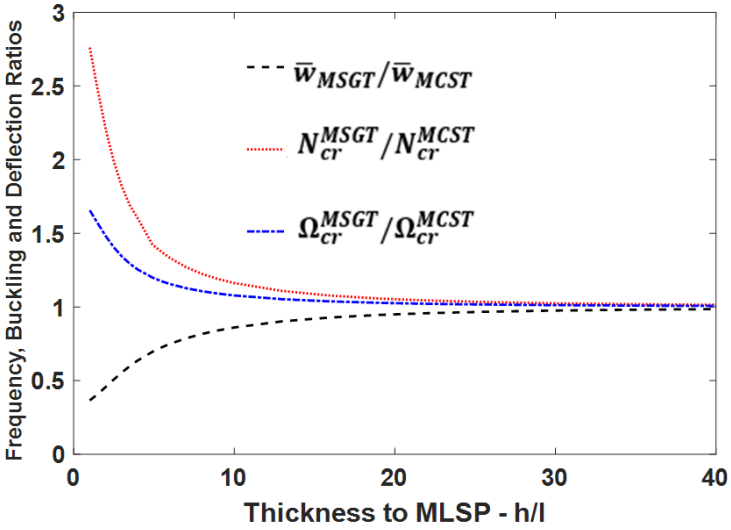

a) SSSS

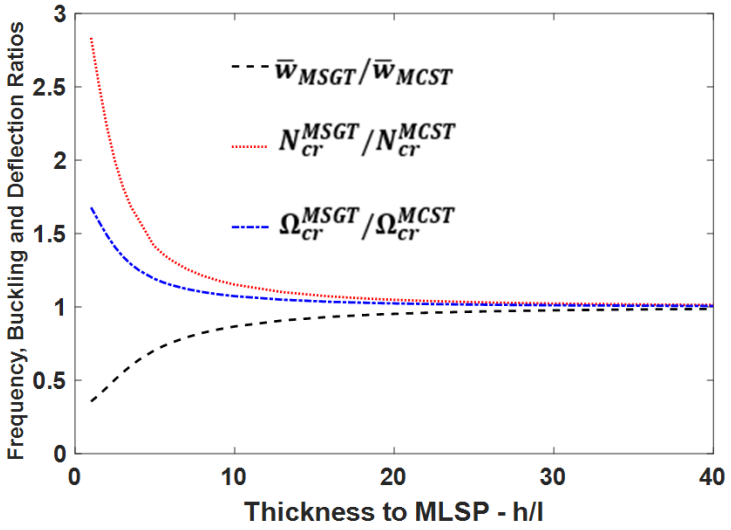

b) SCSC

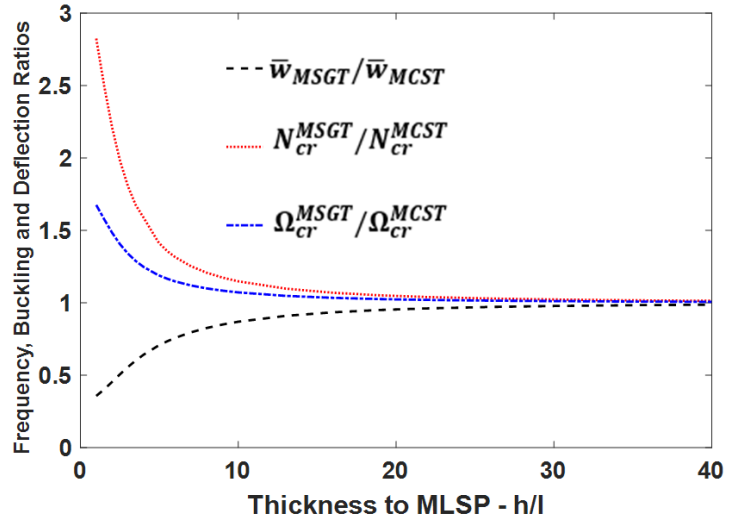

c) CCCC

Figure 7. Comparison between effect of the MCST and MSGT for SSSS, SCSC, and CCCC 2D-FG microplates ($a/h = 10, p_x = p_y = 5$) (uniformly distributed load)

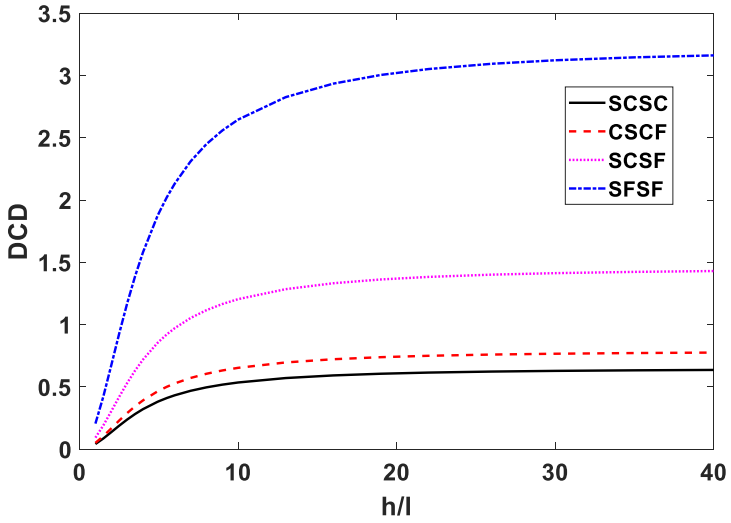

a) DCD

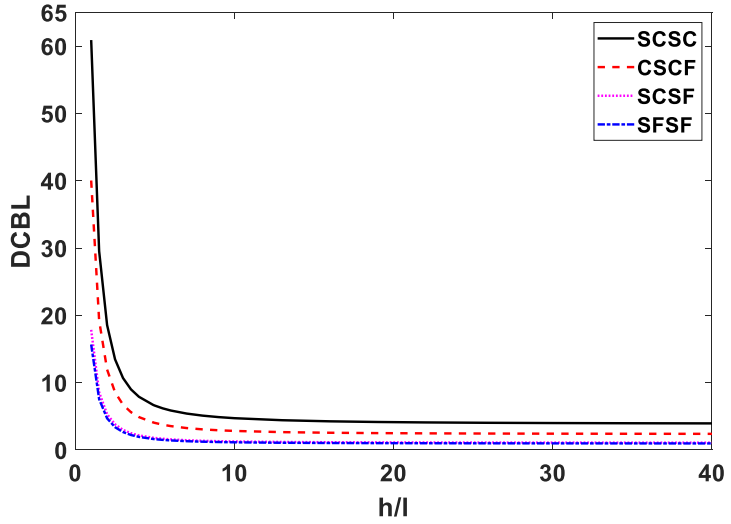

b) DCBL

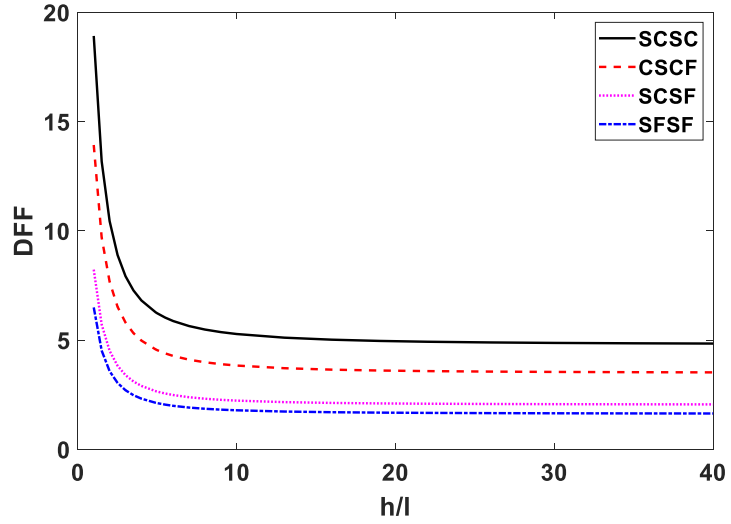

c) DFF

Figure 8. DCDs (sinusoidally distributed load), DCBLs (biaxial) and DFFs of SCSC, CSCF, SCSF and SFSF 2D-FG microplates with respect to h/ℓ_m, $p_x = 5$ and $p_y = 1$ $(a/h = 10)$

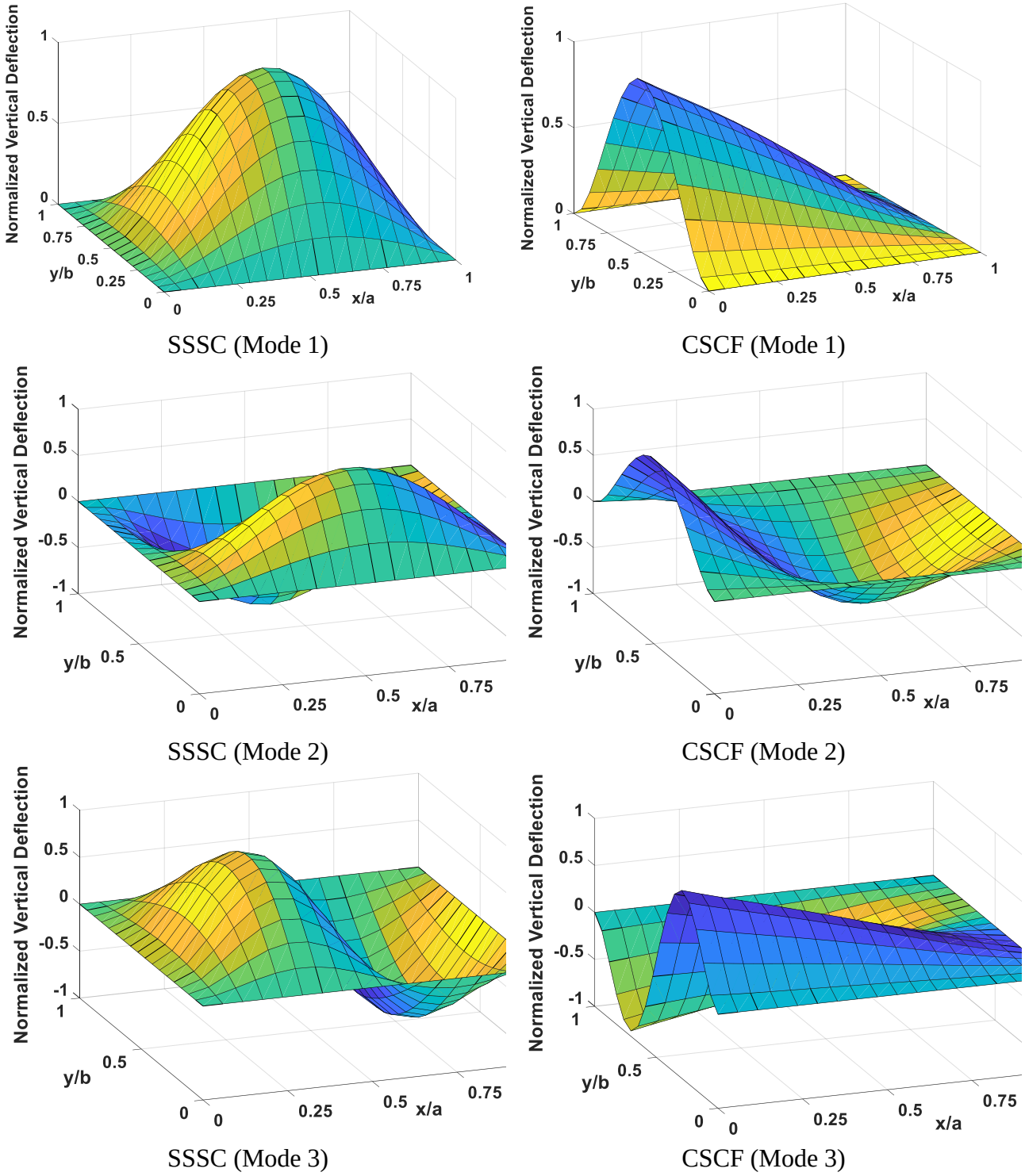

Figure 9. The first three vibration mode shapes of SSSC and CSCF 2D-FG microplates ($a/h = 10, h/\ell_m = 1, p_x = 10, p_y = 1$)

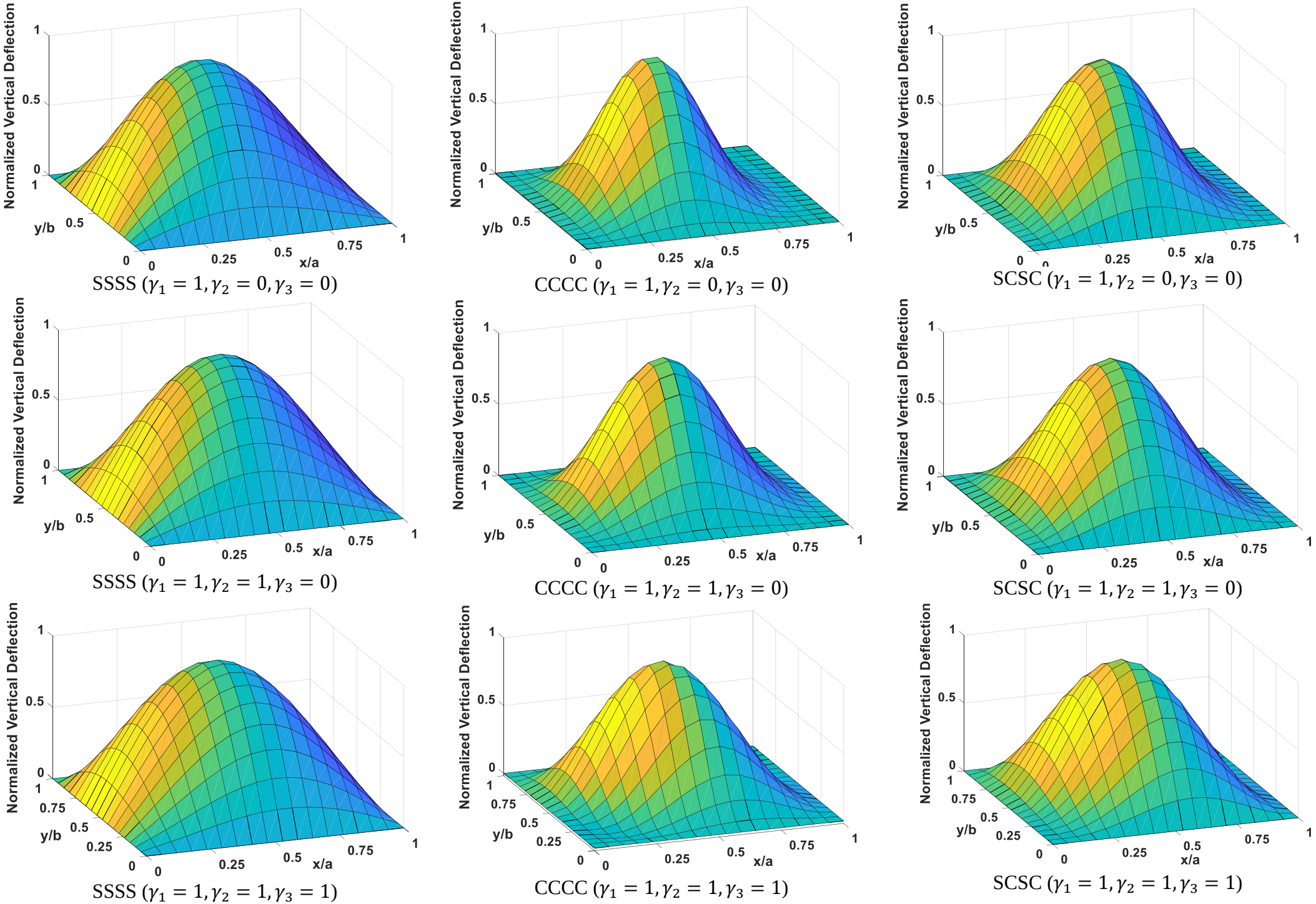

Figure 10. Buckling mode shapes of SSSS, CCCC and SCSC of 2D-FG microplates ($a/h = 10, h/\ell_m = 1, p_x = 10, p_y = 1$)

4.3 3D FG microplates

Due to no available results for the 3D-FG microplates, verification is carried out for their structural responses without the size effect ($\ell = 0$). The first four natural frequencies of the Al/Al_2O_3 and buckling loads of $SUS304/Si_3N_4$ 3D-plates are provided in Tables 15 and 16. They are computed from IGA based on generalized shear deformation theory (GSDT [65]) and 3D elasticity theory [67]. Again, the obtained results are very close to the previous studies.

The DCDs, DCBLs and DFFs of the 3D-FG square microplates for nine BCs are presented in Tables 17 and 18 with respect to the variation of the gradient indexes in tri-directions, h/ℓ and a/h. For the first time, the flexural, stability and free vibration responses of the 3D-FG square microplates are investigated, and the presented results can be used for the benchmark studies.

The results of SSSS, SSSC, SCSC and CCCC 3D-FG microplates are also investigated with respect to the gradient index for tri-directions ($p_x = p_y = p_z = p$) in Fig. 11. It is clear that with the inclusion of the clamped edge leads to have a decrement in the DCDs and an increment in the DCBLs and DFFs. In addition, the effect of the gradient index becomes more visible with the inclusion of clamped edge for DCBLs and DFFs. However, this effect on the DCDs is more pronounced for the microplates with the inclusion of simply supported edge than the inclusion of clamped edge. While $p \geq 6$, the variations of the DCBLs and DFFs are not observed, but those of the DCD are still remarkable.

And finally, the biaxial buckling mode shapes of SCSF, CSCF, SFSF, SSSF, CFFF 3D-FG microplates are revealed in Fig. 12.

Table 15. Verification studies on first four DFFs $\left(\Omega = \omega \frac{a^2}{h}\sqrt{\frac{\rho_m}{E_m}}\right)$ of the Al/Al_2O_3 3D-FG square plates for different BCs, p_x, p_y, p_z, $(a/h = 20)$.

BCs	Theory	Mode	$p_x = p_y = p_z = p$			
			0	1	2	5
SSSS	Present - $\varepsilon_z \neq 0$	1	5.9219	3.9840	3.6029	3.3081
	IGA – 3D Elasticity ([67])		5.9219	3.9430	3.5680	3.2946
	Present - $\varepsilon_z \neq 0$	2	14.6204	9.8297	8.7416	7.9085
	IGA – 3D Elasticity ([67])		14.6199	9.7323	8.6701	7.8877
	Present - $\varepsilon_z \neq 0$	3	23.1081	15.0947	13.4416	12.3539
	IGA – 3D Elasticity ([67])		23.1084	14.9711	13.3670	12.3326
	Present - $\varepsilon_z \neq 0$	4	28.6697	19.3571	17.1036	15.4799
	IGA – 3D Elasticity ([67])		28.6674	19.1597	16.9738	15.4453
CCCC	Present - $\varepsilon_z \neq 0$	1	10.8216	6.8464	6.2929	5.9508
	IGA – 3D Elasticity ([67])		10.6742	6.6877	6.1573	5.8471
	Present - $\varepsilon_z \neq 0$	2	21.6826	14.1338	12.8143	11.8230
	IGA – 3D Elasticity ([67])		21.3315	13.7138	12.4436	11.5707
	Present - $\varepsilon_z \neq 0$	3	31.3898	20.3517	18.3374	16.8998
	IGA – 3D Elasticity ([67])		30.8881	19.7475	17.8457	16.5753
	Present - $\varepsilon_z \neq 0$	4	37.8699	25.0909	22.6301	20.6586
	IGA – 3D Elasticity ([67])		37.3124	24.3297	21.8867	20.1766

Table 16. Verification studies on the DCBLs $\left(N_{cr} = N_0 \frac{a^2}{\pi^2 D_c}\right)$ of the $SUS304/Si_3N_4$ 3D-FG square plates for different BCs ($p_x = p_y = 1$, $D_c = \frac{E_c h^3}{12(1-\nu_c^2)}$) with Mori-Tanaka scheme.

BCs	Theory	a/h	p_z			
			0	1	2	5
SSSS (1,0,0)	Present - $\varepsilon_z \neq 0$	10	2.5896	2.4388	2.4070	2.3717
	IGA – GSDT ([65])		2.6003	2.4470	2.4155	2.3819
	Present - $\varepsilon_z \neq 0$	100	2.7508	2.5903	2.5588	2.5233
	IGA – GSDT ([65])		2.7509	2.5877	2.5564	2.5228
SSSS (1,1,0)	Present - $\varepsilon_z \neq 0$	10	1.2974	1.2201	1.2039	1.1861
	IGA – GSDT ([65])		1.3027	1.2241	1.2081	1.1911
	Present - $\varepsilon_z \neq 0$	100	1.3772	1.2956	1.2797	1.2618
	IGA – GSDT ([65])		1.3772	1.2943	1.2785	1.2615
CFFF (1,0,0)	Present - $\varepsilon_z \neq 0$	10	0.4002	0.3776	0.3730	0.3681
		100	0.4054	0.3826	0.3782	0.3733
CFFF (1,1,0)	Present - $\varepsilon_z \neq 0$	10	0.1577	0.1515	0.1502	0.1488
	IGA – GSDT ([65])		0.1552	0.1492	0.1480	0.1467
	Present - $\varepsilon_z \neq 0$	100	0.1587	0.1525	0.1513	0.1499
	IGA – GSDT ([65])		0.1572	0.1511	0.1500	0.1487

Table 17. DCDs (sinusoidally distributed load) and DFFs of the Al/Al_2O_3 3D-FG square microplates for various BCs, $a/h, p_x, p_y, p_z$ *and* h/ℓ

BCs	h/ℓ	DCD						DFF					
		$a/h=5$			$a/h=10$			$a/h=5$			$a/h=10$		
		$p_x=p_y=p_z=p$											
		1	2	5	1	2	5	1	2	5	1	2	5
CCCC	1	0.0342	0.0449	0.0508	0.0261	0.0344	0.0387	21.4919	19.2848	18.2396	24.1196	21.5994	20.4744
	2	0.1139	0.1495	0.1687	0.0860	0.1129	0.1270	11.3856	10.2246	9.6857	13.2862	11.9199	11.3024
	5	0.3322	0.4354	0.4881	0.2452	0.3182	0.3565	6.6258	5.9570	5.6576	7.8617	7.0920	6.7370
	10	0.4694	0.6138	0.6861	0.3433	0.4425	0.4951	5.5465	4.9928	4.7488	6.6433	6.0111	5.7146
SCSC	1	0.0451	0.0591	0.0669	0.0360	0.0474	0.0533	17.5196	15.7398	14.8861	19.8317	17.7617	16.8389
	2	0.1494	0.1956	0.2206	0.1185	0.1554	0.1746	9.6102	8.6379	8.1839	10.9271	9.8054	9.3024
	5	0.4291	0.5603	0.6281	0.3368	0.4364	0.4886	5.6490	5.0863	4.8319	6.4812	5.8472	5.5570
	10	0.6012	0.7829	0.8750	0.4711	0.6064	0.6781	4.7573	4.2898	4.0806	5.4794	4.9582	4.7156
SSSC	1	0.0595	0.0773	0.0867	0.0499	0.0649	0.0724	15.4666	13.8456	13.0098	16.4479	14.7364	13.9724
	2	0.1961	0.2548	0.2854	0.1638	0.2126	0.2370	8.1986	7.3645	6.9684	9.0751	8.1435	7.7222
	5	0.5571	0.7224	0.8064	0.4619	0.5945	0.6622	4.8531	4.3647	4.1359	5.4030	4.8691	4.6182
	10	0.7771	1.0052	1.1204	0.6450	0.8259	0.9200	4.0991	3.6913	3.5002	4.5707	4.1292	3.9165
SSSS	1	0.0783	0.1029	0.1029	0.0679	0.0898	0.1006	12.7496	11.4135	10.8182	13.8703	12.3732	11.7497
	2	0.2574	0.3381	0.3381	0.2229	0.2937	0.3291	7.0273	6.2925	5.9673	7.6566	6.8394	6.4952
	5	0.7272	0.9528	0.9528	0.6275	0.8201	0.9189	4.1728	3.7418	3.5524	4.5639	4.0919	3.8863
	10	1.0128	1.3236	1.3236	0.8774	1.1408	1.2785	3.5277	3.1674	3.0083	3.8588	3.4676	3.2931
CSCF	1	0.0517	0.0673	0.0760	0.0407	0.0532	0.0596	13.4449	12.3407	11.9469	15.1263	13.9296	13.5363
	2	0.1706	0.2223	0.2501	0.1340	0.1742	0.1950	7.3696	6.7771	6.5712	8.3177	7.6756	7.4635
	5	0.4881	0.6338	0.7089	0.3803	0.4881	0.5444	4.3252	3.9903	3.8779	4.9013	4.5478	4.4300
	10	0.6833	0.8850	0.9870	0.5314	0.6778	0.7548	3.6372	3.3612	3.2699	4.1356	3.8466	3.7489
SCSF	1	0.0928	0.1224	0.1393	0.0805	0.1067	0.1209	8.3169	7.5369	7.2545	8.8522	8.0109	7.7137
	2	0.3067	0.4032	0.4573	0.2663	0.3506	0.3964	4.5581	4.1368	3.9842	4.8422	4.3943	4.2352
	5	0.8798	1.1452	1.2893	0.7650	0.9910	1.1144	2.6566	2.4262	2.3431	2.8223	2.5795	2.4911
	10	1.2321	1.5952	1.7911	1.0742	1.3809	1.5505	2.2355	2.0478	1.9791	2.3761	2.1785	2.1046
SFSF	1	0.1929	0.2570	0.2881	0.1741	0.2332	0.2604	6.5432	5.8206	5.5354	6.9217	6.1343	5.8412
	2	0.6309	0.8384	0.9399	0.5716	0.7624	0.8519	3.6106	3.2131	3.0553	3.8068	3.3819	3.2192
	5	1.7671	2.3295	2.6125	1.6152	2.1296	2.3852	2.1376	1.9120	1.8176	2.2459	2.0075	1.9092
	10	2.4574	3.2264	3.6206	2.2604	2.9641	3.3247	1.8068	1.6201	1.5396	1.8953	1.6988	1.6147
SSSF	1	0.1274	0.1665	0.1874	0.1141	0.1493	0.1672	7.7021	6.9784	6.7124	8.1460	7.3802	7.1097
	2	0.4193	0.5464	0.6138	0.3759	0.4897	0.5477	4.2241	3.8344	3.6921	4.4645	4.0545	3.9087
	5	1.1896	1.5382	1.7201	1.0694	1.3765	1.5363	2.4742	2.2582	2.1796	2.6141	2.3882	2.3058
	10	1.6590	2.1362	2.3859	1.4979	1.9171	2.1396	2.0857	1.9084	1.8428	2.2035	2.0182	1.9486
CFFF	1	0.6539	0.7413	0.7559	0.6146	0.6921	0.7040	2.1679	2.0580	2.0356	2.2139	2.1064	2.1024
	2	2.1466	2.4310	2.4790	2.0202	2.2717	2.3114	1.1967	1.1373	1.1336	1.2209	1.1630	1.1606
	5	6.0476	6.8254	6.9627	5.7024	6.3866	6.5039	0.7129	0.6795	0.6771	0.7262	0.6939	0.6920
	10	8.4157	9.4761	9.6666	7.9342	8.8690	9.0350	0.6040	0.5766	0.5744	0.6149	0.5884	0.5867

Table 18. DCBLs of the Al/Al_2O_3 3D-FG square microplates for various BCs, p_x, p_y, p_z and h/ℓ $(a/h = 10)$

BCs	h/ℓ	$(\gamma_1 = 1, \gamma_2 = 0, \gamma_3 = 0)$			$(\gamma_1 = 1, \gamma_2 = 1, \gamma_3 = 0)$			$(\gamma_1 = 1, \gamma_2 = 1, \gamma_3 = 1)$		
		$p_x = p_y = p_z = p$								
		1	2	5	1	2	5	1	2	5
CCCC	1	175.3083	136.5121	123.5047	95.8715	74.0879	66.5191	80.4783	61.9939	56.3023
	2	53.1287	41.4907	37.5847	29.0932	22.5624	20.2846	24.3684	18.8334	17.1218
	5	18.5575	14.6151	13.2777	10.2117	7.9990	7.2131	8.4973	6.6296	6.0399
	10	13.1679	10.4191	9.4759	7.2736	5.7279	5.1708	6.0285	4.7276	4.3097
SCSC	1	125.5015	96.8767	86.9676	70.8674	55.5185	49.9444	62.7678	48.8834	44.5088
	2	38.1018	29.5133	26.5276	21.5327	16.9260	15.2459	19.0508	14.8845	13.5649
	5	13.3859	10.4683	9.4359	7.5871	6.0202	5.4386	6.6900	5.2741	4.8159
	10	9.5169	7.4814	6.7502	5.4117	4.3164	3.9039	4.7621	3.7729	3.4471
SSSC	1	100.1822	75.3041	65.4284	52.8245	40.6733	36.0019	48.3257	37.0976	33.2487
	5	10.7742	8.2054	7.1367	5.6971	4.4365	3.9309	5.1942	4.0300	3.6157
	10	7.6773	5.8792	5.1145	4.0676	3.1827	2.8203	3.7033	2.8863	2.5898
SSSS	1	77.4609	60.6738	54.6938	39.2471	30.4658	27.3528	36.7160	28.4200	25.8041
	2	23.6060	18.5342	16.7118	11.9607	9.3073	8.3578	11.1838	8.6764	7.8792
	5	8.3829	6.6255	5.9778	4.2482	3.3281	2.9897	3.9663	3.0965	2.8129
	10	5.9838	4.7487	4.2850	3.0327	2.3858	2.1432	2.8291	2.2175	2.0142
CSCF	1	62.1815	54.3957	52.9858	46.0168	40.4679	39.6119	22.4829	20.3317	20.1076
	5	6.1976	5.4612	5.3242	4.5875	4.0680	3.9831	2.1641	1.9720	1.9497
	10	4.3414	3.8349	3.7387	3.2217	2.8638	2.8030	1.5028	1.3724	1.3564
SCSF	1	39.5819	33.4387	31.0644	21.1514	17.5852	16.6303	13.2049	11.5686	11.2834
	2	11.6716	9.8872	9.1825	6.2705	5.2414	4.9660	3.8891	3.4178	3.3341
	5	3.8306	3.2706	3.0386	2.0840	1.7650	1.6781	1.2729	1.1277	1.1004
	10	2.6923	2.3098	2.1487	1.4702	1.2520	1.1907	0.8925	0.7936	0.7743
SFSF	1	39.5819	33.4387	31.0644	18.5207	14.6532	13.3163	12.8082	11.1681	10.6502
	2	11.6716	9.8872	9.1825	5.5486	4.4284	4.0300	3.7732	3.3001	3.1521
	5	3.8306	3.2706	3.0386	1.8826	1.5343	1.4021	1.2359	1.0895	1.0442
	10	2.6923	2.3098	2.1487	1.3330	1.0938	0.9999	0.8667	0.7669	0.7358
SSSF	1	41.3634	35.4755	34.3369	19.6745	16.2574	15.2804	12.9707	11.3863	11.1234
	5	4.0189	3.4874	3.3805	1.9602	1.6511	1.5626	1.2509	1.1095	1.0840
	10	2.8277	2.4637	2.3875	1.3854	1.1729	1.1104	0.8774	0.7809	0.7627
CFFF	1	12.4921	9.9942	9.1883	4.3976	3.6230	3.4293	1.4726	1.1884	1.1040
	2	3.6893	2.9658	2.7273	1.3322	1.1015	1.0421	0.4390	0.3558	0.3304
	5	1.2155	0.9912	0.9123	0.4663	0.3891	0.3677	0.1479	0.1214	0.1127
	10	0.8529	0.7017	0.6462	0.3327	0.2790	0.2635	0.1045	0.0864	0.0802

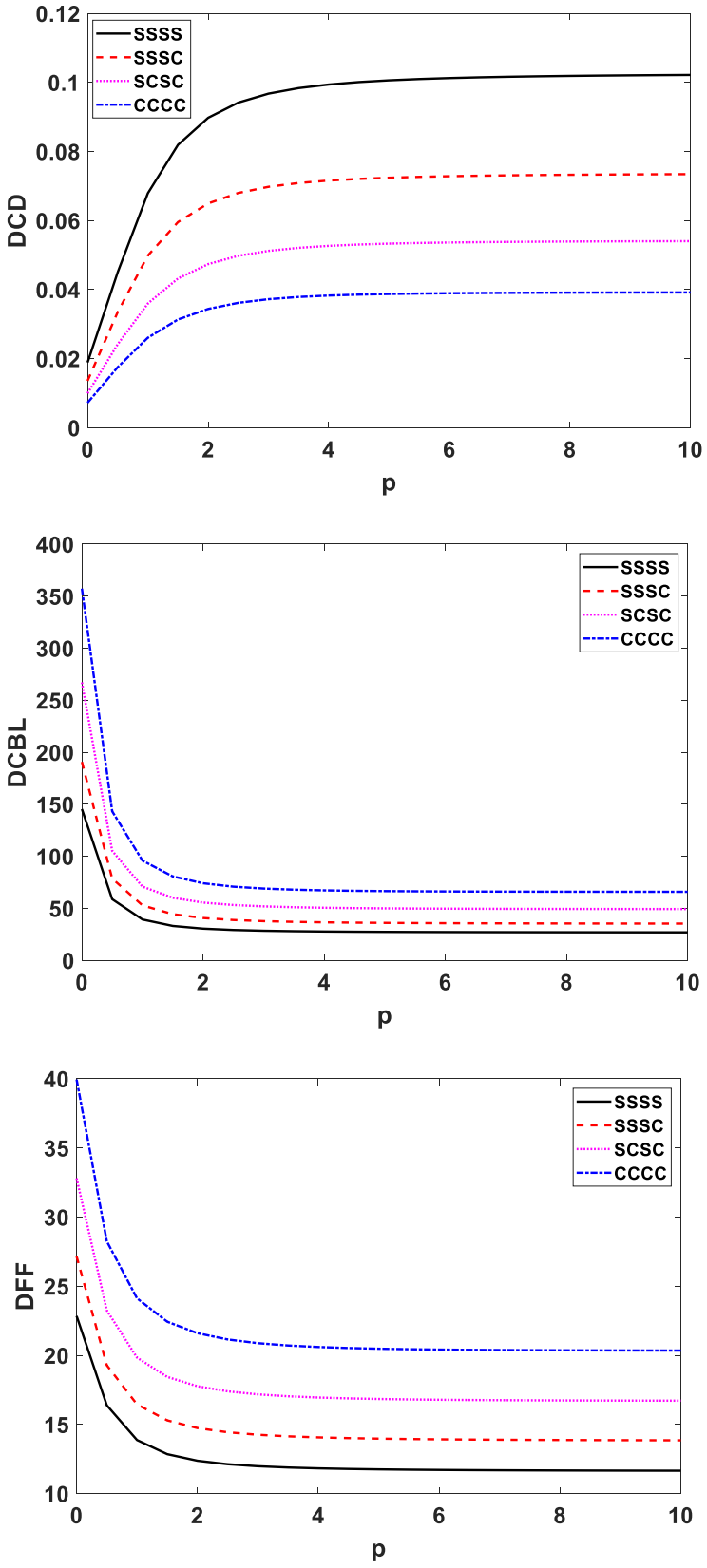

Figure 11. DCDs (sinusoidally), DCBLs (biaxial) and DFFs of CCCC, SCSC, SSSC and SSSS 3D-FG microplates with respect to $p_x = p_y = p_z = p$ $(a/h = 10, h/\ell_m = 1)$

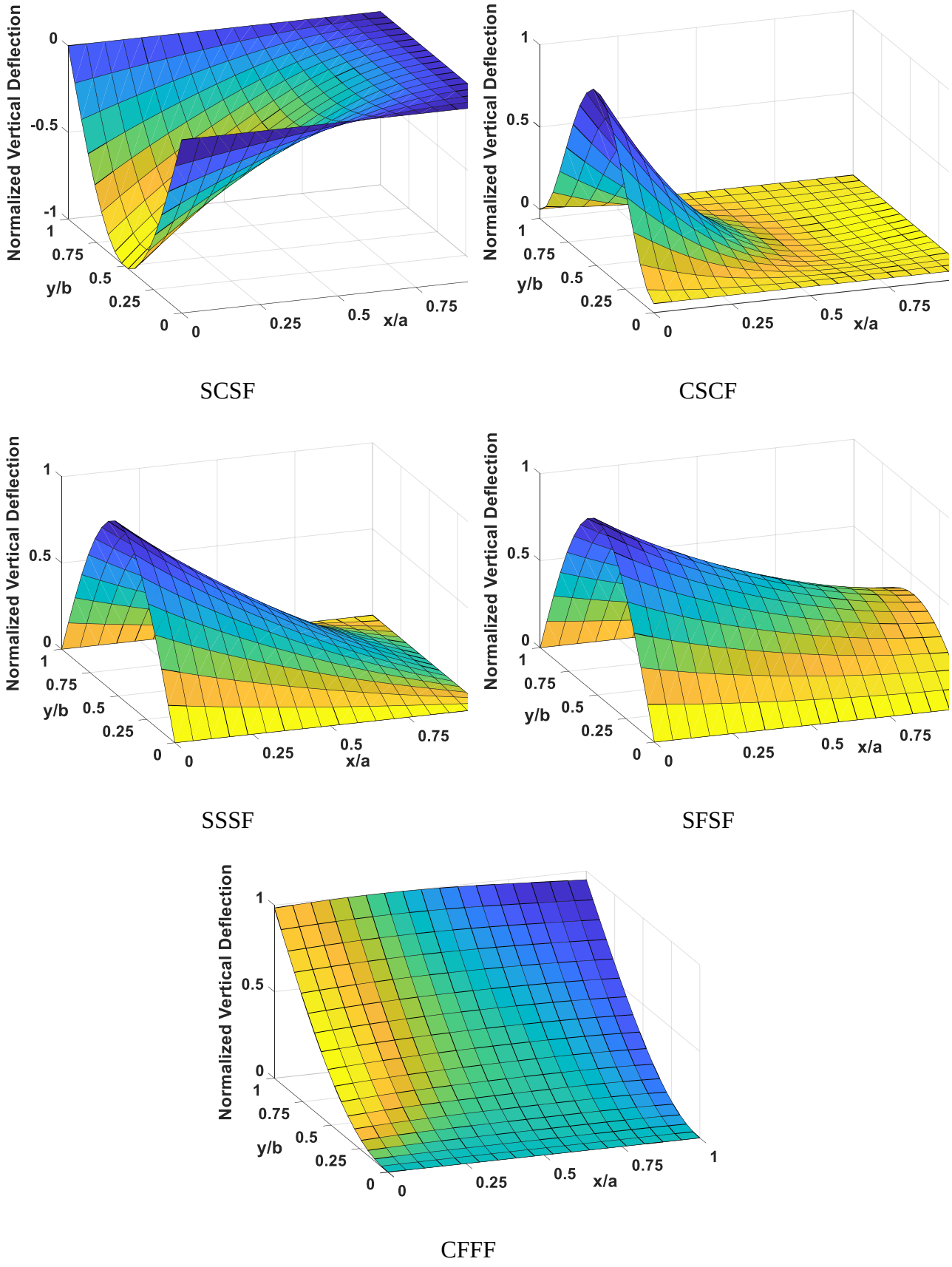

Figure 12. The biaxial buckling mode shapes of SCSF, CSCF, SFSF, SSSF and CFFF 3D-FG microplates ($a/h = 10, h/\ell_m = 1, p_x = 10, p_y = p_z = 1$)

5. Conclusion

The structural behaviors of the multi-directional FG microplates are investigated by using the MSGT and FEM formulation. The material properties vary continuously both in-plane and through-thickness directions. The effect of the material gradient indexes in the x-, y and z-directions are evaluated for nine different BCs with respect to variation of the a/h and h/ℓ. The structural behaviours of the 3D-FG strain gradient microplates can be controlled by the p_x, p_y and p_z. New results for the deflections, natural frequencies and buckling loads of multi-directional FG microplates are presented as benchmark for the future studies. Some of important outputs can be expresses by:

- MSGT should be used for vibration and buckling analysis of the FG microplates when $h/\ell \leq 20$ and bending one when $h/\ell \leq 40$.
- The effect of the p_x, p_y and p_z on the DCDs, DCBLs, and DFFs should be evaluated by considering the BCs and h/ℓ.
- The location of the maximum deflection on the multi-directional FG microplates can be controlled by selecting the p_x and p_y.
- The vibration and buckling mode shapes can be modified by changing the material properties in in-plane directions.

6. Acknowledgement

The first author thanks to Bahcesehir University. This study was funded by Scientific Research Projects Commission of Bahcesehir University. Project number: BAP.2020-1.07.

References

[1] R. A. Toupin, Elastic materials with couple-stresses, Archive for Rational Mechanics and Analysis 11 (1) (1962) 385-414. *doi:https://doi.org/10.1007/BF00253945*.

[2] R. D. Mindlin, H. F. Tiersten, Effects of couple-stresses in linear elasticity, Archive for Rational Mechanics and Analysis 11 (1) (1962) 415-448. *doi:https://doi.org/10.1007/BF00253946.*

[3] N. A. Fleck, J. W. Hutchinson, A phenomenological theory for strain gradient effects in plasticity, Journal of the Mechanics and Physics of Solids 41 (12) (1993) 1825-1857. *doi:10.1016/ 0022-5096(93)90072-N*.

[4] H.-T. Thai, T. P. Vo, T.-K. Nguyen, S.-E. Kim, A review of continuum mechanics models for size-dependent analysis of beams and plates, Composite Structures 177 (2017) 196-219. *doi: https://doi.org/10.1016/j.compstruct.2017.06.040*.

[5] F. Yang, A. Chong, D. Lam, P. Tong, Couple stress based strain gradient theory for elasticity, International Journal of Solids and Structures 39 (10) (2002) 2731 - 2743. *doi:http://dx.doi. org/10.1016/S0020-7683(02)00152-X*.

[6] D. C. C. Lam, F. Yang, A. C. M. Chong, J. Wang, P. Tong, Experiments and theory in strain gradient elasticity, Journal of the Mechanics and Physics of Solids 51 (8) (2003) 1477-1508. *doi:http://dx.doi.org/10.1016/S0022-5096(03)00053-X*.

[7] M. Mirsalehi, M. Azhari, H. Amoushahi, Buckling and free vibration of the FGM thin micro-plate based on the modified strain gradient theory and the spline finite strip method, European Journal of Mechanics - A/Solids 61 (2017) 1 - 13. *doi:https://doi.org/10.1016/j.euromechsol. 2016.08.008*.

[8] A. Ashoori Movassagh, M. Mahmoodi, A micro-scale modelling of Kirchhoff plate based on modified strain-gradient elasticity theory, European Journal of Mechanics - A/Solids. 40 (2013) 50-59. *doi:10.1016/j.euromechsol.2012.12.008.*

[9] A. Li, S. Zhou, S. Zhou, B. Wang, A size-dependent model for bi-layered Kirchhoff micro-plate based on strain gradient elasticity theory, Composite Structures. 113 (2014) 272-280. *doi:10.1016/j.compstruct.2014.03.028.*

[10] M. Kandaz, H. Dal, Two novel Kirchhoff plate finite elements for the modified strain gradient theory, PAMM. 19 (2019). *doi:10.1002/pamm.201900194.*

[11] V. Borjalilou, M. Asghari, Thermoelastic damping in strain gradient microplates according to a generalized theory of thermoelasticity, Journal of Thermal Stresses. 43 (2020) 401-420. *doi:10.1080/01495739.2020.1722771.*

[12] J. Jiang, L. Wang, Vibration of functionally graded Mindlin plate based on a modified strain gradient elasticity theory, IOP Conference Series: Materials Science and Engineering. 531 (2019) 012023. *doi:10.1088/1757-899x/531/1/012023.*

[13] A. Ashoori, M. Mahmoodi, A nonlinear thick plate formulation based on the modified strain gradient theory, Mechanics of Advanced Materials and Structures. 25 (2017) 813-819. *doi:10.1080/15376494.2017.1308588.*

[14] M. Mohammadimehr, M. Emdadi, B. Rousta Navi, Dynamic stability analysis of microcomposite annular sandwich plate with carbon nanotube reinforced composite facesheets based on modified strain gradient theory, Journal of Sandwich Structures & Materials. 22 (2018) 1199-1234. *doi:10.1177/1099636218782770.*

[15] E. Arshid, S. Amir, A. Loghman, Static and dynamic analyses of FG-GNPs reinforced porous nanocomposite annular micro-plates based on MSGT, International Journal Of Mechanical Sciences. 180 (2020) 105656. *doi:10.1016/j.ijmecsci.2020.105656.*

[16] A. Ghasemi Ghalebahman, M. Bigdeli-Yeganeh, E. Cheloeian, M. Khademi-Kouhi, Free vibration of piezoelectric boron nitride nanotube-based composite cylindrical micropanel embedded in an elastic medium subjected to electric potential via modified strain gradient theory, Proceedings Of The Institution Of Mechanical Engineers, Part C: Journal Of Mechanical Engineering Science. 234 (2020) 2309-2328. *doi:10.1177/0954406220907369.*

[17] R. Ansari, R. Gholami, M. F. Shojaei, V. Mohammadi, M. A. Darabi, Thermal Buckling Analysis of a Mindlin Rectangular FGM Microplate Based on the Strain Gradient Theory, Journal of Thermal Stresses 36 (5) (2013) 446-465. *doi:10.1080/01495739.2013.770657*.

[18] R. Ansari, R. Gholami, M. F. Shojaei], V. Mohammadi, S. Sahmani, Bending, buckling and free vibration analysis of size-dependent functionally graded circular/annular microplates based on the modified strain gradient elasticity theory, European Journal of Mechanics - A/Solids 49 (2015) 251 - 267. *doi:https://doi.org/10.1016/j.euromechsol.2014.07.014*.

[19] A. G. Shenas, P. Malekzadeh, Free vibration of functionally graded quadrilateral microplates in thermal environment, Thin-Walled Structures 106 (2016) 294-315. *doi:https://doi.org/10.1016/j.tws.2016.05.001*.

[20] S. Sahmani, R. Ansari, On the free vibration response of functionally graded higher-order shear deformable microplates based on the strain gradient elasticity theory, Composite Structures 95 (2013) 430 - 442. *doi:http://dx.doi.org/10.1016/j.compstruct.2012.07.025*

[21] B. Zhang, Y. He, D. Liu, L. Shen, J. Lei, An efficient size-dependent plate theory for bending, buckling and free vibration analyses of functionally graded microplates resting on elastic foundation, Applied Mathematical Modelling 39 (13) (2015) 3814 - 3845. *doi:http: //dx.doi.org/10.1016/j.apm.2014.12.001*.

[22] B. Zhang, Y. He, D. Liu, J. Lei, L. Shen, L. Wang, A size-dependent third-order shear deformable plate model incorporating strain gradient effects for mechanical analysis of functionally graded circular/annular microplates, Composites Part B: Engineering 79 (2015) 553 - 580. *doi:https: //doi.org/10.1016/j.compositesb.2015.05.017*.

[23] T. Hughes, J. Cottrell, Y. Bazilevs, Isogeometric analysis: CAD, finite elements, NURBS, exact geometry and mesh refinement, Computer Methods in Applied Mechanics and Engineering 194 (39) (2005) 4135 - 4195. *doi:https://doi.org/10.1016/j.cma.2004.10.008*.

[24] T. N. Nguyen, T. D. Ngo, H. Nguyen-Xuan, A novel three-variable shear deformation plate formulation: Theory and Isogeometric implementation, Computer Methods in Applied Mechanics and Engineering, 326, 2017, 376-401, https://doi.org/10.1016/j.cma.2017.07.024.

[25] Q. H. Nguyen, L. B. Nguyen, H. B. Nguyen, H. Nguyen-Xuan, A three-variable high order shear deformation theory for isogeometric free vibration, buckling and instability analysis of FG porous plates reinforced by graphene platelets, Composite Structures, 245, 2020, 112321, https://doi.org/10.1016/j.compstruct.2020.112321.

[26] S. Thai, H.-T. Thai, T. P. Vo, V. I. Patel, Size-dependant behaviour of functionally graded microplates based on the modified strain gradient elasticity theory and isogeometric analysis, Computers and Structures 190 (2017) 219 - 241. *doi:https://doi.org/10.1016/j.compstruc. 2017.05.014*.

[27] S. Thai, H.-T. Thai, T. P. Vo, H. Nguyen-Xuan, Nonlinear static and transient isogeometric analysis of functionally graded microplates based on the modified strain gradient theory, Engineering Structures 153 (2017) 598 - 612. *doi:https://doi.org/10.1016/j.engstruct.2017.10.002*.

[28] S. Thai, H.-T. Thai, T. P. Vo, J. Reddy, Post-buckling of functionally graded microplates under mechanical and thermal loads using isogeomertic analysis, Engineering Structures 150 (2017) 905 - 917. *doi:https://doi.org/10.1016/j.engstruct.2017.07.073*.

[29] C. H. Thai, A. Ferreira, H. Nguyen-Xuan, Isogeometric analysis of size-dependent isotropic and sandwich functionally graded microplates based on modified strain gradient elasticity theory, Composite Structures 192 (2018) 274 - 288. *doi:https://doi.org/10.1016/j.compstruct. 2018.02.060*.

[30] C. H. Thai, A. Ferreira, T. Rabczuk, H. Nguyen-Xuan, Size-dependent analysis of FG-CNTRC microplates based on modified strain gradient elasticity theory, European Journal of Mechanics - A/Solids 72 (2018) 521 - 538. *doi:https://doi.org/10.1016/j.euromechsol.2018.07.012*.

[31] A. Farzam, B. Hassani, Size-dependent analysis of FG microplates with temperature-dependent material properties using modified strain gradient theory and isogeometric approach, Composites Part B: Engineering 161 (2019) 150 - 168. *doi:https://doi.org/10.1016/j.compositesb.2018.10.028*.

[32] H. X. Nguyen, E. Atroshchenko, T. Ngo, H. Nguyen-Xuan, T. P. Vo, Vibration of cracked functionally graded microplates by the strain gradient theory and extended isogeometric analysis, Engineering Structures 187 (2019) 251 - 266. *doi:https://doi.org/10.1016/j.engstruct.2019.02.032*.

[33] B. Akgöz, Ö. Civalek, A microstructure-dependent sinusoidal plate model based on the strain gradient elasticity theory, Acta Mechanica. 226 (2015) 2277-2294. *doi:10.1007/s00707-015-1308-4*.

[34] Q. Li, D. Wu, W. Gao, F. Tin-Loi, Size-dependent instability of organic solar cell resting on Winkler–Pasternak elastic foundation based on the modified strain gradient theory, International Journal Of Mechanical Sciences. 177 (2020) 105306. *doi:10.1016/j.ijmecsci.2019.105306.*

[35] M. Arefi, E. Mohammad-Rezaei Bidgoli, T. Rabczuk, Thermo-mechanical buckling behavior of FG GNP reinforced micro plate based on MSGT, Thin-Walled Structures. 142 (2019) 444-459. *doi:10.1016/j.tws.2019.04.054.*

[36] E. Carrera, S. Brischetto, M. Cinefra, M. Soave, Effects of thickness stretching in functionally graded plates and shells, Composites Part B: Engineering 42 (2) (2011) 123 - 133. *doi:http://dx.doi.org/10.1016/j.compositesb.2010.10.005*.

[37] J. Lei, Y. He, B. Zhang, D. Liu, L. Shen, S. Guo, A size-dependent fFGg micro-plate model incorporating higher-order shear and normal deformation effects based on a modified couple stress theory, International Journal of Mechanical Sciences 104 (2015) 8 - 23. *doi:http://dx.doi.org/10.1016/j.ijmecsci.2015.09.016*.

[38] L. C. Trinh, H. X. Nguyen, T. P. Vo, T.-K. Nguyen, Size-dependent behaviour of functionally graded microbeams using various shear deformation theories based on the modified couple stress theory, Composite Structures 154 (2016) 556 - 572. *doi:https://doi.org/10.1016/j.compstruct.2016.07.033*.

[39] H. X. Nguyen, T. N. Nguyen, M. Abdel-Wahab, S. Bordas, H. Nguyen-Xuan, T. P. Vo, A refined quasi-3D isogeometric analysis for functionally graded microplates based on the modified couple stress theory, Computer Methods in Applied Mechanics and Engineering 313 (2017) 904 - 940. *doi:https://doi.org/10.1016/j.cma.2016.10.002*.

[40] C.-L. Thanh, L. V. Tran, T. Vu-Huu, H. Nguyen-Xuan, M. Abdel-Wahab, Size-dependent nonlinear analysis and damping responses of FG-CNTRC micro-plates, Computer Methods in Applied Mechanics and Engineering 353 (2019) 253 - 276. *doi:https://doi.org/10.1016/j.cma.2019.05.002*.

[41] C. H. Thai, A. Ferreira, T. Tran, P. Phung-Van, A size-dependent quasi-3D isogeometric model for functionally graded graphene platelet-reinforced composite microplates based on the modified couple stress theory, Composite Structures 234 (2020) 111695. *doi:https://doi.org/10.1016/j.compstruct.2019.111695*.

[42] A. Karamanli, M. Aydogdu, Vibration of functionally graded shear and normal deformable porous microplates via finite element method, Composite Structures 237 (2020) 111934. *doi:https://doi.org/10.1016/j.compstruct.2020.111934.*

[43] P. S. Ghatage, V. R. Kar, P. E. Sudhagar, On the numerical modelling and analysis of multidirectional functionally graded composite structures: A review, Composite Structures 236 (2020) 111837. *doi:https://doi.org/10.1016/j.compstruct.2019.111837.*

[44] M. Nemat-Alla, Reduction of thermal stresses by developing two-dimensional functionally graded materials, International Journal of Solids and Structures 40 (26) (2003) 7339 - 7356. *doi:https://doi.org/10.1016/j.ijsolstr.2003.08.017.*

[45] L. Qian, R. Batra, Design of bidirectional functionally graded plate for optimal natural frequencies, Journal of Sound and Vibration 280 (1) (2005) 415 - 424. *doi:https://doi.org/10.1016/j.jsv.2004.01.042.*

[46] A. Farzam, B. Hassani, A new efficient shear deformation theory for FG plates with in-plane and through-thickness stiffness variations using isogeometric approach, Mechanics of Advanced Materials and Structures 26 (6) (2019) 512-525. *doi:https://doi.org/10.1080/15376494.2017.1400623.*

[47] D. Liu, C. Wang, W. Chen, Free vibration of FGM plates with in-plane material inhomogeneity, Composite Structures 92 (5) (2010) 1047 - 1051. *doi:https://doi.org/10.1016/j.compstruct.2009.10.001*.

[48] B. Uymaz, M. Aydogdu, S. Filiz, Vibration analyses of FGM plates with in-plane material inhomogeneity by Ritz method, Composite Structures 94 (4) (2012) 1398 - 1405. *doi:10.1016/j.compstruct.2011.11.002.*

[49] T. Yu, G. Nie, Z. Zhong, F. Chu, Analytical solution of rectangular plate with in-planevariable stiffness, Applied Mathematics and Mechanics 34 (4) (2013) 395-404. *doi:https://doi.org/10.1007/s10483-013-1679-x.*

[50] T. Xiang, S. Natarajan, H. Man, C. Song, W. Gao, Free vibration and mechanical buckling of plates with in-plane material inhomogeneity - a three dimensional consistent approach, Composite Structures 118 (2014) 634 - 642. *doi:https://doi.org/10.1016/j.compstruct.2014.07.043.*

[51] F. Chu, L. Wang, Z. Zhong, J. He, Hermite radial basis collocation method for vibration of functionally graded plates with in-plane material inhomogeneity, Computers and Structures 142 (2014) 79 - 89. *doi:https://doi.org/10.1016/j.compstruc.2014.07.005*.

[52] M-C Trinh, T. Mukhopadhyay, S-E Kim, A semi-analytical stochastic buckling quantification of porous functionally graded plates, Aerospace Science and Technology, 105, 2020, 105928, *doi: https://doi.org/10.1016/j.ast.2020.105928.*

[53] S. Yin, T. Yu, T. Q. Bui, X. Zheng, S. Tanaka, In-plane material inhomogeneity of functionally graded plates: A higher-order shear deformation plate isogeometric analysis, Composites Part B: Engineering 106 (2016) 273 - 284. *doi:https://doi.org/10.1016/j.compositesb.2016.09.008*.

[54] M. Amirpour, R. Das, E. I. S. Flores, Analytical solutions for elastic deformation of functionally graded thick plates with in-plane stiffness variation using higher order shear deformation theory, Composites Part B: Engineering 94 (2016) 109-121. *doi:https://doi.org/10.1016/j.compositesb.2016.03.040*.

[55] M. Esmaeilzadeh, M. Kadkhodayan, Dynamic analysis of stiffened bi-directional functionally graded plates with porosities under a moving load by dynamic relaxation method with kinetic damping, Aerospace Science and Technology, 93, 2019, 105333. *doi:https://doi.org/10.1016/j.ast.2019.105333.*

[56] Q. X. Lieu, S. Lee, J. Kang, J. Lee, Bending and free vibration analyses of in-plane bi-directional functionally graded plates with variable thickness using isogeometric analysis, Composite Structures 192 (2018) 434 - 451. *doi:https://doi.org/10.1016/j.compstruct.2018.03.021*.

[57] Q. X. Lieu, D. Lee, J. Kang, J. Lee, NURBS-based modeling and analysis for free vibration and buckling problems of in-plane bi-directional functionally graded plates, Mechanics of Advanced Materials and Structures 26 (12) (2019) 1064-1080. *doi:https://doi.org/10.1080/15376494.2018.1430273*.

[58] Q. X. Lieu, J. Lee, An isogeometric multimesh design approach for size and shape optimization

of multidirectional functionally graded plates, Computer Methods in Applied Mechanics and Engineering 343 (2019) 407 - 437. *doi:https://doi.org/10.1016/j.cma.2018.08.017*.

[59] T. Van Do, D. Nguyen, N. Duc, D. Doan, T. Bui, Analysis of bi-directional functionally graded plates by FEM and a new third-order shear deformation plate theory, Thin-Walled Structures. 119 (2017) 687-699. *doi:10.1016/j.tws.2017.07.022.*

[60] A. B. Rad, Static analysis of non-uniform 2D functionally graded auxetic-porous circular plates interacting with the gradient elastic foundations involving friction force, Aerospace Science and Technology, 76, 2018, 315-339, *doi: https://doi.org/10.1016/j.ast.2018.01.036.*

[61] Y. Chiker, M. Bachene, M. Guemana, B. Attaf, S. Rechak, Free vibration analysis of multilayer functionally graded polymer nanocomposite plates reinforced with nonlinearly distributed carbon-based nanofillers using a layer-wise formulation model, Aerospace Science and Technology, 104, 2020, 105913, *doi: https://doi.org/10.1016/j.ast.2020.105913.*

[62] M. Adineh, M. Kadkhodayan, Three-dimensional thermo-elastic analysis and dynamic response of a multi-directional functionally graded skew plate on elastic foundation, Composites Part B: Engineering. 125 (2017) 227-240. *doi:10.1016/j.compositesb.2017.05.070.*

[63] A. Karamanli. Size-dependent behaviors of three directional functionally graded shear and normal deformable imperfect microplates Compos. Struct ,257 (2021), doi: 113076,10.1016/j.compstruct.2020.113076

[64] H. Yang, C. Dong, Y. Wu, Postbuckling analysis of multi-directional perforated FGM plates using NURBS-based IGA and FCM, Applied Mathematical Modelling. 84 (2020) 466-500. *doi:10.1016/j.apm.2020.03.043.*

[65] D. Do, H. Nguyen-Xuan, J. Lee, Material optimization of tri-directional functionally graded plates by using deep neural network and isogeometric multimesh design approach, Applied Mathematical Modelling. 87 (2020) 501-533. *doi:10.1016/j.apm.2020.06.002.*

[66] C. Lü, C. Lim, W. Chen, Semi-analytical analysis for multi-directional functionally graded plates: 3-D elasticity solutions, International Journal for Numerical Methods In Engineering. 79 (2009) 25-44. *doi:10.1002/nme.2555.*

[67] T. Son, T. Huu-Tai, Free-vibration analysis of multi-directional functionally graded plates based on 3D isogeometric analysis, Journal of Science And Technology In Civil Engineering (STCE) - NUCE. 13 (2019) 1-11. *doi:10.31814/stce.nuce2019-13(2)-01*.

[68] A. Farzam, B. Hassani, Isogeometric analysis of in-plane functionally graded porous microplates using modified couple stress theory, Aerospace Science and Technology 91 (2019) 508 - 524. *doi:https://doi.org/10.1016/j.ast.2019.05.012*.

[69] A. Bakhsheshy, H. Mahbadi, The effect of multidimensional temperature distribution on the vibrational characteristics of a size-dependent thick bi-directional functionally graded microplate, Noise & Vibration Worldwide 50 (9-11) (2019) 267-290. *doi:https://doi.org/10.1177/0957456519883265*.

Appendix

$$K_{11}(i,j) = \int_{A_e} \Big[A_{11}\varphi_{i,x}\varphi_{j,x} + A_{44}\varphi_{i,y}\varphi_{j,y} + \frac{1}{8}A_{\chi}\big(\varphi_{i,yy}\varphi_{j,yy} + \varphi_{i,xy}\varphi_{j,xy}\big) + J_{\eta}\Big(\frac{7}{5}\varphi_{i,xx}\varphi_{j,xx} + \frac{4}{15}\varphi_{i,yy}\varphi_{j,yy} + \frac{31}{15}\varphi_{i,xy}\varphi_{j,xy} - \frac{1}{5}\varphi_{i,xx}\varphi_{j,yy} - \frac{1}{5}\varphi_{i,yy}\varphi_{j,xx}\Big)\Big] dxdy \qquad (a1)$$

$$K_{12}(i,j) = \int_{A_e} \Big[A_{12}\varphi_{i,x}\varphi_{j,y} + A_{44}\varphi_{i,y}\varphi_{j,x} - \frac{1}{8}A_{\chi}\big(\varphi_{i,yy}\varphi_{j,xy} + \varphi_{i,xy}\varphi_{j,xx}\big) + J_{\eta}\Big(\frac{8}{15}\varphi_{i,xy}\varphi_{j,xx} + \frac{3}{5}\varphi_{i,xx}\varphi_{j,xy} + \frac{3}{5}\varphi_{i,xy}\varphi_{j,yy} + \frac{8}{15}\varphi_{i,yy}\varphi_{j,xy}\Big)\Big] dxdy \qquad (a2)$$

$$K_{13}(i,j) = \int_{A_e} \Big[-B_{11}\varphi_{i,x}\varphi_{j,xx} - B_{12}\varphi_{i,x}\varphi_{j,yy} - 2E_{44}\varphi_{i,y}\varphi_{j,xy} + \frac{1}{8}T_{\chi}\big(\varphi_{i,yy}\varphi_{j,x} - \varphi_{i,xy}\varphi_{j,y}\big) + F_{S\eta}\Big(\frac{1}{15}\varphi_{i,yy}\varphi_{j,x} + \frac{2}{15}\varphi_{i,xy}\varphi_{j,y} + \frac{1}{5}\varphi_{i,xx}\varphi_{j,x}\Big) + T_{S\eta}\Big(-\frac{7}{5}\varphi_{i,xx}\varphi_{j,xxx} - \frac{2}{5}\varphi_{i,xx}\varphi_{j,xyy} - \frac{13}{5}\varphi_{i,xy}\varphi_{j,xxy} - \frac{3}{5}\varphi_{i,xy}\varphi_{j,yyy} + \frac{1}{5}\varphi_{i,yy}\varphi_{j,xxx} - \frac{4}{5}\varphi_{i,yy}\varphi_{j,xyy}\Big)\Big] dxdy \qquad (a3)$$

$$K_{14}(i,j) = \int_{A_e} \Big[-CC_{11}\varphi_{i,x}\varphi_{j,xx} - CC_{12}\varphi_{i,x}\varphi_{j,yy} - 2F_{44}\varphi_{i,y}\varphi_{j,xy} + \frac{1}{8}W_{\chi}\big(\varphi_{i,yy}\varphi_{j,x} - \varphi_{i,xy}\varphi_{j,y}\big) + G_{S\eta}\Big(\frac{1}{5}\varphi_{i,xx}\varphi_{j,x} + \frac{2}{15}\varphi_{i,xy}\varphi_{j,y} + \frac{1}{15}\varphi_{i,yy}\varphi_{j,x}\Big) + X_{S\eta}\Big(-\frac{7}{5}\varphi_{i,xx}\varphi_{j,xxx} - \frac{2}{5}\varphi_{i,xx}\varphi_{j,xyy} - \frac{13}{5}\varphi_{i,xy}\varphi_{j,xxy} - \frac{3}{5}\varphi_{i,xy}\varphi_{j,yyy} + \frac{1}{5}\varphi_{i,yy}\varphi_{j,xxx} - \frac{4}{5}\varphi_{i,yy}\varphi_{j,xyy}\Big)\Big] dxdy \qquad (a4)$$

$$K_{15}(i,j) = \int_{A_e} \Big[GG_{12}\varphi_{i,x}\varphi_j + \frac{1}{8}N_\chi\big(\varphi_{i,yy}\varphi_{j,x} - \varphi_{i,xy}\varphi_{j,y}\big) + N_{S\eta}\left(\frac{3}{5}\varphi_{i,xx}\varphi_{j,x} + \frac{11}{15}\varphi_{i,xy}\varphi_{j,y} - \frac{2}{15}\varphi_{i,yy}\varphi_{j,x}\right)\Big] dxdy \quad (a5)$$

$$K_{22}(i,j) = \int_{A_e} \Big[A_{11}\varphi_{i,y}\varphi_{j,y} + A_{44}\varphi_{i,x}\varphi_{j,x} + \frac{1}{8}A_\chi\big(\varphi_{i,xy}\varphi_{j,xy} + \varphi_{i,xx}\varphi_{j,xx}\big) + J_\eta\left(\frac{7}{5}\varphi_{i,yy}\varphi_{j,yy} + \frac{4}{15}\varphi_{i,xx}\varphi_{j,xx} + \frac{31}{15}\varphi_{i,xy}\varphi_{j,xy} - \frac{1}{5}\varphi_{i,xx}\varphi_{j,yy} - \frac{1}{5}\varphi_{i,yy}\varphi_{j,xx}\right)\Big] dxdy \quad (a6)$$

$$K_{23}(i,j) = \int_{A_e} \Big[-B_{11}\varphi_{i,y}\varphi_{j,yy} - B_{12}\varphi_{i,y}\varphi_{j,xx} - 2E_{44}\varphi_{i,x}\varphi_{j,xy} + \frac{1}{8}T_\chi\big(\varphi_{i,xx}\varphi_{j,y} - \varphi_{i,xy}\varphi_{j,x}\big) + F_{S\eta}\left(\frac{1}{15}\varphi_{i,xx}\varphi_{j,y} + \frac{2}{15}\varphi_{i,xy}\varphi_{j,x} + \frac{1}{5}\varphi_{i,yy}\varphi_{j,y}\right) + T_{S\eta}\left(-\frac{7}{5}\varphi_{i,yy}\varphi_{j,yyy} - \frac{2}{5}\varphi_{i,yy}\varphi_{j,xxy} - \frac{13}{5}\varphi_{i,xy}\varphi_{j,xyy} - \frac{3}{5}\varphi_{i,xy}\varphi_{j,xxx} + \frac{1}{5}\varphi_{i,xx}\varphi_{j,yyy} - \frac{4}{5}\varphi_{i,xx}\varphi_{j,xxy}\right)\Big] dxdy \quad (a7)$$

$$K_{24}(i,j) = \int_{A_e} \Big[-CC_{11}\varphi_{i,y}\varphi_{j,yy} - CC_{12}\varphi_{i,y}\varphi_{j,xx} - 2F_{44}\varphi_{i,x}\varphi_{j,xy} + \frac{1}{8}W_\chi\big(\varphi_{i,xx}\varphi_{j,y} - \varphi_{i,xy}\varphi_{j,x}\big) + G_{S\eta}\left(\frac{1}{5}\varphi_{i,yy}\varphi_{j,y} + \frac{2}{15}\varphi_{i,xy}\varphi_{j,x} + \frac{1}{15}\varphi_{i,xx}\varphi_{j,y}\right) + X_{S\eta}\left(-\frac{7}{5}\varphi_{i,yy}\varphi_{j,yyy} - \frac{2}{5}\varphi_{i,yy}\varphi_{j,xxy} - \frac{13}{5}\varphi_{i,xy}\varphi_{j,xyy} - \frac{3}{5}\varphi_{i,xy}\varphi_{j,xxx} + \frac{1}{5}\varphi_{i,xx}\varphi_{j,yyy} - \frac{4}{5}\varphi_{i,xx}\varphi_{j,xxy}\right)\Big] dxdy \quad (a8)$$

$$K_{25}(i,j) = \int_{A_e} \Big[GG_{12}\varphi_{i,y}\varphi_j + \frac{1}{8}N_\chi\big(\varphi_{i,xx}\varphi_{j,y} - \varphi_{i,xy}\varphi_{j,x}\big) + N_{S\eta}\left(\frac{3}{5}\varphi_{i,yy}\varphi_{j,y} + \frac{11}{15}\varphi_{i,xy}\varphi_{j,x} - \frac{2}{15}\varphi_{i,xx}\varphi_{j,y}\right)\Big] dxdy \quad (a9)$$

$$K_{33}(i,j) = \int_{A_e} \Big[D_{11}\left(\varphi_{i,xx}\varphi_{j,xx} + \varphi_{i,yy}\varphi_{j,yy}\right) + D_{12}\left(\varphi_{i,xx}\varphi_{j,yy} + \varphi_{i,yy}\varphi_{j,xx}\right)$$

$$+ B_{44}\left(\varphi_{i,x}\varphi_{j,x} + \varphi_{i,y}\varphi_{j,y}\right) + 4H_{44}\varphi_{i,xy}\varphi_{j,xy} + \frac{1}{2}B_{\chi}\varphi_{i,xy}\varphi_{j,xy}$$

$$+ \frac{1}{8}B_{\chi}\left(\varphi_{i,xx}\varphi_{j,xx} + \varphi_{i,yy}\varphi_{j,yy} - \varphi_{i,xx}\varphi_{j,yy} - \varphi_{i,yy}\varphi_{j,xx}\right)$$

$$+ \frac{1}{8}H_{\chi}\left(\varphi_{i,x}\varphi_{j,x} + \varphi_{i,y}\varphi_{j,y}\right)$$

$$+ J_{\eta}\left(\frac{4}{15}\varphi_{i,xx}\varphi_{j,xx} + \frac{4}{15}\varphi_{i,yy}\varphi_{j,yy} - \frac{1}{15}\varphi_{i,xx}\varphi_{j,yy} - \frac{1}{15}\varphi_{i,yy}\varphi_{j,xx} + \frac{2}{3}\varphi_{i,xy}\varphi_{j,xy}\right)$$

$$+ S_{\eta}\left(\frac{31}{15}\varphi_{i,xx}\varphi_{j,xx} + \frac{31}{15}\varphi_{i,yy}\varphi_{j,yy} + \frac{11}{15}\varphi_{i,xx}\varphi_{j,yy} + \frac{11}{15}\varphi_{i,yy}\varphi_{j,xx} + \frac{8}{3}\varphi_{i,xy}\varphi_{j,xy}\right)$$

$$+ L_{S\eta}\left(-\frac{16}{15}\varphi_{i,xx}\varphi_{j,xx} - \frac{16}{15}\varphi_{i,yy}\varphi_{j,yy} + \frac{4}{15}\varphi_{i,xx}\varphi_{j,yy} + \frac{4}{15}\varphi_{i,yy}\varphi_{j,xx}\right.$$

$$\left. - \frac{8}{3}\varphi_{i,xy}\varphi_{j,xy}\right) + \frac{4}{15}A_{\eta}\left(\varphi_{i,x}\varphi_{j,x} + \varphi_{i,y}\varphi_{j,y}\right)$$

$$+ \frac{P_{S\eta}}{5}\left(7\varphi_{i,xxx}\varphi_{j,xxx} + 17\varphi_{i,xxy}\varphi_{j,xxy} + 17\varphi_{i,xyy}\varphi_{j,xyy} + 7\varphi_{i,yyy}\varphi_{j,yyy}\right.$$

$$\left. + 2\varphi_{i,xxx}\varphi_{j,xyy} + 2\varphi_{i,xyy}\varphi_{j,xxx} + 2\varphi_{i,xxy}\varphi_{j,yyy} + 2\varphi_{i,yyy}\varphi_{j,xxy}\right)$$

$$- \frac{D_{\eta}}{5}\left(\varphi_{i,x}\varphi_{j,xxx} + \varphi_{i,xxx}\varphi_{j,x} + \varphi_{i,x}\varphi_{j,xyy} + \varphi_{i,xyy}\varphi_{j,x} + \varphi_{i,xxy}\varphi_{j,y} + \varphi_{i,y}\varphi_{j,xxy}\right.$$

$$\left. + \varphi_{i,y}\varphi_{j,yyy} + \varphi_{i,yyy}\varphi_{j,y}\right)\Big] dxdy \qquad (a10)$$

$$K_{34}(i,j) = \int_{A_e} \Big[E_{11}\left(\varphi_{i,xx}\varphi_{j,xx} + \varphi_{i,yy}\varphi_{j,yy}\right) + E_{12}\left(\varphi_{i,xx}\varphi_{j,yy} + \varphi_{i,yy}\varphi_{j,xx}\right)$$

$$+ CC_{44}\left(\varphi_{i,x}\varphi_{j,x} + \varphi_{i,y}\varphi_{j,y}\right) + 4GG_{44}\varphi_{i,xy}\varphi_{j,xy} + \frac{1}{2}C_{\chi}\varphi_{i,xy}\varphi_{j,xy}$$

$$+ \frac{1}{8}C_{\chi}\left(\varphi_{i,yy}\varphi_{j,yy} - \varphi_{i,yy}\varphi_{j,xx} - \varphi_{i,xx}\varphi_{j,yy} + \varphi_{i,xx}\varphi_{j,xx}\right)$$

$$+ \frac{1}{8}P_{\chi}\left(\varphi_{i,x}\varphi_{j,x} + \varphi_{i,y}\varphi_{j,y}\right)$$

$$+ J_{\eta}\left(\frac{4}{15}\varphi_{i,xx}\varphi_{j,xx} + \frac{2}{3}\varphi_{i,xy}\varphi_{j,xy} - \frac{1}{15}\varphi_{i,xx}\varphi_{j,yy} - \frac{1}{15}\varphi_{i,yy}\varphi_{j,xx} + \frac{4}{15}\varphi_{i,yy}\varphi_{j,yy}\right)$$

$$+ \frac{4}{15}B_{\eta}\left(\varphi_{i,x}\varphi_{j,x} + \varphi_{i,y}\varphi_{j,y}\right)$$

$$+ B_{S\eta}\left(\frac{31}{15}\varphi_{i,xx}\varphi_{j,xx} + \frac{8}{3}\varphi_{i,xy}\varphi_{j,xy} + \frac{11}{15}\varphi_{i,xx}\varphi_{j,yy} + \frac{11}{15}\varphi_{i,yy}\varphi_{j,xx}\right.$$

$$\left. + \frac{31}{15}\varphi_{i,yy}\varphi_{j,yy}\right) - \frac{1}{5}E_{\eta}\left(\varphi_{i,x}\varphi_{j,xxx} + \varphi_{i,x}\varphi_{j,xyy} + \varphi_{i,y}\varphi_{j,xxy} + \varphi_{i,y}\varphi_{j,yyy}\right)$$

$$- \frac{1}{5}H_{\eta}\left(\varphi_{i,xxx}\varphi_{j,x} + \varphi_{i,xyy}\varphi_{j,x} + \varphi_{i,xxy}\varphi_{j,y} + \varphi_{i,yyy}\varphi_{j,y}\right)$$

$$+ L_{S\eta}\left(-\frac{8}{15}\varphi_{i,xx}\varphi_{j,xx} - \frac{4}{3}\varphi_{i,xy}\varphi_{j,xy} + \frac{2}{15}\varphi_{i,xx}\varphi_{j,yy} + \frac{2}{15}\varphi_{i,yy}\varphi_{j,xx}\right.$$

$$\left. - \frac{8}{15}\varphi_{i,yy}\varphi_{j,yy}\right)$$

$$+ M_{S\eta}\left(-\frac{8}{15}\varphi_{i,xx}\varphi_{j,xx} - \frac{4}{3}\varphi_{i,xy}\varphi_{j,xy} + \frac{2}{15}\varphi_{i,xx}\varphi_{j,yy} + \frac{2}{15}\varphi_{i,yy}\varphi_{j,xx}\right.$$

$$\left. - \frac{8}{15}\varphi_{i,yy}\varphi_{j,yy}\right)$$

$$+ E_{S\eta}\left(\frac{7}{10}\varphi_{i,xxx}\varphi_{j,xxx} + \frac{2}{5}\varphi_{i,xxx}\varphi_{j,xyy} + \frac{17}{5}\varphi_{i,xxy}\varphi_{j,xxy} + \frac{2}{5}\varphi_{i,xyy}\varphi_{j,xxx}\right.$$

$$+ \frac{17}{5}\varphi_{i,xyy}\varphi_{j,xyy} + \frac{2}{5}\varphi_{i,xxy}\varphi_{j,yyy} + \frac{2}{5}\varphi_{i,yyy}\varphi_{j,xxy}$$

$$\left. + \frac{7}{5}\varphi_{i,yyy}\varphi_{j,yyy}\right)\Big] dxdy \qquad (a11)$$

$$K_{35}(i,j) = \int_{A_e} \Big[-H_{12}\left(\varphi_{i,xx}\varphi_j + \varphi_{i,yy}\varphi_j\right) + N_{44}\left(\varphi_{i,x}\varphi_{j,x} + \varphi_{i,y}\varphi_{j,y}\right) + \frac{1}{2}F_\chi \varphi_{i,xy}\varphi_{j,xy}$$

$$+ \frac{1}{8}F_\chi\left(\varphi_{i,yy}\varphi_{j,yy} + \varphi_{i,xx}\varphi_{j,xx} - \varphi_{i,xx}\varphi_{j,yy} - \varphi_{i,yy}\varphi_{j,xx}\right)$$

$$+ \frac{1}{8}R_\chi\left(\varphi_{i,x}\varphi_{j,x} + \varphi_{i,y}\varphi_{j,y}\right) - \frac{3}{5}N_\eta\left(\varphi_{i,xx}\varphi_j + \varphi_{i,yy}\varphi_j\right)$$

$$- \frac{8}{15}C_\eta\left(\varphi_{i,x}\varphi_{j,x} + \varphi_{i,y}\varphi_{j,y}\right)$$

$$- \frac{3}{5}Y_\eta\left(\varphi_{i,xxy}\varphi_{j,y} + \varphi_{i,yyy}\varphi_{j,y} + \varphi_{i,xxx}\varphi_{j,x} + \varphi_{i,xyy}\varphi_{j,x}\right)$$

$$- \frac{1}{5}H_{S\eta}\left(\varphi_{i,xx}\varphi_j + \varphi_{i,yy}\varphi_j\right)$$

$$+ Y_{S\eta}\left(\frac{2}{3}\varphi_{i,xy}\varphi_{j,xy} - \frac{1}{15}\varphi_{i,xx}\varphi_{j,yy} - \frac{1}{15}\varphi_{i,yy}\varphi_{j,xx} + \frac{4}{15}\varphi_{i,yy}\varphi_{j,yy} + \frac{4}{15}\varphi_{i,xx}\varphi_{j,xx}\right)$$

$$+ C_{S\eta}\left(-\frac{8}{15}\varphi_{i,xx}\varphi_{j,xx} - \frac{4}{3}\varphi_{i,xy}\varphi_{j,xy} + \frac{2}{15}\varphi_{i,xx}\varphi_{j,yy} + \frac{2}{15}\varphi_{i,yy}\varphi_{j,xx}\right.$$

$$\left. - \frac{8}{15}\varphi_{i,yy}\varphi_{j,yy}\right)\Big] dxdy \qquad (a12)$$

$$K_{44}(i,j) = \int_{A_e} \Big[F_{11}\left(\varphi_{i,xx}\varphi_{j,xx} + \varphi_{i,yy}\varphi_{j,yy}\right) + F_{12}\left(\varphi_{i,xx}\varphi_{j,yy} + \varphi_{i,yy}\varphi_{j,xx}\right)$$

$$+ D_{44}\left(\varphi_{i,x}\varphi_{j,x} + \varphi_{i,y}\varphi_{j,y}\right) + 4L_{44}\varphi_{i,xy}\varphi_{j,xy} + \frac{1}{2}D_{\chi}\varphi_{i,xy}\varphi_{j,xy}$$

$$+ \frac{1}{8}D_{\chi}\left(\varphi_{i,yy}\varphi_{j,yy} + \varphi_{i,xx}\varphi_{j,xx} - \varphi_{i,xx}\varphi_{j,yy} - \varphi_{i,yy}\varphi_{j,xx}\right)$$

$$+ \frac{1}{8}L_{\chi}\left(\varphi_{i,x}\varphi_{j,x} + \varphi_{i,y}\varphi_{j,y}\right)$$

$$+ J_{\eta}\left(\frac{4}{15}\varphi_{i,xx}\varphi_{j,xx} + \frac{4}{15}\varphi_{i,yy}\varphi_{j,yy} - \frac{1}{15}\varphi_{i,xx}\varphi_{j,yy} - \frac{1}{15}\varphi_{i,yy}\varphi_{j,xx} + \frac{2}{3}\varphi_{i,xy}\varphi_{j,xy}\right)$$

$$+ \frac{4}{15}F_{\eta}\left(\varphi_{i,x}\varphi_{j,x} + \varphi_{i,y}\varphi_{j,y}\right)$$

$$+ T_{\eta}\left(\frac{31}{15}\varphi_{i,xx}\varphi_{j,xx} + \frac{31}{15}\varphi_{i,yy}\varphi_{j,yy} + \frac{11}{15}\varphi_{i,xx}\varphi_{j,yy} + \frac{11}{15}\varphi_{i,yy}\varphi_{j,xx} + \frac{8}{3}\varphi_{i,xy}\varphi_{j,xy}\right)$$

$$+ M_{S\eta}\left(-\frac{16}{15}\varphi_{i,xx}\varphi_{j,xx} - \frac{16}{15}\varphi_{i,yy}\varphi_{j,yy} + \frac{4}{15}\varphi_{i,xx}\varphi_{j,yy} + \frac{4}{15}\varphi_{i,yy}\varphi_{j,xx}\right.$$

$$\left. - \frac{8}{3}\varphi_{i,xy}\varphi_{j,xy}\right)$$

$$- \frac{L_{\eta}}{5}\left(\varphi_{i,x}\varphi_{j,xxx} + \varphi_{i,xxx}\varphi_{j,x} + \varphi_{i,x}\varphi_{j,xyy} + \varphi_{i,xyy}\varphi_{j,x} + \varphi_{i,xxy}\varphi_{j,y} + \varphi_{i,y}\varphi_{j,xxy}\right.$$

$$\left. + \varphi_{i,y}\varphi_{j,yyy} + \varphi_{i,yyy}\varphi_{j,y}\right)$$

$$+ \frac{R_{S\eta}}{5}\left(7\varphi_{i,xxx}\varphi_{j,xxx} + 17\varphi_{i,xxy}\varphi_{j,xxy} + 17\varphi_{i,xyy}\varphi_{j,xyy} + 7\varphi_{i,yyy}\varphi_{j,yyy}\right.$$

$$+ 2\varphi_{i,xxx}\varphi_{j,xyy} + 2\varphi_{i,xyy}\varphi_{j,xxx} + 2\varphi_{i,xxy}\varphi_{j,yyy}$$

$$\left. + 2\varphi_{i,yyy}\varphi_{j,xxy}\right)\Big] dxdy \qquad (a13)$$

$$K_{45}(i,j) = \int_{A_e} \Big[-L_{12}\left(\varphi_{i,xx}\varphi_{j} + \varphi_{i,yy}\varphi_{j}\right) + P_{44}\left(\varphi_{i,x}\varphi_{j,x} + \varphi_{i,y}\varphi_{j,y}\right) + \frac{1}{2}G_{\chi}\varphi_{i,xy}\varphi_{j,xy}$$

$$+ \frac{1}{8}G_{\chi}\left(\varphi_{i,yy}\varphi_{j,yy} + \varphi_{i,xx}\varphi_{j,xx} - \varphi_{i,xx}\varphi_{j,yy} - \varphi_{i,yy}\varphi_{j,xx}\right)$$

$$+ \frac{1}{8}S_{\chi}\left(\varphi_{i,x}\varphi_{j,x} + \varphi_{i,y}\varphi_{j,y}\right) - \frac{3}{5}P_{\eta}\left(\varphi_{i,xx}\varphi_{j} + \varphi_{i,yy}\varphi_{j}\right) - \frac{8}{15}G_{\eta}\left(\varphi_{i,x}\varphi_{j,x} + \varphi_{i,y}\varphi_{j,y}\right)$$

$$- \frac{3}{5}A_{S\eta}\left(\varphi_{i,xxy}\varphi_{j,y} + \varphi_{i,yyy}\varphi_{j,y} + \varphi_{i,xxx}\varphi_{j,x} + \varphi_{i,xyy}\varphi_{j,x}\right)$$

$$- \frac{1}{5}H_{S\eta}\left(\varphi_{i,xx}\varphi_{j} + \varphi_{i,yy}\varphi_{j}\right)$$

$$+ Y_{S\eta}\left(\frac{2}{3}\varphi_{i,xy}\varphi_{j,xy} - \frac{1}{15}\varphi_{i,xx}\varphi_{j,yy} - \frac{1}{15}\varphi_{i,yy}\varphi_{j,xx} + \frac{4}{15}\varphi_{i,yy}\varphi_{j,yy} + \frac{4}{15}\varphi_{i,xx}\varphi_{j,xx}\right)$$

$$+ D_{S\eta}\left(-\frac{8}{15}\varphi_{i,xx}\varphi_{j,xx} - \frac{4}{3}\varphi_{i,xy}\varphi_{j,xy} + \frac{2}{15}\varphi_{i,xx}\varphi_{j,yy} + \frac{2}{15}\varphi_{i,yy}\varphi_{j,xx}\right.$$

$$\left. - \frac{8}{15}\varphi_{i,yy}\varphi_{j,yy}\right)\Big] dxdy \qquad (a14)$$

$$K_{55}(i,j) = \int_{A_e} \Big[GG_{11}\varphi_i\varphi_j + M_{44}\big(\varphi_{i,x}\varphi_{j,x} + \varphi_{i,y}\varphi_{j,y}\big) + \frac{1}{2}E_\chi\varphi_{i,xy}\varphi_{j,xy} + \frac{1}{8}E_\chi\big(\varphi_{i,yy}\varphi_{j,yy} + \varphi_{i,xx}\varphi_{j,xx} - \varphi_{i,xx}\varphi_{j,yy} - \varphi_{i,yy}\varphi_{j,xx}\big) + \frac{1}{8}M_\chi\big(\varphi_{i,x}\varphi_{j,x} + \varphi_{i,y}\varphi_{j,y}\big) + \frac{70}{5}M_\eta\varphi_i\varphi_j + \frac{31}{15}X_\eta\big(\varphi_{i,x}\varphi_{j,x} + \varphi_{i,y}\varphi_{j,y}\big) - \frac{1}{5}R_\eta\big(\varphi_i\varphi_{j,xx} + \varphi_{i,xx}\varphi_j + \varphi_i\varphi_{j,yy} + \varphi_{i,yy}\varphi_j\big) + S_{S\eta}\Big(\frac{4}{15}\varphi_{i,xx}\varphi_{j,xx} + \frac{2}{3}\varphi_{i,xy}\varphi_{j,xy} + \frac{4}{15}\varphi_{i,yy}\varphi_{j,yy} - \frac{1}{15}\varphi_{i,xx}\varphi_{j,yy} - \frac{1}{15}\varphi_{i,yy}\varphi_{j,xx}\Big)\Big] dxdy \quad (a15)$$

$$M_{11}(i,j) = \int_{A_e} I_0\varphi_i\varphi_j dxdy \quad (a16)$$

$$M_{13}(i,j) = -\int_{A_e} I_1\varphi_i\varphi_{j,x} dxdy \quad (a17)$$

$$M_{14}(i,j) = -\int_{A_e} J_1\varphi_i\varphi_{j,x} dxdy \quad (a18)$$

$$M_{22}(i,j) = \int_{A_e} I_0\varphi_i\varphi_j dxdy \quad (a19)$$

$$M_{23}(i,j) = -\int_{A_e} I_1\varphi_i\varphi_{j,y} dxdy \quad (a20)$$

$$M_{24}(i,j) = -\int_{A_e} J_1\varphi_i\varphi_{j,y} dxdy \quad (a21)$$

$$M_{33}(i,j) = \int_{A_e} I_0\varphi_i\varphi_j dxdy + \int_{A_e} I_2\big(\varphi_{i,x}\varphi_{j,x} + \varphi_{i,y}\varphi_{j,y}\big) dxdy \quad (a22)$$

$$M_{34}(i,j) = \int_{A_e} I_0\varphi_i\varphi_j dxdy + \int_{A_e} J_3\big(\varphi_{i,x}\varphi_{j,x} + \varphi_{i,y}\varphi_{j,y}\big) dxdy \quad (a23)$$

$$M_{35}(i,j) = \int_{A_e} J_2\varphi_i\varphi_j dxdy \quad (a24)$$

$$M_{44}(i,j) = \int_{A_e} I_0\varphi_i\varphi_j dxdy + \int_{A_e} K_1\big(\varphi_{i,x}\varphi_{j,x} + \varphi_{i,y}\varphi_{j,y}\big) dxdy \quad (a25)$$

$$M_{45}(i,j) = \int_{A_e} J_2 \varphi_i \varphi_j dxdy \qquad (a26)$$

$$M_{55}(i,j) = \int_{A_e} K_2 \varphi_i \varphi_j dxdy \qquad (a27)$$

$$M_{12}(i,j) = 0, M_{15}(i,j) = 0 \; and \; M_{25}(i,j) = 0 \qquad (a28)$$

$$G_{33}(i,j) = \int_{A_e} N_x \varphi_{i,x} \varphi_{j,x} dxdy + \int_{A_e} N_y \varphi_{i,y} \varphi_{j,y} dxdy + 2 \int_{A_e} N_{xy} \varphi_{i,x} \varphi_{j,y} dxdy \qquad (a29)$$

$$G_{34}(i,j) = \int_{A_e} N_x \varphi_{i,x} \varphi_{j,x} dxdy + \int_{A_e} N_y \varphi_{i,y} \varphi_{j,y} dxdy + \int_{A_e} N_{xy} \left(\varphi_{i,x} \varphi_{j,y} + \varphi_{i,y} \varphi_{j,x}\right) dxdy \qquad (a30)$$

$$G_{35}(i,j) = \int_{A_e} N_x \varphi_{i,x} \varphi_{j,x} dxdy + \int_{A_e} N_y \varphi_{i,y} \varphi_{j,y} dxdy + \int_{A_e} N_{xy} \left(\varphi_{i,x} \varphi_{j,y} + \varphi_{i,y} \varphi_{j,x}\right) dxdy \qquad (a31)$$

$$G_{44}(i,j) = \int_{A_e} N_x \varphi_{i,x} \varphi_{j,x} dxdy + \int_{A_e} N_y \varphi_{i,y} \varphi_{j,y} dxdy + 2 \int_{A_e} N_{xy} \varphi_{i,x} \varphi_{j,y} dxdy \qquad (a32)$$

$$G_{45}(i,j) = \int_{A_e} N_x \varphi_{i,x} \varphi_{j,x} dxdy + \int_{A_e} N_y \varphi_{i,y} \varphi_{j,y} dxdy + \int_{A_e} N_{xy} \left(\varphi_{i,x} \varphi_{j,y} + \varphi_{i,y} \varphi_{j,x}\right) dxdy \qquad (a33)$$

$$G_{55}(i,j) = \int_{A_e} N_x \varphi_{i,x} \varphi_{j,x} dxdy + \int_{A_e} N_y \varphi_{i,y} \varphi_{j,y} dxdy + 2 \int_{A_e} N_{xy} \varphi_{i,x} \varphi_{j,y} dxdy \qquad (a34)$$

$$G_{11}(i,j) = 0, G_{12}(i,j) = 0, G_{13}(i,j) = 0, G_{14}(i,j) = 0, G_{15}(i,j) = 0, G_{22}(i,j) = 0,$$
$$G_{23}(i,j) = 0\,, G_{24}(i,j) = 0 \;\; and \; G_{25}(i,j) = 0 \qquad (a35)$$

$$F_3(i,j) = \int_{A_e} q \varphi_i \varphi_j \, dxdy \qquad (a36)$$

$$F_4(i,j) = \int_{A_e} q\varphi_i\varphi_j \, dxdy \qquad (a37)$$

$$(A_{11}, B_{11}, CC_{11}, D_{11}, E_{11}, F_{11}, GG_{11}) = \int_{-\frac{h}{2}}^{+\frac{h}{2}} C_{11}\left(1, f_1, f_2, {f_1}^2, f_1 f_2, {f_2}^2, {f_3}'^2\right) dz \qquad (a38)$$

$$(A_{12}, B_{12}, CC_{12}, D_{12}, E_{12}, F_{12}, GG_{12}, H_{12}, L_{12})$$
$$= \int_{-\frac{h}{2}}^{+\frac{h}{2}} C_{12}\left(1, f_1, f_2, {f_1}^2, f_1 f_2, {f_2}^2, {f_3}', f_1 {f_3}', f_2 {f_3}'\right) dz \qquad (a39)$$

$$(A_{44}, B_{44}, CC_{44}, D_{44}, E_{44}, F_{44}, GG_{44}, H_{44}, L_{44}, M_{44}, N_{44}, P_{44})$$

$$= \int_{-\frac{h}{2}}^{+\frac{h}{2}} C_{44}[1, (1-{f_1}')^2, (1-{f_1}')(1-{f_2}'), (1-{f_2}')^2, f_1, f_2,$$

$$f_1 f_2, {f_1}^2, {f_2}^2, {f_3}^2, (1-{f_1}')f_3, (1-{f_2}')f_3]dz \qquad (a40)$$

$$\left(A_\chi, B_\chi, C_\chi, D_\chi, E_\chi, F_\chi, G_\chi, H_\chi, L_\chi, M_\chi, N_\chi, P_\chi, R_\chi, S_\chi, T_\chi, W_\chi\right)$$

$$= \int_{-h/2}^{+h/2} Q_\chi[1, (1+{f_1}')^2, (1+{f_1}')(1+{f_2}'), (1+{f_2}')^2, {f_3}^2, (1+{f_1}')f_3,$$

$$(1+{f_2}')f_3, {f_1}''^2, {f_2}''^2, {f_3}'^2, {f_3}', {f_1}''{f_2}'', {f_1}''{f_3}', {f_2}''{f_3}', {f_1}'', {f_2}'']dz \qquad (a41)$$

$$\left(J_\eta, A_\eta, B_\eta, C_\eta, D_\eta, E_\eta, F_\eta, G_\eta, H_\eta, L_\eta, M_\eta, N_\eta, P_\eta, R_\eta, S_\eta, T_\eta, X_\eta, Y_\eta, A_{S\eta}, B_{S\eta}, C_{S\eta}, D_{S\eta}, E_{S\eta}, F_{S\eta}, G_{S\eta},\right.$$

$$\left. H_{S\eta}, L_{S\eta}, M_{S\eta}, N_{S\eta}, P_{S\eta}, R_{S\eta}, S_{S\eta}, T_{S\eta}, X_{S\eta}, Y_{S\eta}\right)$$

$$= \int_{-h/2}^{+h/2} Q_\eta[1, {f_1}''^2, {f_1}''{f_2}'', {f_1}''{f_3}', {f_1}''f_1, {f_1}''{f_2}', {f_2}''^2, {f_2}''{f_3}', {f_2}''f_1, {f_2}''{f_2}', {f_3}''^2, {f_3}''f_1', {f_3}''{f_2}', {f_3}''f_3,$$

$${f_1}'^2, {f_2}'^2, {f_3}'^2, {f_3}'f_1, {f_3}'f_2, f_1'f_2', f_1'f_3, f_2'f_3, f_1f_2, f_1'', f_2'', f_3'', f_1', f_2', f_3', {f_1}^2, {f_2}^2, {f_3}^2, f_1, f_2, f_3]dz \quad (a42)$$

$$(I_0, I_1, I_2, J_1, J_2, J_3, K_1, K_2) = \int_{-\frac{h}{2}}^{+\frac{h}{2}} \rho\left(1, f_1, {f_1}^2, f_2, f_3, f_1 f_2, {f_2}^2, {f_3}^2\right) dz \qquad (a43)$$